Volume 1, Number 3

September-October, 1960

JOURNAL OF STRUCTURAL CHEMISTRY

ЖУРНАЛ СТРУКТУРНОЙ ХИМИИ
(ZHURNAL STRUKTURNOI KHIMII)

TRANSLATED FROM RUSSIAN

CONSULTANTS BUREAU

ZHURNAL STRUKTURNOI KHIMII
EDITORIAL BOARD:

S. S. Batsanov *(Secretary)*
G. B. Bokii *(Editor)*
A. V. Nikolaev *(Acting Editor)*
B. V. Ptitsyn
O. Ya. Samoilov
Yu. T. Struchkov
Ya. K. Syrkin
V. V. Voevodskii
M. V. Vol'kenshtein

JOURNAL OF

STRUCTURAL CHEMISTRY

A translation of ZHURNAL STRUKTURNOI KHIMII,

a publication of the Academy of Sciences of the USSR

© 1961 CONSULTANTS BUREAU ENTERPRISES, INC.
227 West 17th Street, New York 11, N. Y.

Volume 1, Number 3 September-October, 1960

CONTENTS

	PAGE ENG.	PAGE RUSS.
Anatolii Fedorovich Kapustinskii	253	275
Comparative Calculation of Interatomic Distances. M. Kh. Karapet'yants and Ling T'ing-ch'ing	255	277
Mutual Orientation of Water Molecules in Ionic Solutions and Salting-Out of Nonelectrolytes. Yu. V. Gurikov	264	286
Investigation of the Influence of the Structures of Solid and Liquid Phases on the Solubility of Salts in Water. I. On Solubility in the Systems $NH_4NO_3-NH_4I-H_2O$ and KNO_3-KI-H_2O at 25°. P. S. Bogoyavlenskii	281	305
Investigation of the Structure of Certain Unsaturated Compounds by the Method of Combination Scattering of Light. Ya. S. Bobovich and V. V. Perekalin	288	313
Acceptor-Donor Concepts Applied to Extraction. A. V. Nikolaev, N. M. Sinitsyn, and S. M. Shubina	294	319
Conditions of Solubility of Organic Substances in the Solid State. A. I. Kitaigorodskii	299	324
The Structure of $K_2[RuCl_5H_2O]$. T. S. Khodashova	308	333
The Crystal Structure of the Isomorphous Dihalogeno-Dipyridineates of Cobalt and Zinc. (The Problem of the Nature of the Isomeric Cobalt Compounds with Composition CoA_2X_2). M. A. Porai-Koshits, L. O. Atovmyan, and G. N. Tishchenko.	312	337
The Structural Unity of Structural Types. N. L. Smirnova	317	342
The Different Forms and Some Properties of Neutral Zinc Selenite. L. Ya. Markovskii and Yu. P. Sapozhnikov	321	346
The Use of Overlap Integrals for the Determination of the Ionic Character of Bonds in Molecules. S. S. Batsanov and V. I. Durakov	329	353
REVIEWS	REVIEWS	
Contemporary X-ray Spectral Analysis. E. E. Vainshtein	336	360
The Structure of Normal Paraffins and of Their Solid Solutions. Yu. V. Mnyukh	346	370
BRIEF COMMUNICATIONS	BRIEF COMMUNICATIONS	
Oxanium Compounds of Oxygen. Ya. K. Syrkin	366	389
Lithium Uranate (V) $LiUO_3$. L. M. Kovba and A. N. Golubenko	367	390

Annual Subscription: $80 **Single Issue: $20** **Single Article: $12.50**

Note: The sale of photostatic copies of any portion of this copyright translation is expressly prohibited by the copyright owners.

ANATOLII FEDOROVICH KAPUSTINSKII

Anatolii Fedorovich Kapustinskii, a famous Soviet scientist in the fields of physical chemistry and inorganic chemistry and a Corresponding Member of the Academy of Sciences of the USSR, died prematurely in his 54th year on August 26, 1960.

Anatolii Fedorovich was born in Zhitomir on December 29, 1906. He entered the first gymnasium in Warsaw in 1914, and finished his secondary schooling in Moscow in 1922. In 1923, he became a student in the Chemical Division of the Physicomathematical Faculty of Moscow State University. He completed his university course there when he presented his diploma thesis "An investigation of the thermal dissociation of cadmium sulfide" in 1929. He had studied under the famous Academicians I. A. Kablukov and É. V. Britske. On leaving the university, he became a research worker in the Thermal Laboratory of É. V. Britske in the Moscow Institute of Applied Mineralogy. In this Institute (later called the All-Union Institute for Mineral Raw Materials) Anatolii Fedorovich worked from 1929 to 1941 as research worker, aspirant, engineer, senior scientific coworker, scientific consultant, and laboratory and group director. In 1935 he was sent by the People's Commissariat of Heavy Industry to the U.S.A., England, and France to study arrangements for scientific research work in these countries. He worked for six months in G. N. Lewis' laboratory at the University of California. In the fall of the same year he presented a paper on "Problems of Crystal Chemistry" at a conference of the American Chemical Society. In 1939 Anatolii Fedorovich became a Corresponding Member of the Division of Chemical Sciences of the Academy of Sciences of the USSR. In 1941, he transferred to the Institute of General and Inorganic Chemistry of the Academy of Sciences of the USSR as Director of the Thermal Chemistry Laboratory. He later worked in the Solutions Laboratory of the Institute.

Anatolii Fedorovich began his teaching activities in 1930 in the physical chemistry department of the Moscow School for Higher Technology (MVTU). In later years Anatolii Fedorovich was Professor and Head of the Department of Physical Chemistry in the Gor'kii State University (1933-1937), the Moscow Institute of Steel (1937-1941), and the Kazan State University (1941-1943). In 1943, he became Professor in charge of the Department of General and Inorganic Chemistry of the D. I. Mendeleev Moscow Chemicotechnological Institute, where he worked till the end of his life.

The activities of Anatolii Fedorovich form one of the bright chapters in Soviet chemical sciences. He carried out a large number of profound and always original investigations on many important problems in chemistry. Of these, we may refer to a series of papers on the physical chemistry of metallurgical reactions, on crystal chemistry, on thermochemistry (particularly on the heats of formation of inorganic compounds), theoretical papers on the periodic law and on geochemistry, and papers on the theory of solutions, particularly on ionic solvation in electrolyte solutions. His work on the history of chemistry should also be noted. His most important contribution to science was his work on the energetics of crystals. His equation for the lattice energy of ionic crystals – the widely used Kapustinskii equation (1933, 1943, 1956) – is now always referred to in all monographs and textbooks on crystal chemistry.

The same series of crystal chemistry papers includes the investigations from which he developed a new ionic constant – the crystallochemical electronegativity – characterizing the electron affinity of an ion in a crystal structure. In 1956 Anatolii Fedorovich derived a very general equation, relating the radius of a cation, having the eight electron structure of a rare gas atom, to the charge and the total number of electrons of the cation. He used this equation to calculate the radii of cations of the transuranic elements with different charges. His collected work on crystal chemistry was published in 1956 by the English Chemical Society as a review "The Lattice Energy of Ionic Crystals."

Great interest was aroused by his profound investigation on the theory of solvation of ions in electrolyte solutions. The object of this research was to build up a theory of the thermodynamic characteristics of individual ions in solutions. In Kapustinskii's series of papers on ionic solvation, as with all his work, there is a characteristically remarkable combination of approaches from the point of view of thermodynamics and from the point of view of structural chemistry.

Anatolii Fedorovich possessed great and original talents which included an extraordinary ability to aim for extreme clarity in the understanding of the most complex phenomena. His results were distinguished by great simplicity and ease in demonstration, which made them particularly effective. He achieved wide generalizations in all his series of papers. The extent of his scientific interests can only be described as encyclopedic.

There were many facets to the creative work of Anatolii Fedorovich for publishing and for scientific societies. For nearly 20 years he was the chief editor of the journal "Izvestiya Akademii Nauk SSSR, Otdelenie Khimicheskikh Nauk." In 1946 he became a member of the chief editorial board of the second edition of the Great Soviet Encyclopedia. A series of Russian and translated monographs and textbooks were published under his editorship. In 1957 he was elected President of the National Association of Soviet Chemical Historians. For his outstanding merits, A. F. Kapustinskii was awarded the order of the Worker's Red Badge and medals.

Many scientists and all who knew Anatolii Fedorovich will always retain vivid memories of this outstanding Soviet scientist, brilliant speaker, and remarkable personality.

COMPARATIVE CALCULATION OF INTERATOMIC DISTANCES

M. Kh. Karapet'yants and Ling T'ing-ch'ing

D. I. Mendeleev Chemicotechnological Institute of Hsiamên University
Amoi, Chinese Peoples' Republic
Translated from Zhurnal Strukturnoi Khimii, Vol. 1, No. 3, pp. 277-285,
September-October, 1960
Original article submitted January 15, 1959

Approximate relationships between the interatomic distances, d, in groups of similar molecules are described. The results are particular cases of two methods of comparative calculation. These relationships are illustrated with examples of crystalline and gaseous substances. Some of the results are applied to determine values of d in some gas molecules not yet investigated and to obtain more precise values of d for gas molecules already investigated.

It is known that approximate calculations of various properties can be made by the method of comparative calculation. Up to now most investigators have applied this method to investigations of various macroproperties (energy involved in phase and chemical transformations, boiling point, vapor pressure, viscosity, etc.); few comparisons have been made of microproperties, particularly of the dimensions of particles (interatomic distances, atomic radius of atoms and ions, etc.), which vary regularly in a group of similar substances. Some of these comparisons were made in [1] as particular examples of the first [2] and second [3] methods of comparative calculation. Some of these relationships are described in the present work.

Comparison of Interatomic Distances in Crystalline Substances

1

For the purpose of orientation in calculating constants of the crystal lattice, we can use the following approximate relationship:

$$a_{II} = A_1 a_I + B_1, \tag{1}$$

$$c = A_2 a + B_2 \tag{2}$$

and

$$x_N = A_2 x_M + B. \tag{3}$$

Equation (1) refers to the comparison of the periods of the elementary cell, a, in two groups of substances with similar structures. Figure 1 * shows a few examples. Equation (2) refers to the comparison of two constants, a and c, of the crystal lattice in a group of elements with the same structure; examples are given in Figs. 2 and 3.

* The lines are numbered in the most convenient order. The scales of the axes are equal; the scale is indicated on the figure. The substances corresponding to the points of the lines are indicated in the legend to the left. The values necessary for construction of this and most of the following graphs are taken from the same source [4] for the sake of similarity.

In the left corner of Fig. 3 are given the data corresponding to chlorides, $MeCl_3$, of some elements of the actinide and lanthanide series [4, 5]. All these compounds correspond to the structural type of UCl_3, although for some of them the points do not lie on the same line; in most cases this deviation is apparently within the limit of the experimental error in the values of the properties which are compared. This curve directly indicates the similarity between the elements of the actinide and lanthanide series. However, these data in [4] are insufficient to confirm quantitatively [according to Eq. (2)] the similarity of the elements of the actinide and lanthanide series to the compounds of the elements in groups IVa and VIa [6].

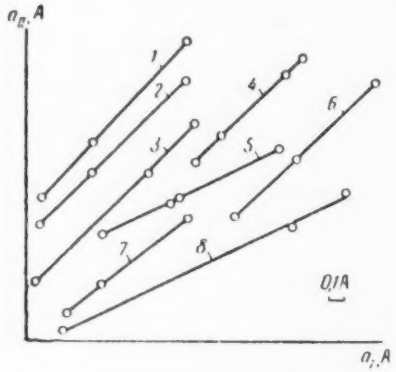

Fig. 1. Interrelations between the periods of the elementary cells for two series of similar substances: 1) $Co(NH_3)_6X_2$ and $Mn(NH_3)_6X_2$ (X = Cl, Br, I); 2) $Co(NH_3)_6X_2$ and $Ni(NH_3)_6X_2$ (X = Cl, Br, I); 3) MeSH and MeSeH (Me = Na, K, Rb); 4) PrX and CeX (X = P, As, Sb, Bi); 5) $MeClO_4$ (cubical) and $MeClO_4$ (rhombohedral) (Me = K, NH_4, Rb, Cs); 6) RuX_2 and OsX_2 (X = S, Se, Te); 7) AlX and GaX (X = P, As, Sb); 8) CuX and AgX (X = F, Cl, Br). For 1, 2, 4, 6, and 7, the values of a are the periods of the elementary cubic cell.

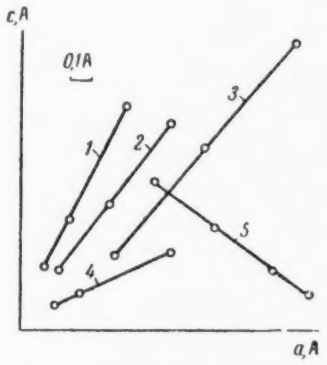

Fig. 2. Relationships between the periods of elementary cells in a series of similar substances. 1) TiX_2 (X = S, Se, Te); 2) MeC_2 (Me = Ca, Sr, Ba); 3) MeH_2 (Me = Ca, Sr, Ba); 4) $Ca(H_2O)_6X_2$ (X = Cl, Br, I); 5) $X(C_6H_5)_4$ (X = Si, Ge, Sn, Pb).

Figure 4 represents the periods of the elementary cell of different substances with hexagonal lattices; all the points are near the same straight line. The difference in coordination does not have a significant effect.

Equation (3) corresponds to the third type of comparison. This equation refers to the comparison of periods of the elementary cell, x (a, b, c), of two structurally similar substances. Equation (3) is illustrated in Fig. 5 in the case of some compounds.

We could present other examples confirming the possibility of using the relationships under consideration, particularly from the investigations of recent years. Thus, Eq. (1) reproduces very well the results obtained in [7] and [8], Eq. (2) could be used to describe the results in [9] and [10], etc. As to the three methods of comparative calculation (see [1], for example), it is difficult as yet to check the degree of their applicability. However, one can assume, for example, that between two intermolecular distances in a molecule of naphthalene at 20 and − 195° [11] there exists an approximately linear relationship: out of 17 distances (8 within a layer and 9 between layers) 11 follow a straight line within the limits of the expected experimental error.

2

Calculation of interatomic distances on the basis of the regular variation of properties (reflected in the periodic table), contrary to the determination of many other properties, is limited by the fact that the type of structure may change from one element to another within a period.

However, even in this case the possibility of comparison is not excluded. In fact, according to the results presented in [4], we can propose for the isostructural halides of the elements of the lithium subgroup the following approximate equations, which are particular examples of relationship (1):

$$a_{LiX} = 1{,}08201\, a_{NaX} - 0{,}9741, \tag{4}$$

$$a_{KX} = 0{,}9284\, a_{NaX} - 1{,}052, \tag{5}$$

$$a_{RbX} = 0{,}9208\, a_{NaX} - 1{,}368, \tag{6}$$

where X = F, Cl, Br, and I, and

$$a_{MeF} = 1{,}1378 a_{MeCl}, \tag{7}$$

$$a_{MeBr} = 0{,}96553\, a_{MeCl} + 0{,}5257, \tag{8}$$

$$a_{MeI} = 0{,}93255\, a_{MeCl} + 1{,}215. \tag{9}$$

where Me = Li, Na, K, and Rb. For LiX and NaX the difference between the experimental and calculated values of a are somewhat greater than the probable error; for KX and RbX they are within the limits of this error. The average deviation for all 15 substances is equal to 0.009 A, the maximum being 0.024 A.

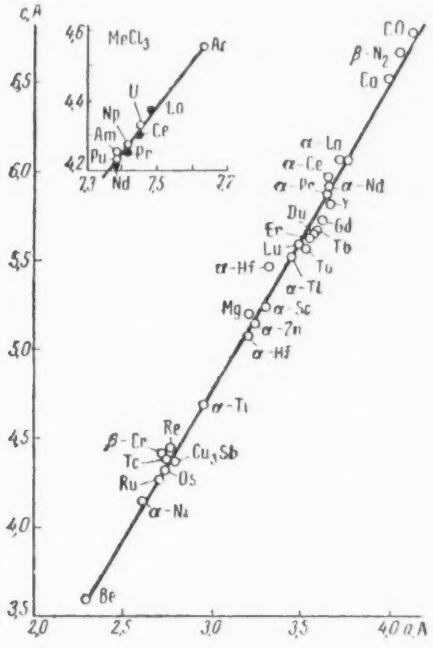

Fig. 3. Relationship between the periods of elementary cells of substances with hexagonal lattices.

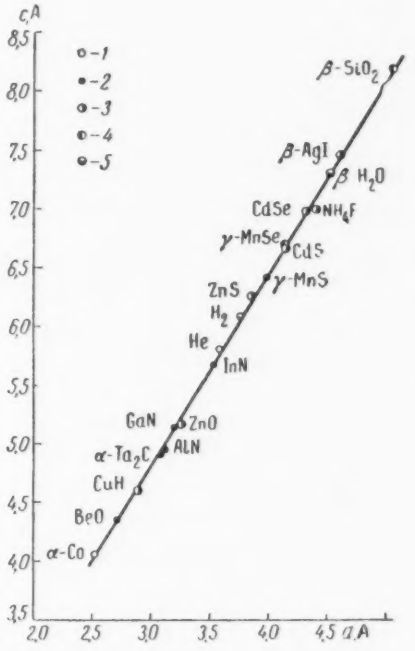

Fig. 4. Relationship between the periods of elementary cells of substances with hexagonal lattices. 1) Dense coordination V; 2) tetrahedral coordination T/T; 3) T/T coordination; 4) T/*l* coordination, 5) tetrahedral coordination T.

For isostructural compounds of the same elements and elements of group VI we can use the following approximate equations:

$$a_{Li_2X} = 1{,}102\, a_{K_2X} - 2{,}460, \tag{10}$$

$$a_{Na_2X} = 1{,}025\, a_{K_2X} - 1{,}048, \tag{11}$$

$$a_{Rb,X} = 0{,}9508\, a_{K,X} + 0{,}623, \tag{12}$$

where X = O, S, Se, and Te, and

$$a_{MeO} = 1{,}083\, a_{MeS} + 1{,}547 \tag{13}$$

$$a_{MeSe} = 0{,}9936\, a_{MeS} + 0{,}914, \tag{14}$$

$$a_{MeTe} = 0{,}9791\, a_{MeS} + 0{,}329, \tag{15}$$

where Me = Li, Na, K, and Rb. For 13 compounds the average deviation is equal to 0.009 A, the maximum deviation being 0.025 A. The values calculated according to this equation, a_{Rb_2Se} = 7.926 A and a_{Rb_2Te} = = 8.389 A, will be close to the real value only under the condition that these compounds have the same structure as the other compounds within the same group.

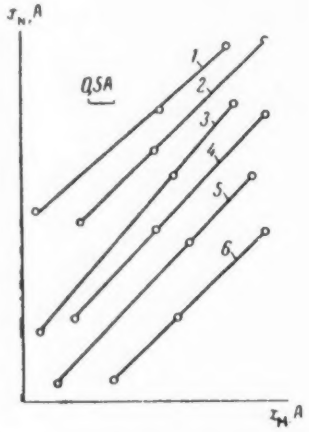

Fig. 5. Relationship between the periods of elementary cells a, b, and c of two similar substances. 1) $PbCl_2$ and $PbBr_2$; 2) Rb_2SO_4 and K_2SO_4; 3) $BaCl_2$ and BaI_2; 4) Rb_2SO_4 and Cs_2SO_4; 5) $BaCl_2$ and $BaBr_2$; 6) $Zn(NH_3)_2Cl_2$ and $Zn(NH_3)_2Br_2$. On curves 2, 4, and 6, contrary to all others, the sequence is different: a, c, b.

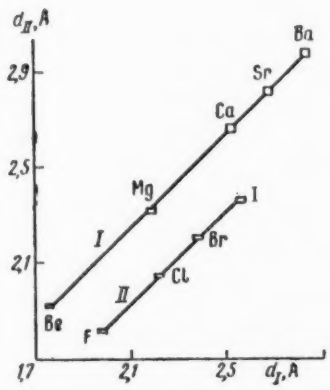

Fig. 6. Relationship between the interatomic distances in some series of similar gaseous substances. I) MeCl, MeBr; II) CdX, ZnX.

For isostructural compounds of the beryllium subgroup with elements of group VI the following approximate relationships are valid:

$$a_{BeX} = 1{,}178\, a_{CaX} - 1{,}846, \tag{16}$$

$$a_{MgX} = 1{,}119\, a_{CaX} - 1{,}168, \tag{17}$$

$$a_{SrX} = 0{,}9734\, a_{CaX} - 0{,}780, \tag{18}$$

$$a_{CaX} = 0{,}9491\, a_{CaX} + 0{,}980, \tag{19}$$

where X = O, S, Se, Te, and

$$a_{MeO} = 1{,}057\, a_{MeS} - 1{,}208 \tag{20}$$

$$a_{MeSe} = 0{,}9828\, a_{MeS} + 0{,}327, \tag{21}$$

$$a_{MeTe} = 0{,}9421\, a_{MeS} + 0{,}990, \tag{22}$$

where Me = Be, Mg, Ca, Sr, and Ba. For the 17 substances the average deviation is 0.019 A and the maximum deviation is 0.038 A. The values, $a_{BeO} = 3.825$ and $a_{MgTe} = 5.90$ A, calculated according to this equation will not correspond to the real values, since these substances have structures which are not similar to the other compounds. Somewhat larger deviations in the case of BeS, BeSe, and BeTe are apparently due to the fact that their type of lattice is different from that of other compounds of group VI.

The average error in the value of a calculated by Eqs. (4) to (22) for 45 substances is less than 0.01 A, i.e., for most of the compounds it is within the limits of the experimental error.

Comparison of Interatomic Distances in Gaseous Substances

1

The method of comparative calculation of interatomic distances in gaseous compounds is more precise and can be applied to a greater number of elements; contrary to crystalline substances, the effect of structural differences on the value of d is insignificant.

Data concerning interatomic distances of gaseous substances are not very numerous (see [12], for example). Furthermore, although the error in d for a number of cases is insignificant (often of the order of 0.01 A), it is also often large; in addition, one must keep in mind the discrepancies between the results obtained by different investigators, and the experimental difficulties (particularly the decomposition of the substance during heating). But even for these relatively limited and sometimes contradictory results, it is easy to show the usefulness of the method of comparative calculation. This can be seen, for example, in the following equations:

$$d_{Me-Br} = 1{,}01\, d_{Me-Cl} + 0{,}13, \tag{23}$$

$$d_{Zn-X} = 0{,}98\, d_{Cd-X} - 0{,}12, \tag{24}$$

which describe the relationship between the interatomic distances, metal– halogen, in bromides and chlorides of the elements of the beryllium subgroup [13-17] and halides of cadmium [18] and zinc [19, 20].

It can be seen directly from Fig. 6, in which the dimensions of each rectangle correspond to the error of values of d, that the error in calculation by Eqs. (23) and (24) is within the limits of precision of the experimental results. It is also important that the points corresponding to fluorides, for example on the curve representing the variation of d as a function of the number of the element, Z [21], are practically on the same straight line as the points corresponding to other halides. This confirmation can be extended from F to Be (see Fig. 6) and to other elements of the second period. At the same time, it can be seen that equations of the type of (23) and (24) eliminate a certain nonlinearity in the relationship, $d = f(Z)$, for the elements of groups III (IV) - VI.

Equations (23) and (24) are examples of the approximate relationship,

$$d_{II} = A_1 d_I + B \tag{25}$$

between the interatomic distances in two groups of related elements; this relationship represents a particular example of the first method of comparative calculation (see [2], for example). The fact that in (23) and (24) the value of the coefficient, A_1, is close to unity is due to the closeness of the properties of the elements in the different groups being compared; this also explains the fact that the point corresponding to MeF falls on the common straight line.

In particular cases, Eq. (25) can be used also to increase the precision of the results in determining d. Thus, it makes it possible to reveal the lack of precision and the contradiction between the values of d, summarized in [12], for some compounds of the lithium subgroup. One can assume in particular that the most precise value of d_{Cs-Cl} is between the values found in the literature, 2.88 A [21], and 3.06 A [22] (see [4]). The fact that the points fall satisfactorily on the straight line, $d_{Me-H} = f(d_{Me-Br})$, indicates that the properties of the hydride and the halides are close; on the other hand, the difference between the hydrides and the halides is revealed by the fact that for the hydrides the value of the coefficient, A_1, differs considerably from unity.

2

Comparison of the values of d in several groups of similar substances is of considerable interest, especially if these values are reliable and from one laboratory. This comparison is possible due to a summary of results [23] obtained by Akishin and co-workers [13-17]. From this comparison one can not only predict new values but see clearly that the value of d for a series of similar substances forms a system of values. This system of values is illustrated in Fig. 7, using the values of d from [13-17] for halides of the elements of the beryllium subgroup. This figure also shows the values concerning the hydrides, illustrating their similarity to fluorides, and also values for cadmium [18] and zinc [19] halides, illustrating the difference between them and the halides from the beryllium subgroup: a different slope of the straight line and the fact that the points for the fluorides do not lie on the curve.

From this comparison, we can draw a few conclusions. For all molecules (probably with the exception of BeF_2) the results of the calculation according to Eq. (25) are within the limits of the experimental error, indicated by the height and width of the rectangle surrounding the point. If the values of $d_{Be-F} = 1.36$ and $d_{Be-Cl} = 1.7$ A given in [12] are correct, the same cannot be said of the values of $d_{Ca-F} = 2.02$, or particularly of $d_{Ca-Cl} = 1.86$ A, from the same publication. Figure 7 makes it possible to calculate the value for d_{Mg-I}, which equals 2.53 A. *

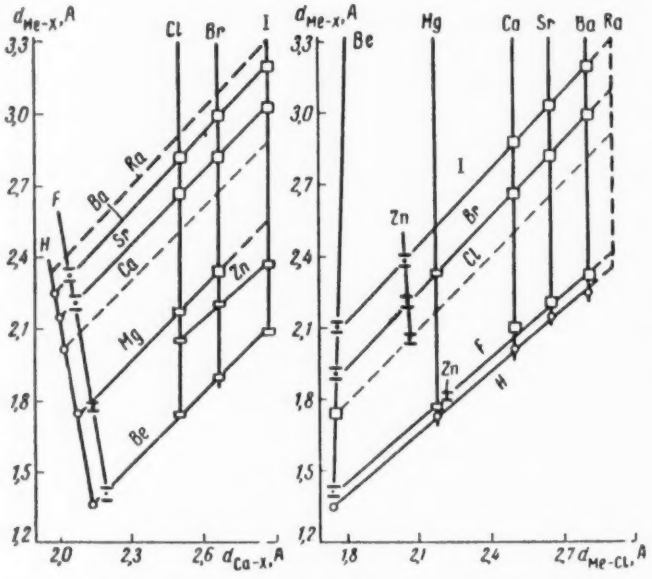

Fig. 7. Relationship between the interatomic distances, d_{Me-X}, for gaseous halides and hydrides of elements of the beryllium subgroup, and also for zinc.

Figure 8 represents the relationship between the values of d for the halides of the carbon subgroup. The diagram was drawn mainly on the basis of the values given in [25]; other values were taken from [12] and [26]. Aside from the value for d_{E-X} (X, F, Cl, Br, I) we have also drawn the value of d for hydrides, metal-metal compounds, CH_3-X, and also for Pb^{**} and Sn^{**}. This diagram shows that the deviation from the additivity of the interatomic distances of the elements of group IV is considerably larger than for the elements of group II. The fact that the compounds C-X and Me-F do not follow the straight line is due to the fact that the compounds

* After completion of this work the authors became acquainted with the investigation [24], in which it was found experimentally that $d_{Mg-I} = 2.52 \pm 0.03$ A; (determination of this value according to the curve, $d = f(Z)$ [21], gives $d_{Mg-I} = 2.54$ A).

of C and F are the first elements in the series of similar compounds. It must be noted that the straight line representing the value of $\underline{d}$ given here for the compounds Me-F is approximate, since the points corresponding to different metals can be considered as belonging to the straight line only in the first approximation. A deviation from the straight line for $Pb^{\cdot\cdot}$ and $Sn^{\cdot\cdot}$ indicates that their properties differ from the properties corresponding to the quadrivalent cations. Figure 8 shows that $d_{Pb-Br} \approx 2.58$, $d_{Pb-I} \approx 2.77$, $d_{Sn-Sn} \approx 2.75$, and the most precise value of d_{Si-Br} is apparently close to 2.20, d_{Ge-C} to 1.95, d_{Ge-Br} to 2.27, and d_{Sn-Br} to 2.50 A.

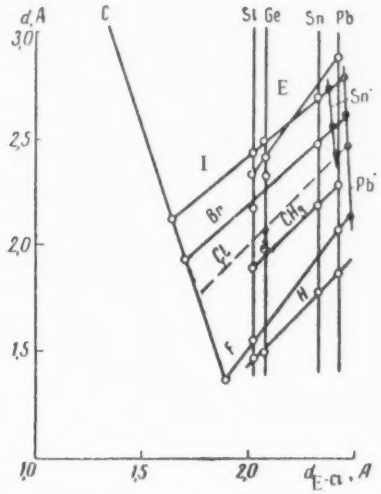

Fig. 8. Relationship between interatomic distances for some gaseous compounds of the carbon subgroup.

Similar results are obtained for the compounds of group V. However, the insufficient number and uncertainty of the values of $\underline{d}$ (see [26], for example) do not allow us to treat these data by the method described.

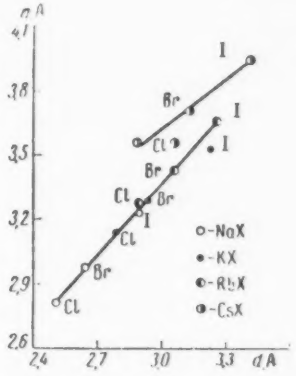

Fig. 9. Relationship between the constants, $\underline{a}$, of the crystal lattice and the interatomic distances, d_{Me-X}, for some halides of the lithium subgroup in the gaseous state.

The similarity between the $Pb^{\cdot\cdot}$ and $Sn^{\cdot\cdot}$ compound is seen much more clearly from the curve, $d_{Sn^{\cdot\cdot}-X} = f(d_{Pb^{\cdot\cdot}-X})$. If we had drawn this graph according to the values recommended in [27] and [28] we would have obtained results similar to those represented in Fig. 8.

3

In some cases the method of comparative calculation makes it possible to evaluate $\underline{d}$ for a whole series of elements. We shall illustrate this with the example of radium halides for which we shall use the second method of comparative calculation (see [3], for example) in the form:

$$d = A_2 a + B_2, \tag{26}$$

in which $\underline{a}$ is a lattice constant of the corresponding crystalline compound. A comparison according to this equation has a meaning, of course, only under the condition that the substances compared are isostructural. This assumption is illustrated by the data in Fig. 9. For Na, K, and Rb halides the points follow practically a straight line* while the points corresponding to CsX fall on the side. This is due to the fact that CsCl, CsBr, and CsI are crystallized with a different coordination. This graph (as well as the graph of $d_{Me-Cl} = f(d_{Me-Br})$ indicates also that the value of d_{Cs-Cl} is between those given in [4] and is closer to the first of them.

* The fact that the point corresponding to KI is out of line is probably due, to a considerable degree, to the error in the value of d_{K-I} [4].

Returning now to the problem of evaluating d_{Ra-X}, we shall use the Ca-Ra group of fluorides, since they are isostructural [4]. Therefore, we can apply Eq. (26) to them, according to which

$$d_{Me-F} = A_2 a_{MeF_2} + B. \quad (27)$$

By extrapolation we found $d_{Ra-F} \approx 2.4$ A. Using this value and Fig. 7, we determined that $d_{Ra-Cl} \approx 2.92$, $d_{Ra-Br} \approx 3.1$, $d_{Ra-I} \approx 3.3$, and $d_{Ra-H} \approx 2.35$ A.

It is well known that interatomic distances depend on the type of bond, which is determined by the different valence states of the atoms [29]. It was determined [29] that there exists a relationship between the interatomic distances and the valence states of the carbon atoms in different compounds; the interatomic distance decreases when the "tetrahedral system" of valences of the carbon atom is replaced by a "plane" or "linear" system of valences.

In this case, we can also use Eq. (25). This can be seen from Fig. 10, drawn according to values obtained in [20]. The fact that in this case the atoms are the same and only the type of bond is different leads to the possibility of using in Eq. (25), $B_1 \approx 0$, i.e., using the equation:

$$d = A_1 d_{>C-X} \quad (28)$$

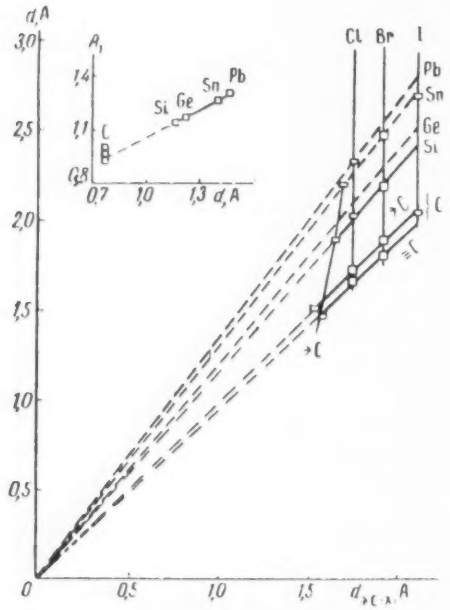

Fig. 10. Relationship between the values of d_{E-X} for some gaseous compounds of the carbon subgroup.

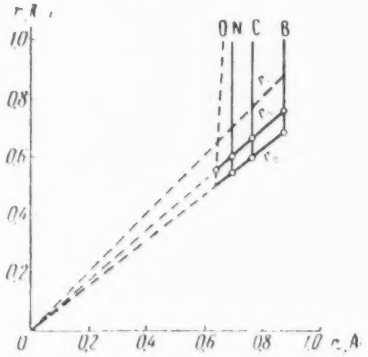

Fig. 11. Relationship between the covalent radii of some elements of the second period.

Although in the majority of cases the difference between $d_{>C-X}$, $d_{=C-X}$ and $d_{\equiv C-X}$ is only slightly greater than the experimental error of these values, there is no question of the validity of Eq. (28). Figure 10 shows that the value of the constant, A_1, in this equation varies regularly.

The existence of similar regularities in the relationship between covalent radii, r, and the binding multiplicity factor is seen in Fig. 11.

SUMMARY

1. We have described some approximate relationships between interatomic distances in a series of similar molecules which are particular cases of two methods of comparative calculation.

2. We have calculated the approximate value of interatomic distances, d, in a gaseous molecule for the following previously uninvestigated compounds: Ra-Cl (2.92), Ra-Br (3.1), Ra-I (3.3), and Ra-H (2.35), $Sn^{\cdots\cdot}$ - $Sn^{\cdots\cdot}$ (2.75), $Pb^{\cdots\cdot}$-Br (2.58), $Pb^{\cdots\cdot}$ - I (2.77 A). More precise values of d were found for: Si-Br (2.22), Ge-Br (2.27), $Sn^{\cdots\cdot}$ - Br (2.50), and Ba-H (2.17 A).

LITERATURE CITED

1. M. Kh. Karapet'yants, Doctoral Dissertation [in Russian] (Khim.-Tekh. Inst. im. D. I. Mendeleev, Moscow, 1957).
2. M. Kh. Karapet'yants, Zhur. Fiz. Khim. 27, 775, 934 (1953); 28, 1136 (1954); 29, 938, 1328 (1955); 30, 593, 2218 (1956); 32, 949 (1958); Neft. Khoz., 4, 66 (1955); Tr. D. I. Mendeleev Khim. Tekh. Inst. 19, 17 (1953); 23, No. 3 (1954); 25, No. 3 (1957); Zhur. Obshch. Khim. 27, 3379 (1957).*
3. M. Kh. Karapet'yants, Zhur. Fiz. Khim. 28, 353 (1954); 29, 938, 1328 (1955); 30, 1104 (1956).
4. B. F. Ormont, Structure of Inorganic Substances [in Russian] (Gostekhteoretizdat, Moscow-Leningrad, 1950).
5. Collection: Actinides, Ed. by G. Siborg and J. Katz [Russian translation] (IL, Moscow, 1955).
6. E. S. Makarov, Zhur. Neorg. Khim. 5, 1079 (1958).
7. P. I. Kripyakevich and E. I. Gladyshevskii, Doklady Akad. Nauk SSSR 95, 525 (1954).
8. G. Giesecke and H. Pfister, Acta Cryst. 11, 369 (1958).
9. D. H. Temleton and G. F. Carter, J. Phys. Chem. 58, 940 (1954).
10. H. A. Eick, J. Am. Chem. Soc. 80, 43 (1958).
11. V. M. Kozhin and A. I. Kitaigorodskii, Zhur. Fiz. Khim. 29, 1897 (1955).
12. T. Cottrell, Strength of Chemical Bonds [Russian translation] (IL, Moscow, 1956).
13. P. A. Akishin, V. P. Spiridonov, and G. A. Sobolev, Doklady Akad. Nauk SSSR 118, 1134 (1958).*
14. P. A. Akishin, et al., Zhur. Fiz. Khim. 31, 461 (1957).
15. P. A. Akishin, V. P. Spiridonov, and G. A. Sobolev, Zhur. Fiz. Khim. 31, 648 (1957).
16. P. A. Akishin, et al., Zhur. Fiz. Khim. 31, 1871 (1957).
17. P. A. Akishin, et al., Zhur. Fiz. Khim. 32, 58 (1958).
18. P. A. Akishin, et al., Zhur. Fiz. Khim. 30, 155 (1956).
19. P. A. Akishin, L. V. Volkov, and V. P. Spiridonov, Doklady Akad. Nauk SSSR 101, 77 (1955).
20. P. A. Akishin, V. P. Spiridonov, and V. A. Naumov, Zhur. Fiz. Khim. 30, 951 (1956).
21. R. G. Luce and J. W. Trischka, J. Chem. Phys. 21, 105 (1953).
22. P. W. Allen and L. E. Sutton, Acta Cryst. 3, 46 (1950).
23. P. A. Akishin and V. P. Spiridonov, Kristallografiya 2, 475 (1957).
24. P. A. Akishin and V. P. Spiridonov, Zhur. Fiz. Khim. 32, 1682 (1958).
25. V. M. Tatevskii, Uch. Zap. MGU 174, 235 (1957).
26. M. E. Dyatkina, Zhur. Fiz. Khim. 20, 7 (1946).
27. P. A. Akishin, V. P. Spiridonov, and A. N. Khodchenkov, Zhur. Fiz. Khim. 32, 1679 (1958).
28. M. Lister and L. Sutton, Trans. Faraday Soc. 37, 406 (1941).
29. V. M. Tatevskii, Doklady Akad. Nauk SSSR 101, 901 (1955).

* Original Russian pagination. See C. B. translation.

MUTUAL ORIENTATION OF WATER MOLECULES IN IONIC SOLUTIONS AND SALTING-OUT OF NONELECTROLYTES

Yu. V. Gurikov

V. G. Khlopin Radium Institute, Academy of Sciences of the USSR, Leningrad
Translated from Zhurnal Strukturnoi Khimii, Vol. 1, No. 3, pp. 286-304, September-October, 1960
Original article submitted February 25, 1960

This work is devoted to the investigation of phenomena of disorder in the structure of water in ionic solutions. It is assumed that when water is condensed and a network of hydrogen bonds is formed, a redistribution of electron density in the molecule and the hydrogen bridge occurs, which is equivalent to the appearance of a dipole whose positive end is located at the proton, while its negative end lies in the center of the electron cloud corresponding to the unshared electron pair of the oxygen atom in the neighboring molecule. A specific disruptive action of "hydrogen dipoles" on the structure of water in the electrostatic field of an ion has been found. The theory is applied to the calculation of the structural contribution to salting-out coefficients. Good agreement is achieved with experimental values of the salting-out coefficients of benzene and the changes in the height of energy barriers separating equilibrium positions of water molecules in pure water and ionic solutions (which, as Samoilov showed, are the principal characteristic of the inner hydration of ions), if the "inherent dipole moment of the hydrogen bond" is taken to be 0.83 D.

Works on the molecular-theoretical analysis of salting-in – salting-out phenomena may be divided into three groups. In the first group of works [1] salting-out is connected with dielectric polarization in the ion field. In these theories the solvent (water) is regarded as a continuous medium. The free energy of solvation is calculated on the basis of formal electrostatics. A great number of facts contradict the indicated theories. It is impossible to confirm unambiguously the proposed theory of inverse proportionality between the salting-out coefficient* and the "average ionic radius," although general tendencies – increase of salting-out capacity with increase of charge and decrease of ionic radius – are confirmed by experiment (see, for instance, [2]).

In the second group of works the contraction of water on solution of ionic salts in it, leading to increase of the internal pressure in the solution, is taken into account. In a recent work [3], however, where this point of view is developed, very high values of the salting-out coefficients are obtained.

Finally, a generalization [4] of the electrostatic theory of salting-out, taking into account the action of noncoulombic (dispersion) forces between ions and molecules of the solvent and the nonelectrolyte being salted out, like the theory of McDevitt and Long, correctly predicts the sign of the effect but leads to salting-out coefficients which are one-third to one-half the actual values.

* The proportionality coefficient in the Sechenov equation $\log f = K_S C_S$, where f is the activity coefficient of the nonelectrolyte in a salt solution of concentration C_S moles/liter.

None of the enumerated theories takes note of the molecular nature of the solvent and its structure. In the present article an attempt is made to estimate the order of magnitude of structural influences on the salting-out coefficients, proceeding from modern ideas on the structure of water.

If nonlinear concentration effects (interionic interaction, overlapping of ionic spheres of influence) are avoided, i.e., if sufficiently dilute solutions are considered, the analysis of salting-in – salting-out phenomena naturally falls into two parts: 1) investigation of the interaction of ions with water molecules and the influence of ions on its structure; 2) study of the changes that occur when neutral molecules are added to water.

The latter group of questions was discussed qualitatively by Frank and Wen [5]. Here we confine ourselves to the analysis and estimation of effects connected with the action of inorganic ions on the structure of water. Unfortunately, the quantitative theory of the thermodynamic properties of water is not sufficiently developed as yet. One variant of this theory, which, though by no means complete or exact, permits a satisfactory approach to the analysis of phenomena connected with changes in the structure of water in ionic solutions, is proposed in Section 1. These questions are discussed in Section 3, special attention being paid to ascertaining the role of distant effects of disorder, determined by the specific properties of the hydrogen bond (Section 2). In Section 4 the concepts developed are applied to the investigation of salting-in – salting-out phenomena.

Thermodynamic Properties and Order of Water in the Liquid State

Modern ideas on the tetrahedral structure of water were developed qualitatively by Bernal and Fowler [6]. An extensive review of various approaches to the calculation of the interactions and distribution of water molecules is given in Samoilov's monograph [7].

It is well-known that water molecules in ice have tetrahedral coordination and are so disposed that just one proton is located on each line connecting the centers of adjacent molecules. Thermal motion of the molecules may disturb this ideal order, since some of the adjacent molecules will be so oriented that either two protons or none are located on the oxygen–oxygen line. The number of such "irregular" configurations in ice is very small. According to Bjerrum's estimate [8], the proportion of these states does not exceed $3.4 \cdot 10^{-6}$. Besides intramolecular vibrations, water molecules in ice describe two main types of motion: 1) translational vibration within a cell whose walls are formed by the force fields of the neighboring molecules, and 2) small vibrations about various equilibrium orientations (restricted rotation or oscillation in Bjerrum's terminology [8]).

The transition from the solid to the liquid state leads to the appearance of new elements of disorder:

a) In the less-ordered liquid structure the number of "irregular" types of H–H and O–O neighborhoods may increase considerably.

b) A qualitative change in the character of the molecular oscillation is possible; in particular, Pople [9] introduced the concept of independent bending of the bonds* formed by a molecule in water.

c) The appearance of structures with coordination differing from that of the molecules in ice. Bernal and Fowler [6] presumed that three structures exist simultaneously in liquid water: ice-type (I), quartz-type (II), and close-packed (III). On the basis of investigations of the compressibility of water, Hall [11] developed a bistructural water model, according to which the ice-type and close-packed structures are simultaneously present in liquid water. Grjotheim and Krogh-Moe [12] developed a similar point of view in order to explain the volume anomaly of water. Recently, Mikhailov and Syrnikov [13] proposed a comparison of the ice-like and close-packed structures determined formally by Hall, with the obvious model of the tetrahedral structure with partly filled voids. The possibility of explaining the peculiarities of the radial distribution functions of water, obtained from x-ray data, and other anomalous properties of water by the filling of voids in the structure, was pointed out long ago by Samoilov [14].

* The concept of independent bending of bonds in the liquid state is not wholly consistent with the results of Fox and Martin [10], who studied the infrared absorption spectra of ice and water. In this work, it was found that the intensity of the absorption band at about 1600 cm^{-1}, which is ascribed to deformation vibrations of the water molecule, increases with temperature. At the same time the width of this band decreases. These peculiarities may be explained by an increase in the number of molecules whose intramolecular vibrations are not excited by neighbors.

d) The appearance of vacant nodes in the tetrahedral lattice.

In calculations of thermodynamic properties it is essential to estimate correctly the potential interactions and changes of interaction energy with change in the relative positions of the molecules and their neighbors. At present a single point of view on the mechanism of bond breaking in water does not exist. Different authors interpret this concept differently and give different quantitative estimates of hydrogen-bond energy. With any of the above-listed methods of thermal disordering, probably, different types of interactions (hydrogen-bond, dipole-dipole, dispersion, repulsion interactions) change to a different degree.

In the present article only orientational disorder connected with the appearance of "irregular" types of H−H and O−O neighborhoods in liquid water are considered. Here, we do not confine ourselves to a definite model of the water molecule and the nature of the hydrogen bond, but introduce a set of energy parameters ε_{HH}, ε_{OO}, $\varepsilon_{OH} = \varepsilon_{HO}$, which are contributions to the energy of interaction of a water molecule with its nearest neighbors in nodes of the tetrahedral lattice, from the corresponding types of neighborhoods; these parameters are so chosen as to obtain agreement with experimental data for the enthalpy and entropy of water.

Simplifying the actual situation somewhat, we shall consider the distribution $N_{HH} = x_{HH}N$, $N_{OO} = x_{OO}N$ and $N_{OH} = x_{OH}N + x_{HO}N$ of numbers of different types of H−H, O−O, and O−H, H−O neighborhoods (the symbol O−H corresponds to the case where the molecule under consideration is oriented by the oxygen atom to a proton of a neighboring molecule) out of 2N possible positions in a system of N water molecules, assuming that this distribution does not depend on the character of the vibratory and oscillatory motions described by the water molecules.

In the theory of free volume the statistical integral of a system of N water molecules may be represented in the form

$$Q = \left(\frac{2\pi mkT}{h^2}\right)^{3N/2} \psi^N \frac{G}{G_0} v_f^N \exp\left(-E/kT\right). \tag{1.1}$$

Here ψ is the function of state, corresponding to intramolecular vibrational degrees of freedom. At room temperature $\psi \sim 1$ and is practically independent of temperature. Therefore, the contribution of vibrational degrees of freedom of the water molecule to the thermodynamic properties may be neglected [8].

The free energy of water F = − kT ln Q is determined in conformity with Eq. (1.1) by three main factors:

1) The configuration factor G/G_0, for which, as a quasichemical approximation, one may put [15]*

$$\frac{G}{G_0} = \frac{(N/2)!}{N_{HH}!} \cdot \frac{(N/2)!}{N_{OO}!} \cdot \frac{(N/2)!}{N_{OH}!} \cdot \frac{(N/2)!}{N_{HO}!}.$$

2) The potential factor exp (− E/kT), where E is the potential energy of interaction of N water molecules located in their average positions in nodes of the quasicrystal lattice:

$$E = N\left(x_{HH}\varepsilon_{HH} + x_{OH}\varepsilon_{OH} + x_{HO}\varepsilon_{HO} + x_{OO}\varepsilon_{OO}\right).$$

The energy parameters ϵ are functions only of the system density.

3) The free volume v_f simultaneously takes into account many influences: a) vibration and oscillation of the molecules about equilibrium positions in lattice nodes; b) distortion of the regular tetrahedral structure as a result of thermal motion of the molecules (bending of bonds according to Pople, fluctuations of the coordination number, and the like); c) the interrelation between vibratory motion of the molecules and orientational disorder.

* The normalizing factor G_0 is so determined that $G/G_0 \to 1$ as $T \to \infty$, when the distribution of protons with respect to bonds becomes disordered and $N_{HH} = N_{OO} = N_{OH} = N_{OH} = N/2$.

An exact description of the latter relation would be very difficult. As a very simple, rough estimate, however, an approximate expression of the free volume through $x_{OH}, x_{HO}, x_{HH}, x_{OO}$, analogous to the free-volume approximation in hole theories of simple liquids [16], may be used:

$$\ln (v_f / v) = g_{HH} x_{HH} + g_{OH} x_{OH} + g_{HO} x_{HO} + g_{OO} x_{OO}.$$

The g coefficients depend on the density and to a slight degree on the temperature.

Thermodynamically, the equilibrium distribution of protons with respect to bonds, characterized by the "concentrations" x of different types of neighborhoods will be found from the condition of minimum free energy. In this case, the conditions of normalization $x_{HH} + x_{OH} = 1$ and symmetry $x_{HH} = x_{OO} = 1 - x$, $x_{HO} = x_{OH} = x$. must be fulfilled.

The temperature and volume dependence of x (the proportion of hydrogen bonds) is given by the equation

$$\left(\frac{x}{1-x}\right)^2 = \exp [q - (\varepsilon/RT)], \tag{1.2}$$

where $q = q_{OH} - (q_{OO} + q_{HH})/2$ and $\varepsilon = 2\varepsilon_{OH} - \varepsilon_{HH} - \varepsilon_{OO}$.

Now the temperature and volume dependence of any thermodynamic property of water may be calculated from Eq. (1.1) if it is known how ϵ depends on the density and q on the temperature and density. In particular, for the internal energy and entropy of water, we obtain

$$\bar{E} = \frac{3}{2} RT + x\varepsilon + RT^2 \left(\frac{\partial \Phi}{\partial T}\right)_v + RT^2 x \left(\frac{\partial q}{\partial T}\right)_v + \text{const}\,(v),$$

$$S = \frac{3}{2} R \ln T + Rqx + R \ln (G/G_0) + RT \left(\frac{\partial \Phi}{\partial T}\right)_v + RTx \left(\frac{\partial q}{\partial T}\right)_v + \text{const}\,(v),$$

$$\ln (G/G_0) = -2 \ln 2 - 2(1-x) \ln (1-x) - 2x \ln x,$$

where $\Phi = (g_{OO} + g_{HH})/2$.

Our equations contain four unknown parameters: ϵ, q and the derivatives $(\partial\Phi/\partial T)$ and $(\partial q/\partial T)_v$. We developed a special method of successive approximations in order to calculate the temperature and volume dependence of unknown parameters from experimental data for the enthalpy and entropy of liquid water.

It can be shown that the contribution of the configuration term $R \ln (G/G_0)$ to the entropy is about 5% of the contribution to the enthalpy, which is proportional to x. In the first approximation, therefore, one may write for two arbitrarily chosen temperatures T_1 and T_2:

$$\varepsilon \{x(T_2) - x(T_1)\} = \bar{E}(T_2) - \bar{E}(T_1) - \frac{3}{2} R (T_2 - T_1) - R (T_2^2 - T_1^2) \zeta \equiv \alpha;$$

$$Rq \{x(T_2) - x(T_1)\} = S(T_2) - S(T_1) - \frac{3}{2} R \ln \frac{T_2}{T_1} - R (T_2 - T_1) \zeta \equiv \beta,$$

where $\zeta = (\partial\Phi/\partial T)_v + x (\partial q/\partial T)_v$.

For known values of T_1, T_2, and v and with fixed ζ, values of α and β are calculated from experimental data for the enthalpy and entropy of liquid water [17]. From (1.3) we obtain $\epsilon / Rq = \alpha / \beta$, this ratio being known. Now the first of Eqs. (1.3) contains only one unknown parameter ϵ, since, according to (1.2), x(T) depends only on q and ϵ. This equation was solved graphically.

We carried out quantitative calculations for the specific volume 1.0018 cm^3/g. Water has this specific volume under atmospheric pressure at 20°. We took 0° and 20° for T_1 and T_2 in Eqs. (1.3). The relation between the parameters figuring in our equations, and ζ, is given in Table 1. For these same values of ζ the enthalpy of water at 60° was calculated (Table 2), ζ and q being regarded as constant in the temperature

interval under consideration. Calculated values of H vary linearly with respect to ζ. Finally ζ is so chosen that the calculated enthalpy coincides with the experimental value, 1.21 kcal/mole at 60°. This value of $\zeta = -0.0104$ (Table 2). In Fig. 1 are shown several calculated values of the enthalpy of liquid water for $\zeta = -0.0104$ and the somewhat lower value $\zeta = -0.0110$. The solid curve is drawn from experimental data [17]. At $\zeta = -0.0104$ the calculated values of enthalpy at several temperatures in the interval 0-60° agree excellently with experiment.

TABLE 1

$-\zeta$	$-\varepsilon$, kcal/mole	$-q$
0,010	7,51	10,4
0,011	8,18	11,2
0,012	9,20	12,4
0,0104	7,82	10,75

TABLE 2

ζ	H, kcal/mole
—0,010	1,16
—0,011	1,28
—0,012	1,40
—0,0104	1,21

In the next approximation the difference $\Delta\beta$ between values of R ln (G/G_0) for 0 and 20° must be calculated by using the determined parameters ϵ and q, the new value $\beta' = \beta - \Delta\beta$ being obtained. The entire procedure is repeated for this β', etc. However, these calculations are very laborious. Therefore, we confine ourselves here to the first approximation. As a consequence of this, the calculated entropy at 60° is 30% higher than the experimental value. Thus, the results obtained must be regarded as rough estimates.

TABLE 3

Percentage of Bonds Broken in the Fusion of Ice

Cross, Burnham, and Leighton [18]	50	Taft and Sisler [21]	11
Ewell and Eyring [19]	44	Lagunov [22]	10
Grjotheim and Krogh-Moe [12]	33*	Haggis, Hasted, and Buchanan [23]	9
Pauling [20]	15	Pople [9]	0
Our work	14		

* Grjotheim and Krogh-Moe considered a bistructural model of water and identified the proportion of the close-packed structure, which they estimated from density data, with the proportion of broken bonds. We calculated this quantity again, assuming that half the bonds are retained in the close-packed structure. These data are given in Table 3 and Fig. 2.

The change in the structure of water and its thermodynamic and other properties on melting is connected by several authors with the breaking of hydrogen bonds. Since, practically, $x_{HH} = 0$ in the solid state, the value of x_{HH} may be regarded as the proportion of bonds broken on melting. We calculated the temperature dependence of x_{HH} by means of Eq. (1.2) and the data of Table 1. From these calculations it follows that 13.8% of the bonds are broken on melting. In Table 3 this result is compared with the data of other authors.

Table 3 shows that all estimates are divided into two groups: 10-15% and 30-50%. It is interesting to note that the higher estimates were obtained through analysis of properties (viscosity [19], density [12]) for which mechanisms of disordering (filling of voids in the structure, appearance of vacant nodes in the lattice) which we did not take into account are very important. The lower values were obtained through analysis of the dielectric properties of water and ice [22, 23]. Pople [9], who in principle does not consider the possibility of bond breaking, notes that a high percentage of broken bonds is incompatible with the high dielectric constant of water. Apparently, the passing of a water molecule into a void in the structure is accompanied only by a change in the character of the bond (transition from a covalent hydrogen bond to dipole-dipole interaction [24]). The strong orientational correlation inherent in the ice-like structure is weakened in this case, probably

to an insignificant degree. This conclusion is consistent with the great number of broken bonds in water, found by Cross, Burnham, and Leighton [18], who studied the Raman spectrum of water, if the shift of bands in the vibration spectrum of liquid water is ascribed to the appearance of a partly covalent bond between hydrogen and oxygen atoms of neighboring molecules.

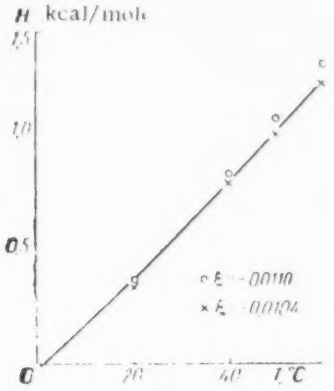

Fig. 1. Enthalpy of water for v = = 1.0018 cm^3/g. Standard state (H = 0): liquid water at 0° in equilibrium with the solid phase.

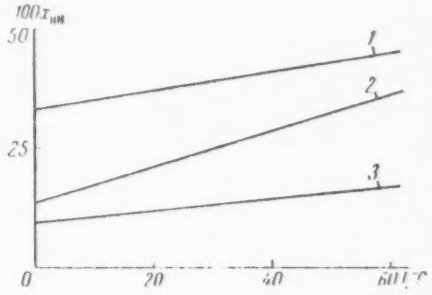

Fig. 2. Percentage of broken bonds in water: 1) Grjotheim and Krogh-Moe [12]; 2) our work; 3) Haggis, Hasted, and Buchanan [23].

Values of the temperature dependence of the percentage of broken bonds, obtained by Haggis, Hasted, and Buchanan [23], Grjotheim and Krogh-Moe [12], and by us, are compared in Fig. 2. In all cases, the temperature dependence proved to be almost linear between 0 and 60°

TABLE 4

Energy of the Hydrogen Bond (kcal/mole)

Rowlinson [25]	4.86	Our work	3.9
Pauling [20]	4.5	Cross, Burnham, and Leighton [18]	3.0
Taft and Sisler [21]	4.25	Grjotheim and Krogh-Moe [12]	2.6

It is of interest to estimate the energy of the hydrogen bond by means of our values of the parameter $\varepsilon = 2\varepsilon_{OH} - \varepsilon_{HH} - \varepsilon_{OO}$. For different types of neighborhoods the quantities ϵ are the result of addition of interactions of different nature. In the absence of a specific hydrogen bond having a sharply directional character, it would follow from the requirement of spherical symmetry that $\epsilon \sim 0$. Therefore $\epsilon/2$ may be regarded as the energy of the hydrogen bond proper. Various estimates of this quantity are compared in Table 4. Here also is observed a clear division into two groups: 4.5 kcal/mole and 3 kcal/mole.

2. Structure of the Water Molecule and the Nature of the Hydrogen Bond

An exact expression for the electrostatic interaction energy of an ion and the system of water molecules surrounding it can be written only if the charge distribution in the molecule is known. The question of the relative position of the two protons and the oxygen nucleus may be considered solved [7]: on the basis of study of the infrared spectrum of water vapor, it may be concluded that the three nuclei are located at the vertices of an isosceles triangle. The oxygen – proton distance is 0.96 A, and the interbond angle is 105°.

Unfortunately, there are practically no data on the real electron-density distribution in the water molecule. In early works [20] the entire dipole moment of the water molecule was ascribed to the partly ionic character of the O–H bond. If a dipole moment of 1.54 D is ascribed to each O–H bond, it may be said that each of the protons bears a concentrated charge of 0.33 e, which is compensated by a total charge of – 0.66 e on the oxygen. At various times somewhat similar point charge models were proposed. In order to take into account

displacement of the center of the electron shell surrounding the oxygen atom in the field of the protons, Bernal and Fowler [6], assuming a triangular arrangement of charges, put a charge of 0.5 e on the proton and at the same time shifted the negative charge 0.15 A inside the triangle. In the model of Fervei [26] a positive charge of 6 e on the oxygen nucleus and 0.5 e each on the two protons is compensated by a negative charge of − 7e, located on the axis of the molecule within the triangle. Campbell [27] held that concentration of the entire negative charge at one point leads to considerable overestimation of the higher multipole moments, and put two negative charges of 0.37e on each line of the O−H bond, at a distance of 0.054 A from the oxygen nucleus. On the other hand, Rowlinson [25] showed that certain structural peculiarities of ice can be explained by assuming that the negative charge on the oxygen atom is divided into two charges located on a line perpendicular to the plane of the nuclear triangle, and at a distance of 0.5 A from one another. The only requirement which the described model must meet consists in obtaining the observed dipole moment of 1.87 D. However, this problem admits of many solutions. The situation is further complicated by the fact that none of these models unambiguously determines thermodynamic characteristics, with the observed values of which a comparison can be made. With the appropriate choice of parameters for interactions of a nonelectrostatic nature, any of these models leads to relatively good agreement with experiment.

Complete information on the electron-density distribution in the water molecule can be obtained in principle by means of quantum-mechanical theory. It is generally known that, of the ten electrons in the water molecule, the two 1 s electrons of the oxygen atom practically are not excited when the molecule is formed, whereas four electrons take part in two σ-bonds with protons. Pople [28] showed that the remaining four nonbonding electrons are disposed in pairs in hybrid orbitals forming approximately tetrahedral angles with each other and with the O−H bonds. The existence of the regular tetrahedral structure of ice confirms this conclusion. Bjerrum [8] obtained good agreement with experimental values of the heat of sublimation and the temperature variation of the heat capacity of ice, for a symmetrical model of an equilateral tetrahedron at whose corners positive and negative charges of 0.17 e are located. Pople [28] was the first to take note of the fact that the unshared electrons of the oxygen atom play an important part in determining the dipole moment of the water molecule, since the centers of the electron clouds corresponding to the unshared electrons are quite distant from the oxygen nucleus. Coulson [29] showed that the simple conception of ionic-covalent resonance, in which the influence of nonbonding electrons in the oxygen atom is not taken into account, may lead one to overestimate seriously the contribution of the ionic structure to the dipole moment of the O−H bond. Recently, the results of quantum-mechanical calculations of the dipole moment of the water molecule were published [30], based on wave functions [31] more exact than those available earlier. These calculations lead to rather unexpected conclusions on the electron-density distribution in the water molecule. It was found that practically all the observed dipole moment is due to the atomic dipole moment of oxygen, the polarity of the O− H bond being exceedingly low. The corresponding dipole moment is equal to 0.16 D instead of the value of 1.54 D, usually ascribed to the O−H bond. Thus, the triangular models described above contradict the exact theory.

The results of Burnell and Coulson [30] make necessary a different approach to hydrogen-bond theory. As is generally known [32], the simple electrostatic conception of the hydrogen bond [8, 20, 25, 27, 33] is not adequate to explain the principal manifestation of the latter − the shift of valence vibration frequencies in the infrared spectra toward the long-wave region. The correct sign of frequency shift is obtained only if it is assumed that a donor-acceptor bond appears between a hydrogen atom of one molecule and the oxygen atom of a neighboring molecule as a result of overlapping of the wave functions of an unshared electron pair and the electron of the hydrogen atom. A prerequisite for the appearance of a donor-acceptor bond is a sufficiently high positive charge concentrated on the hydrogen atom [32]. Since, as Burnell and Coulson showed, the polarity of the O−H bond is very slight, Aleksandrov and Sokolov [34] recently suggested that considerable polarization of the O−H bond occurs in the process of hydrogen-bond formation. Polarization of the electron cloud about the oxygen atom of the neighboring molecule occurs simultaneously [35]. Moreover, it may be thought that the appearance of a positive charge on the protons causes additional deformation (change in the degree of s− p hybridization) of the electron cloud of this same water molecule, produced by the two unshared electron pairs of the oxygen atom, which is expressed in a certain decrease in the atomic dipole moment. Thus, the formation of the hydrogen bond is accompanied by drastic redistribution of the electron density in the water molecule. If, it is assumed that the final charge distribution coincides with the highly symmetrical distribution suggested by Bjerrum [8], we come to the conclusion that the formation of a hydrogen bond between initially free water molecules is equivalent to the appearance of a dipole whose positive end is located at the proton, whereas its negative end

lies in the center of the deformed electron cloud formed by an unshared electron pair of the oxygen atom. In the following paragraphs, it will be shown that with the proper choice of "inherent dipole moment of the hydrogen bond" this hypothesis makes it possible to explain and to connect satisfactorily a great number of facts.

3. Influence of Ions on the Degree of Order in Water

Analysis of the phenomena occurring when salts dissolve in water leads to a very complex picture. There are a number of facts which make it possible to bring out the existence of specific effects connected with the change in the structure of the solvent near the ions.

Very often, especially in early works, concepts of ion hydration were employed in order to interpret the results of investigation of various properties of ionic solutions (ionic mobility, density, compressibility, entropy, vapor pressure, salting-out, etc.). However, hydration numbers determined by various methods do not agree with each other but lie in a very wide range (0-1000). Bockris [36] suggested that one distinguish primary hydration, consisting in binding of the nearest water molecules by the ion, and secondary hydration, due to interaction of the ion with more distant molecules. In a number of works by Samoilov [7] is developed a detailed, dynamic picture of exchange of water molecules between the layer next to the ion and the remaining mass of "free" water, and it is shown that concepts of strong binding of water in the hydration shell of the ion cannot give a comprehensive description of all the observed phenomena. It was found that some ions (e.g., Cs^+, I^-) increase the mobility of the nearest water molecules (negative hydration).

In order to describe the structural changes of the solvent in ionic solutions, Bernal and Fowler [6] introduced the concept of structural temperature. Williams and Millet [37] analyzed the infrared spectra of salt solutions in a wide range of wavelengths and found, in conformity with Bernal and Fowler's point of view, that solution of a salt and increase in temperature shift the absorption-band maxima in the same direction. Such parallelism of changes is also found on investigation of the heat capacity of aqueous solutions [38]. Stewart [39] notes similar effects on consideration of the x-ray scattering, adiabatic compressibility, and density of ionic solutions, especially emphasizing that remote influences of ions on the structure of water are manifested here.

Frank and Evans [40] analyzed a number of experimental data of a thermodynamic nature (entropy of hydration, partial molar heat capacity) and came to the conclusion that, apart from the strong binding of water in the layer next to the ion as a result of electrostatic ion-dipole interaction, ions have a disorganizing effect on more distant water molecules, disrupting their intrinsic structure. By means of very rough approximate estimates these authors calculated the contribution from the effect of the change in the structure of water near ions to the entropy of hydration. With the exception of Li^+ and F^-, which strongly bind water molecules, remote interaction amounts to pure disruption of the structure of water by ions.

Frank and Evans come to the conclusion that three layers of water molecules must be distinguished near the ion: layer A of water molecules next to the ion, strongly bound owing to electrostatic ion-dipole interaction; layer B, where the water structure is less ordered than in the first, and the third layer C of the remaining mass of water, which does not undergo structural changes (apart from the "super-remote" effect of polarization of the medium). The contributions of layers B and C to the entropy of hydration have different signs and can compensate one another. The thicknesses of the first and second layers may be different for different ions. However, Frank and Evans hold that layer A of strongly bound water molecules always exists near ions of any nature. This differs from Samoilov's point of view, according to which negatively hydrated ions increase the mobility of water molecules next to the ion [41].

In a recent work by Frank and Wen [5] the complex picture of ion hydration, proposed earlier, is supported by a number of new experimental data (dielectric relaxation, diffusion, thermal conductivity). The question as to the reasons for the appearance of the anomalously disordered layer B is more difficult. Frank and Wen suggest a qualitative explanation which reduces to the following. Water molecules in layer B undergo two orienting influences: "one of them is the normal structural orienting influence of the neighboring water molecules" of layer C; "the other is the orienting influence of the spherically symmetrical ion field on the dipole." The latter influence predominates in layer A, and the former predominates in layer C. Frank and Wen write: "It is not unlikely that between A and C there is a region of finite width, in which much greater orientational disorder exists than in A or C." Gurney [42], taking a similar position, holds that considerable orientational disorder may appear even in layer A of water molecules next to the ion.

However, the given explanation raises objections. Actually, it is far more likely that the degree of order in the water, very high in layer A, steadily falls, reaching a limiting value corresponding to the degree of order of pure water at a sufficiently great distance from the ion (in layer C). Although the change in the orientation of individual molecules in pure water is complicated, nevertheless, the numbers of molecules oriented with the field and against it are the same on the average. In this sense, there is no difference between layer B and layer C. It seems to us that the remote effects of disorder of the structure of water in layer B, manifested on a background of the strong binding effect of the ionic electrostatic field on the dipolar water molecules, also are electrostatic in nature and cannot be explained by the disorganizing action of water molecules in layer C. A new explanation of the observed phenomena, based on concepts of special properties of the hydrogen bond (Section 2) manifested in the ionic electrostatic field, is proposed in the present article.

Orientation of Water Molecules in the Ionic Electrostatic Field. It is well known that the electrostatic interaction energy of two charge systems can be resolved into a series in multipole moments [43]. Confining ourselves to the first two terms of the expansion, we write, following Buckingham [44], the equation for the energy of electrostatic interaction of an ion with a water molecule thus:

$$E_{ion} = -\frac{Ze}{M}\left[\frac{\mu_{eff}}{r^2}\cos\varphi_z + \frac{1}{2r^3}\left\{\theta_a(3\cos^2\varphi_x - 1) + \theta_b(3\cos^2\varphi_y - 1)\right\}\right]. \quad (3.1)$$

Here r is the distance from the center of the ion, Ze is its charge, M the dielectric constant, and μ_{eff} the effective dipole moment of the water molecule; θ_a and θ_b are expressed through the diagonal components of the tensor of the quadrupole moment;* φ_x, φ_y, φ_z are the angles formed by the principal axes of the molecule and the direction of the ionic electrostatic field. The omitted terms, as well as interactions of a nonelectrostatic nature, diminish with distance as $1/r^4$ or even faster.

The drastic rearrangement of the electronic structure in the water molecule on formation of a hydrogen bond does not mean that molecules lose their individuality in the ice lattice. This is confirmed by Pauling's well-known calculation [20] of the residual entropy of ice, since the hypothesis of the equal probability of two possible positions of the proton on the oxygen – oxygen line is consistent with the results of neutron-diffraction investigations [45]. On the other hand, the electrical characteristics of the molecule may change considerably.

It is necessary to distinguish the inherent μ_0 from the effective dipole moment of the water molecule. The first depends on the electron density distribution within the molecule, and in liquid water may differ from the value 1.87 D, corresponding to a free water molecule in the vapor. The effective dipole moment determines the behavior of the molecule in an external electric field. Its value depends on the electron density distribution in the hydrogen bridge. If the formation of the hydrogen bond is equivalent to the appearance of a dipole with moment μ_H, then

$$\mu_{eff} = \mu_0 - t\mu_H\cos 54°, \quad (3.2)$$

where t is the number of hydrogen bonds formed by the molecule. It is easy to see that $\mu_{eff} \leq \mu_0$ regardless of the mutual orientations of the neighboring molecules.

The formation of a network of hydrogen bonds also changes the quadrupole moment of the individual molecules. Unfortunately, there are no experimental data on the quadrupole moment of the water molecule. Not having independent estimates, we shall therefore adhere to Bjerrum's symmetrical tetrahedral model [8]. In this case, $\theta_\sigma = 0$, and the only nonzero component of the quadrupole moment $\theta = \theta_a = -\theta_b$ is unambiguously determined by the value of the charge $\pm$ ql, concentrated on each corner of the tetrahedron, if $\theta = 6.28 \cdot 10^{-26}$ q. It should be noted that it is unnecessary to fix the value of q exactly, since the combination

* $\theta_b = \theta_{zz} - \theta_{yy}$ characterizes the division of charges in the plane of the nuclear triangle, whereas $\theta_a = \theta_{zz} - \theta_{xx}$ characterizes that in the perpendicular plane containing the centers of the electron clouds corresponding to unshared electron pairs of the oxygen atom. The sum $\theta_\sigma = \theta_a + \theta_b$ is a measure of the electrical asymmetry of the molecule: the more symmetrical the charge distribution is, the less is θ_σ.

q/M figures in all equations. It is customary to assume that the dielectric constant near the ion is different from the macrodielectric constant. Recently Rudakov [46] demonstrated that this is a general property of associated liquids. There is no established point of view with respect to the value of the microdielectric constant of water. Sometimes M is regarded as a function of the distance from the ion [47]. It is more convenient to use the average constant value of M. Samoilovich and Goryunov [48] arbitrarily set M = 20. Pasynskii [49] showed that the Debye equation for the compressibility of salt solutions agrees with experiment if M is set at about 10. In the main calculations, we used q/M = 0.017 , which corresponds to M = 10 and $\underline{q}$ = 0.17.

In order to simplify the analysis, we shall assume that the water molecule takes up several discrete orientations in space with respect to the ion. Four pairs of configurations having the same energy may be distinguished. They are shown in Fig. 3. Configurations 1 and 3 are characterized by the fact that the dipole moment of the molecule is directed with the ionic field or against it. If the positive ion is located on the left in Fig. 3, the energy of interaction with an ion in these configurations, according to (3.1), is found to be

$$E_{iw}^{(1)} = -E_{iw}^{(3)} = -\frac{Ze\mu_{\text{eff}}}{M r^2}.$$

In configurations 2 and 4 the dipole moment is directed perpendicular to the field and does not contribute to the interaction energy. In these positions the energy of interaction of the water molecule with the ion is wholly determined by the quadrupole moment. With the preceding condition (positive ion on the left in Fig. 3) we obtain

$$E_{iw}^{(4)} = -E_{iw}^{(2)} = -\frac{3}{2} \cdot \frac{Ze\theta}{M r^3};$$

The question as to the degree to which any given configuration is represented at a definite distance from the ion at a fixed temperature, is of the greatest interest. In the first approximation it may be assumed that the statistical weights x_i (i = 1, 2, 3, 4) of the different configurations are determined by the corresponding Boltzmann factors

$$x_i = Q^{-1} \exp(-E_{iw}^{(i)}/kT), \tag{3.3}$$

where $Q = \sum_{i=1}^{4} \exp(-E_{iw}^{(i)}/kT)$, so that as a whole, $\sum_{i=1}^{4} x_i = 1$. In these equations, the anions and cations are fully equivalent. On the other hand, it is generally known that anions and cations of the same radius interact differently with water molecules. The heat of hydration of F^- is greater than that of K^+ (the radius of both ions is 1.33 A) by 35-45 kcal/mole [26]. Buckingham [44], who ascribed the difference to electrical asymmetry

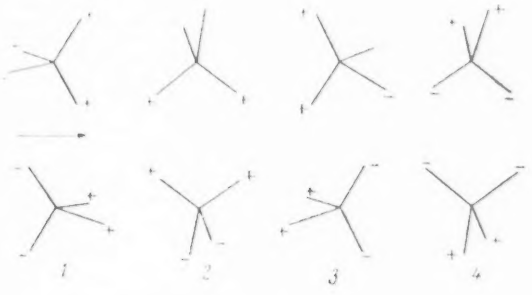

Fig. 3.

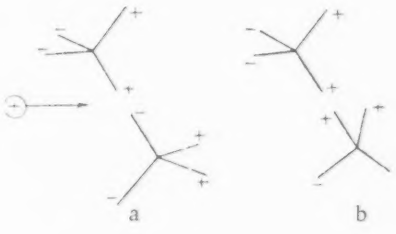

Fig. 4.

of the water molecule, found $\theta_\sigma = 3.9 \cdot 10^{-26}$. This value is much greater than the result of quantum-mechanical calculation [50]: $\theta_\sigma = 0.43 \cdot 10^{-26}$. On the other hand, Waldron [51] and Syrnikov [52], who analyzed the infrared absorption spectra of ionic solutions, suggested that the interaction of the anion with the nearest water molecules, in contrast to the cation, approximates in character to hydrogen bonds in pure water. This explanation is compatible with the symmetrical model of the water molecule in the condensed phase, adopted in the present article, where $\theta_\sigma = 0$.

Direct calculations by Eq. (3.3) are as yet impossible, since the relation between the number of hydrogen bonds formed by the molecule in water and the distance to the ion is unknown. A rough estimate at $t = 0$ shows that, as should have been expected, configuration 1 is practically the only one found near the ion, and that the proportion of configurations 4 and 2 sharply increases even within the limits of the first hydration layer* $1 \lesssim r^* \lesssim 3$ and almost reaches the limiting maximum value $x_4 \gtrsim x_2 \approx 1/4$ in the second hydration layer. At $t \neq 0$ this increase becomes even more pronounced.

Inherent Disorder of Water Near Ions. The inherent disorder of water, determined by the stability of the hydrogen bond ϵ, is superimposed on the forced orientation of water molecules near the ion. Near the ion, however, the hydrogen bond assumes the new, quite unexpected role of structure disrupter.

For concreteness, we shall consider a positively charged ion and two neighboring molecules of the first and second layers of its hydration shell. If both molecules occur in configuration 1, which predominates at short distances from the ion, a hydrogen bond is formed between them (Fig. 4a). In this case, the positive end of the hydrogen dipole (Section 2) is located closer to the ion than the negative end. This leads to a certain increase in the energy of the system. But in a state of thermodynamic equilibrium the free energy is minimal. Hence, under certain conditions a disposition in which a molecule of the first layer occurs in configuration 1 and a molecule of the second layer goes over to configuration 4 (Fig. 4b) may prove more favorable. In this case, the probability of formation of a hydrogen bond between the two molecules is decreased, since a H − H neighborhood becomes possible.

On considering the order of the structure of pure water in Section 1, we chose as the criterion of structural disorganization the quantity x_{HH} − the proportion of types of H − H neighborhoods or, what is the same, the proportion of broken hydrogen bonds. Thus, when conditions arise where it is more favorable for a molecule of the second or, in general, any higher layer to pass over from configuration 1 to configuration 4 or 2, the inherent disorganization of water increases. Clearly the necessary conditions arise at rather short distances from the ion, where the number of configurations 1 is still large − otherwise, "unfavorable" hydrogen bonds simply would not exist − but where the number of configurations 4 and 2 is already considerable, i.e., in the second-third layer of water molecules around the ion.

The quantitative consideration of the question may be simplified by assuming that processes of forced orientation in the ionic electrostatic field and the inherent order of water are statistically independent. Then the proportion of broken hydrogen bonds $x_{HH}^{i}(r^*)$ may be expressed as the product $\gamma x_{HH}^{w} \cdot x_{HH}^{i0}$ of the proportion of H − H pairs x_{HH}^{i0}, appearing under conditions of forced orientation, and the proportion of broken hydrogen bonds x_{HH}^{w} arising on account of the inherent order of the water near the ion in the absence of electrostatic interaction of the ion with water molecules. The normalizing constant γ is so chosen that as $r^* \to \infty$ $x_{HH}^{i0} \to x_{HH}$. The quantity x_{HH} is the proportion of broken hydrogen bonds in pure water. At 20° $x_{HH} = 0.206$.

The quantity x_{HH}^{i0} may be connected with the concentrations of different configurations in the following manner:

$$x_{HH}^{i0} = \frac{1}{2}(x_1x_2 + x_1x_3 + x_1x_4 + x_2x_3 + x_2x_4 + x_3x_4 + x_2^2 + x_4^2). \tag{3.4}$$

* Here and everywhere below, the radius of the water molecule $r_w = 1.38$ A is adopted as the unit of length ($r^* = r/r_w$).

Each term in this expression is the contribution to the probability of appearance of a H – H neighborhood from a pair of corresponding configurations.

The question of the inherent order of water near the ion is solved by the same methods which were developed in Section 1. Here, we can apply Eq. (1.2) directly, replacing ϵ by

$$\varepsilon^i = \varepsilon + 4\frac{Zq\mu_H}{Mr^2}\langle\cos\varphi\rangle. \tag{3.5}$$

Here φ is the angle between the direction of the ionic field and the hydrogen dipole. Obviously

$$\langle\cos\varphi\rangle = \cos 54^\circ(x_1 - x_3). \tag{3.6}$$

On taking into account the fact that the effective dipole moment of the water molecule according to (3.2) depends on x^i_{HH}, we come to a complex system of nonlinear equations for x_1, x_2, x_3, x_4, and x^i_{HH}. The exact solution of this system by the method of successive approximations requires very cumbersome calculations and is scarcely expedient in view of the roughness of the theory as a whole. We proceeded in the following manner. The x_i values in the zeroth approximation were calculated with $\mu_{eff} = \mu_0$. These values were substituted in (3.5), and the radial dependence of x^w_{HH} was calculated by Eq. (1.2). With the aid of x^w_{HH} a new value of μ_{eff} was calculated by Eq. (3.2), where we put $t = 2x^w_{OH}$. The total number of bonds formed by the molecule is equal to $4x^w_{OH}$. The factor $^1/_2$ is introduced to allow for the fact that disordering hydrogen dipoles are absent between the ion and the nearest water molecules. If μ_{eff} is known, the next approximation for x_i may be derived and x^{i0}_{HH} calculated by Eq. (3.4). In Fig. 5 is shown the radial functionality $x^i_{HH} = 4x^{in}_{HH} \cdot x^w_{HH}$ for $q/M = 0.017$ and three values of μ_H. The curve for $q/M = 0.020$ and $\mu_H = 0.83$ D is shown for comparison. All calculations were performed for singly charged ions. It is easily seen that the resulting picture corresponds closely to the ideas of Frank, Evans, and Wen. At short distances from the center of the ion strong binding of water molecules occurs (layer A). As the distance increases, the proportion of broken bonds sharply increases, becoming greater than the value corresponding to the degree of disorganization of pure water, and reaches a maximum in the first-second layer of water molecules (layer B). At greater distances x^i_{HH} falls relatively slowly, approaching the value 0.206 (layer C). The value of the maximum sharply rises on increase of the inherent dipole moment of the hydrogen bond. At low values of μ_H disordering of the water structure does not occur: x^i_{HH} rises steadily, approaching the value 0.206. The curve for $\mu_H = 0.56$ D behaves in this way. As q/M increases, the maximum value of x^i_{HH} decreases.

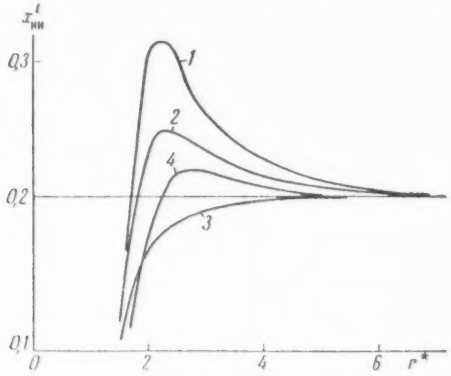

Fig. 5. Disorder of the structure of water near an ion at 20°: 1) q/M = 0.017, $\mu_H = 1.12 \cdot 10^{-18}$; 2) q/M = 0.017, $\mu_H = 0.83 \cdot 10^{-18}$; 3) q/M = 0.017, $\mu_H = 0.56 \cdot 10^{-18}$; 4) q/M = 0.020, $\mu_H = 0.83 \cdot 10^{-18}$

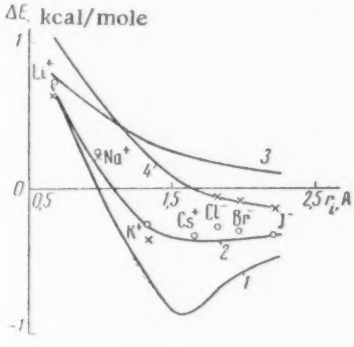

Fig. 6. Change in energy barriers separating equilibrium positions of H_2O molecules in an ionic solution in comparison with pure H_2O at 20°: ○) Samoilov [7]; ×) Vdovenko and Shcherbakov [53]. The theoretical curves were calculated for the parameters: 1) q/M = 0.017, $\mu_H = 1.12 \cdot 10^{-18}$; 2) q/M = 0.017, $\mu_H = 0.83 \cdot 10^{-18}$; 3) q/M = 0.017, $\mu_H = 0.56 \cdot 10^{-18}$; 4) q/M = 0.020, $\mu_H = 0.83 \cdot 10^{-18}$.

It is interesting to follow the change in the degree of order of water in the first hydration layer with respect to the ionic radius. The hydration energy is usually used as a measure of the binding action of the ion. However, Samoilov [7] noted that the hydration energy is a summary effect, whereas the character of the motion of water molecules in the first hydration layer is actually determined by small changes in the interaction energy on displacement of the molecules through relatively short distances. Samoilov suggested that the state of water molecules in ionic solution be described by changes in the energy barrier ΔE separating the instantaneous equilibrium positions in pure water and near the ion. Within the scope of the concepts developed in the present article, ΔE may be identified * with the change in the bond energy of a water molecule in the first hydration layer of the ion, and may be quantitatively evaluated as follows:

$$\Delta E = \varepsilon \left(x^{i}_{\mathrm{HH}} - x_{\mathrm{HH}}\right)|_{r=r_i+r_w},$$

where r_i is the ionic radius. Figure 6 shows the relation between ΔE and the ionic radius for various choices of μ_H and q/M. In the same figure are shown values found by Samoilov [7] from data for coefficients of self-diffusion and mobility of ions, as well as values calculated from the data of Vdovenko and Shcherbakov [53], who measured directly, by the method of nuclear magnetic resonance, the ratio τ_i/τ ** of residence times of the molecules in relative equilibrium positions near the ion and in pure water.

If μ_H is large enough, ΔE goes over from positive to negative values at some value of r_i. In the case $\Delta E < 0$, water molecules in the layer next to the ion are less strongly attached to neighboring molecules than in pure water. Samoilov suggested that this phenomenon be called negative hydration. With the best choice of $q/M = 0.017$, better agreement with Samoilov's, as well as Vdovenko and Shcherbakov's, data is obtained if $\mu_H = 0.83$ D. In particular, the radius determining the boundary between positively and negatively hydrated ions is equal to 1.09 A. Samoilov gives 1.11 A [7].

In earlier works [54, 55, 48], where water was regarded as a mixture of polymers $(H_2O)_n$, it was considered obvious that the dipole moment of the component water molecules in the polymeric formations was diminished. Recently, Mikhailov and Syrnikov [13] analyzed the temperature dependence of the density of salt solutions and showed in a different way that the effective dipole moment of the molecule in the close-packed structure is greater than in the ice lattice. If half the bonds are retained in the close-packed structure, Eq. (3.2) gives for the difference between effective dipole moments in the two structures $\Delta\mu_{eff} = 2\mu_H \cos 54°$. If $\mu_H = 0.83$ D, $\Delta\mu_{eff} = 0.96$ D. This value is in good agreement with the value $\Delta\mu_{eff} = 0.8$ D, found by Mikhailov and Syrnikov. The inherent dipole moment of the hydrogen bond may be evaluated exactly for the Bjerrum model of the water molecule in ice: $\mu_H = qe \cdot 0.78$ A = 0.64 D. In the liquid, this value should be increased to 0.79 D, since the oxygen – oxygen distance at 20° is increased to about 2.95 A. The values found above agree satisfactorily with this estimate. The value $\mu_{eff} = 0.5$ D also is in good agreement with it (if 20.6 % of the bonds are broken at 20°, this value corresponds to $\mu_H = 0.75$ D); Evjen and Zwicky [55] using

* The departure of a water molecule from the hydration shell of the ion takes place in two stages. First the water molecule passes from a lattice node to a void in the structure, next to the ion; this process requires the activation energy $E^{(i)}_{ww}$, necessary for the breaking of two bonds with the external environment of the hydrated ion. Then the water molecule jumps from the void next to the ion into a lattice node in the second layer of water molecules near the ion; the activation energy in this case is equal to the change Δh in the electrostatic energy of interaction of ion and water molecule on displacement through a distance $\Delta r = 0.8$ A [7]. Obviously, $\Delta h < h < Ze_{\mu_0}/M\ (0.68 + 1.38)^2 \approx 3$ kcal/mole. On the other hand, even if 50% of the bonds are broken in the hydration layer, $E^{(i)}_{ww}$ is about 4 kcal/mole. Thus $\Delta h < E^{(i)}_{ww}$ always. Hence the lifetime of the molecule in the hydration shell of the ion, which is determined by the first, slowest process, depends only on the height of the energy barrier $E^{(i)}_{ww}$.

** Strictly speaking, the "lifetime of the bond" between water molecules of the ion hydration shell and the external environment was measured in these experiments. The good agreement of Vdovenko and Shcherbakov's results with Samoilov's confirms the conclusion reached above, that the lifetime of a water molecule in the ion hydration shell is determined by the lifetime of the bond between two neighboring water molecules near the ion.

this value were able to explain quantitatively the concentration dependence of the coefficient of thermal expansion of salt solutions.

4. Structure of Ionic Solutions and Salting-Out Coefficients

In the preceding section it was shown that every ion, including such strongly hydrated ions as Li^+, is surrounded by a rather extensive region where the water structure is disordered much more than in pure water, which is not subject to the action of ionic electrostatic fields. Disruption of the structure is accompanied by a decrease in the energy of the bond between the water molecule and the environment. Hence, the replacement of a water molecule by a nonelectrolyte molecule in ionic solution requires a smaller expenditure of energy. Clearly, this influence is opposite in character to the constrictive action of the ionic electrostatic field and must decrease salting-out coefficients calculated without allowing for structural changes in the solution.

In the present article a very simple case is considered, in which the nonelectrolyte molecule is nonpolar, so that its effect on the water structure may be neglected. The activity coefficient of a nonelectrolyte in a salt solution is determined by the difference between the average potential energies of the nonelectrolyte molecules in the salt solution and pure water, $RT \ln F = \overline{\Delta E}$. If the change in interaction energy of nonelectrolyte and water molecules is negligible, ΔE is determined only by the change in the degree of bonding of water molecules in the salt solution.

When an ion is introduced in the solution, effects of two types are possible: 1) ordering and disruption of the structure; 2) change in the cell potential acting on the water molecule, leading to a decrease in the free volume; the latter is equivalent to an increase of internal pressure and is expressed in the contraction observed when salts dissolve in water. In the first approximation, if volume effects on solution of ions in water are small, $\overline{\Delta E}$ consists of the change $\Delta(\delta E/\delta V)\, v_n$ and the changes $\overline{\Delta E'}$, which are connected with the first of the effects noted above:

$$\overline{\Delta E} = \Delta (\delta E/\delta V)\, v_n + \overline{\Delta E'}, \tag{4.1}$$

where v_n is the partial molar volume of the nonelectrolyte at infinite dilution.

When the solution is sufficiently dilute with respect to the salt, $\overline{\Delta E'}$ is equal to the sum of the individual contributions from each of the types of ions present in the solution: $\overline{\Delta E'} = \Sigma_i \overline{\Delta E'_i}$. At low salt concentrations the spheres of influence of the individual ions do not overlap. In this case *

$$\overline{\Delta E'_i} = 2\,\frac{N_i}{N_w} \cdot \overline{\Delta U_i}. \tag{4.2}$$

Here N_i is the number of gram-ions of Type i and N_W is the number of moles of water per liter of solution. $\overline{\Delta U_i}$ is the average change in the potential energy of water surrounding one ion of Type i:

$$\overline{\Delta U_i} = \int_{1+r_i^*}^{\infty} \varepsilon\,(x^i_{HH} - x_{HH})\,\frac{dV}{v_w} \tag{4.3}$$

(v_W is the molar volume of water).

The first component in (4.1), connected with the manifestation of internal pressure, was discussed rigorously and in detail by McDevitt and Long [3]. The total salting-out coefficient is the sum of the quantity K_S^0, calculated by McDevitt and Long, and a structural correction for salting-in, ΔK_S:

$$K_s = K_s^0 + \Delta K_s,$$

* The factor 2 takes into account the fact that when a water molecule in the quasicrystal lattice is replaced by a nonelectrolyte molecule, the maximum number of bonds broken is not two but four.

where, according to (4.2) and (4.3),

$$\Delta K_s = -\frac{4\pi r_w^3 N_0}{v_w} \cdot \frac{2\varepsilon}{2{,}302RT \cdot 55{,}5} \sum_i \int_{1+r_i^*}^{\infty} (x_{HH}^i - x_{HH})\, r^{*2}\, dr^* \qquad (4.4)$$

(N_0 is Avogadro's number). In order to calculate the integral in (4.4) with greater accuracy, it is convenient to expand x_{HH}^i in powers of μ_H, since the energy of hydrogen dipoles at great distances from the ion is small in comparison with $(RTq - \epsilon)/2 = 1.35RT$ kcal/mole. Confining ourselves to the first term of the expansion, we obtain

$$\Delta K_s = -\frac{0{,}136}{RT} \sum_i \left[\frac{2Ze\mu_H \cos 54^\circ}{Mr_w^2 kT} \psi(1{,}35)\, I_i^{(2)} - 4x_{HH} I_i^{(1)} \right], \qquad (4.5)$$

where

$$I_i^{(2)} = \int_{1+r_i^*}^{\infty} 4x_{HH}^{io} (x_1 - x_3)\, dr^*,$$

$$I_i^{(1)} = \int_{1+r_i^*}^{\infty} \left(\frac{1}{4} - x_{HH}^{io} \right) r^{*2}\, dr^*$$

and

$$\psi(x) = \exp x/(1 + \exp x)^2.$$

ΔK_s was calculated by Eq. (4.5) using the previous choice of constants, q/M = 0.017, M = 10 for singly charged ions at 20°. It must be noted that the integrals $I^{(1)}$ and $I^{(2)}$ are practically independent of the nature of the ions, since ionic radii lie in a relatively narrow range, and the main contribution to $I^{(1)}$ and $I^{(2)}$ comes from the diffuse region beyond the disorder maximum in the curves $x_{HH}^i(r^*)$. Integrals $I^{(1)}$ and $I^{(2)}$ were evaluated numerically at nine points for a fixed value of $r_i^* = 1.0$. The maximum error for Li^+ ($r^* = 0.56$) does not exceed 10%. Results are given in Table 5.

TABLE 5

$\mu_H \cdot 10^{18}$	$I^{(1)}$	$I^{(2)}$	ΔK_s
1,12	0,50	1,07	—0,230
0,83	1,07	1,28	—0,087
0,56	1,41	1,40	+0,058

In Table 6 are given the total coefficients of salting-out of benzene by certain salts at 20° with corrections for structural salting-in at $\mu_H = 0.83$ D. McDevitt and Long's results [3] are more than twice the experimental values. Our values agree satisfactorily with experiment.

NH_4Cl is somewhat peculiar. Theory predicts salting-in for this salt, whereas just the opposite occurs in fact. Apparently, the discrepancy in the case of NH_4Cl can be explained by the participation of protons of the ammonium ion in the formation of hydrogen bonds with neighboring water molecules and the strong additional ordering effect of NH_4 on water.

It is interesting that the salting-out coefficients obtained by McDevitt and Long [56] for O_2 and H_2 are in excellent agreement with experiment without introducing corrections for structural salting-in. This difference may be explained by the fact that the mechanism of solution of gases in water is very different from the mechanism of solution of benzene. Above, we assumed that benzene molecules displace water molecules. Eley [57] studied the solubility of inert gases in water and found that the solution process in this case is related not to the displacement of water molecules but to the entry of gas molecules into voids of the structure. Clearly the change in the degree of bonding of water molecules in nodes of the quasicrystal lattice does not noticeably affect the latter process.

TABLE 6

Salt	K_s^0 [3]	K_S, calc.	K_S, expt.	Salt	K_s^0 [3]	K_S, calc.	K_S, expt.
NaCl	0,42	0,245	0,195	KCl	0,34	0,165	0,166
NaBr	0,35	0,175	0,155	RbCl	0,31	0,135	0,14
NaI	0,27	0,095	0,095	CsCl	0,26	0,085	0,088
$NaNO_3$	0,31	0,135	0,119	NH_4Cl	0,15	—0,025	0,103
LiCl	0,31	0,135	0,141				

I sincerely thank V. M. Vdovenko, Corresponding Member Acad. Sci. USSR, for his constant support and assistance in the work, and also Doctor of Chemical Sciences O. Ya. Samoilov and Professor N. D. Sokolov for valuable advice and comments.

LITERATURE CITED

1. H. Harned and B. Owen, Physical Chemistry of Electrolyte Solutions [Russian translation] (IL, Moscow, 1952).
2. V. M. Vdovenko and T. V. Kovaleva, Zhur. Neorg. Khim. 2, 1682 (1957).
3. W. F. McDevitt and F. Long, J. Am. Chem. Soc. 74, 1773 (1952).
4. J. Bockris, J. Bowler-Reed, and J. A. Kitchener, Trans. Faraday Soc. 47, 184 (1951).
5. H. S. Frank and Wen-Yang Wen, Disc. Faraday Soc. 24, 133 (1957).
6. J. Bernall and R. Fowler, J. Chem. Phys. 1, 515 (1933).
7. O. Ya. Samoilov, Structure of Aqueous Electrolyte Solutions and Ion Hydration [in Russian] (Izd. AN SSSR, Moscow, 1957).
8. N. Bjerrum, Dan. Mat. Fys. Medd. 27, No. 1 (1951).
9. J. A. Pople, Proc. Roy. Soc. A 205, 163 (1951).
10. J. Fox and E. Martin, Proc. Roy. Soc. A 174, 234 (1940).
11. L. Hall, Phys. Rev. 73, 775 (1948).
12. K. Grjotheim and J. Krogh-Moe, Acta Chem. Scand. 8, 1193 (1954).
13. I. G. Mikhailov and Yu. P. Syrnikov, Zhur. Strukt. Khim. 1, 1, 12 (1960).*
14. O. Ya. Samoilov, Zhur. Fiz. Khim. 20, 1411 (1946).
15. E. A. Guggenheim, Mixtures (Oxford, 1952).
16. J. S. Rowlinson and C. F. Curtiss, J. Chem. Phys. 19, 1519 (1951).
17. N. Dorsey, Properties of Ordinary Water-Substance (New York, 1940).
18. P. Cross, S. Burnham, and P. Leighton, J. Am. Chem. Soc. 59, 1134 (1937).
19. R. Ewell and H. Eyring, J. Chem. Phys. 5, 726 (1937).
20. L. Pauling, Nature of the Chemical Bond [Russian translation] (Goskhimizdat, Moscow-Leningrad, 1947).
21. R. W. Taft and H. H. Sisler, J. Chem. Educ. 24, 175 (1947).
22. M. D. Lagunov, Zhur. Fiz. Khim. 32, No. 3 (1958).
23. G. Haggis, J. Hasted, and T. Buchanan, J. Chem. Phys. 20, 1452 (1952).
24. H. S. Frank, Proc. Roy. Soc. A247, 481 (1958).
25. J. S. Rowlinson, Trans. Faraday Soc. 47, 120 (1951).
26. B. E. Conway and J. O'M. Bockris, Collection: Some Problems of Modern Electrochemistry [Russian translation] (IL, Moscow, 1958) p. 63.
27. E. S. Campbell, J. Chem. Phys. 20, 1411 (1952).
28. J. A. Pople, Proc. Roy. Soc., A 202, 323 (1950).
29. C. A. Coulson, Proc. Roy. Soc. A 207, 63 (1951).
30. L. Burnell and C. A. Coulson, Trans. Faraday Soc. 53, 403 (1957).
31. F. O. Ellison and H. Shull, J. Chem. Phys. 23, 2348 (1955).
32. N. D. Sokolov, Uspekhi Fiz. Nauk 57, 205 (1955).
33. J. Lennard-Jones and J. A. Pople, Proc. Roy. Soc. A 205, 155 (1951).
34. I. V. Aleksandrov and N. D. Sokolov, Doklady Akad. Nauk SSSR 124, 115 (1959).*

* Original Russian pagination. See C. B. translation.

35. I. Fisher-Hjalmars and R. Grahn. Acta Chem. Scand. 12, 584 (1958).
36. J. O'M. Bockris, Quart. Rev. 3, 173 (1949).
37. D. Williams and W. Millet, Phys. Rev. 66, No. 6 (1944).
38. N. K. Voskresenskaya and T. N. Yankovskaya, Izvest. Akad. Nauk SSSR, Otdel. Khim. Nauk 1, No. 3 (1945).
39. G. W. Stewart, J. Chem. Phys. 11, 72 (1943); 7, 869 (1939).
40. H S. Frank and M. W. Evans, J. Chem. Phys. 13, 507 (1945).
41. O. Ya. Samoilov, Disc. Faraday Soc. 24, 216 (1957).
42. R. W. Gurney, Ionic Processes in Solution (New York, 1953).
43. L. Landau and E. Lifshits, Field Theory [in Russian] (Moscow-Leningrad, 1948).
44. A. D. Buckingham, Disc. Faraday Soc. 24, 151 (1957).
45. E. O. Wallen, W. L. Davidson, and C. G. Shull, Phys. Rev. 75, 1348 (1949).
46. E. S. Rudakov, Doklady Akad. Nauk SSSR 127, 1058 (1959).*
47. G. I. Mikulin, Zhur. Fiz. Khim. 33, 2419 (1959).
48. A. G. Samoilovich and A. A. Goryunov, Zhur. Éksp. i Teoret. Fiz. 4, 892 (1934).
49. A. Pasynskii, Zhur. Fiz. Khim. 11, 606 (1938).
50. A. B. Duncan and J. A. Pople, Trans. Faraday Soc. 49, 217 (1953).
51. R. D. Waldron, J. Chem. Phys. 26, 809 (1957).
52. Yu. P. Syrnikov, Doklady Akad. Nauk SSSR 118, 760 (1958).*
53. V. M. Vdovenko and V. A. Shcherbakov, Zhur. Strukt. Khim. 1, 1, 28 (1960).*
54. A. G. Samoilovich, Physik Z. Sowjetunion 4, 843 (1933).
55. H. M. Evjen and F. Zwicky, Phys. Rev. 33, 860 (1929).
56. W. F. McDevitt and F. Long, Chem. Rev. 51, 119 (1952).
57. D. D. Eley, Trans. Faraday Soc. 35, 1281 (1939).

* Original Russian pagination. See C. B. translation.

INVESTIGATION OF THE INFLUENCE OF THE STRUCTURES OF SOLID AND LIQUID PHASES ON THE SOLUBILITY OF SALTS IN WATER

I. ON SOLUBILITY IN THE SYSTEMS $NH_4NO_3 - NH_4I - H_2O$ AND $KNO_3 - KI - H_2O$ AT 25°

P. S. Bogoyavlenskii

L'vov Zooveterinary Institute

Translated from Zhurnal Strukturnoi Khimii, Vol. 1, No. 3, pp. 305-312, September-October, 1960
Original article submitted October 13, 1959

Solubility in the systems $NH_4NO_3 - NH_4I - H_2O$ and $KNO_3 - KI - H_2O$, which were studied at 25°, is explained with the aid of the crystallochemical characteristics of salts and concepts of the structure of aqueous electrolyte solutions. A special quantity – the displacement coefficient – is introduced for quantitative characterization of the joint solubility of salts in ternary solutions.

Structural consideration of experimental data on the indicated systems leads to the conclusion that the solubility of the component salts in binary and ternary solutions is determined to a certain extent by the relative stability of ionic close order which determines the crystallization of salts from saturated solutions: the more stable this order is, the less soluble is the salt.

The change of individual solubilities of salts in ternary solutions of both systems is characterized by linear dependence of the molar quantities of the salted-out salt on the molar quantities of the dissolved, unsaturated salt and by approximately constant displacement coefficients, which, in general, indicates that the joint solubility is determined by the structural state of the saturated solutions.

In our works [1-4] the solubilities of certain salts in water were explained with the aid of the crystallochemical characteristics of ions and salts, the Bernal-Fowler [5] model of liquid water, and Kapustinskii and Samoilov's ideas on the structure of aqueous electrolyte solutions and the hydration of ions [6, 7].

Obviously, the influence of the structures of crystals and liquid solutions on the solubility of salts in water may be followed most distinctly in those systems, the readily soluble salts of which contain ions having negative hydration [7] and relatively weak interaction with water molecules. In the present article certain over-all premises of our comparison of the solubilities of uni-univalent salts having large ions, with the structures of the solid salts and their aqueous solutions, are generalized, and solubility in the systems $NH_4NO_3 - NH_4I - H_2O$ and $KNO_3 - KI - H_2O$ is considered. Our comparative evaluation of the solubilities of readily soluble uni-univalent salts with large ions, containing potassium and ammonium cations, on a structural basis [3] is continued by the study of the systems named.

Our investigation is based to a certain extent on the interpretation of joint solubility in ternary water-salt systems, with allowance for the fact that the attainment of equilibrium in them involves the partial displacement

of some ions by others in the structure of a saturated solution of the given salt. This displacement, which determines the change in the individual solubilities of salts in ternary solutions, takes place in a mobile but relatively ordered liquid system and hence has a definite relation to the structure of the original saturated solution and the structural characteristics of the ions and salts.

On ordered displacement of the given salt in its saturated solution by another salt one may expect the molar quantity of the salted-out salt to be a linear function of that of the dissolved salt, the ratio of the salts being approximately constant; i.e., the same regularity should obtain as in the formation of substitutional solid solutions by two isomorphous salts. The displacement of the saturating salt in the ternary solution by the dissolving salt may be characterized [2] by the displacement coefficient

$$K = (x_0 - x)/y,$$

where x_0 is the number of moles of a given salt in a saturated binary solution, x is the number of moles of the same salt in a saturated ternary solution, and y is the number of moles of the salt not saturating the ternary solution.

In evaluating the structural heterogeneity [7, 8, 9] of a saturated solution of an anhydrous, readily soluble salt we proceed from the idea that in such a solution effective (i.e., capable of crystallization) close order of ions and close order formed from ions and water molecules [2] are simultaneously present, and they interchange. Apparently, it may be assumed that structural ion groups which determine crystallization and are the effective part of the structure of the saturated anhydrous-salt solution correspond as nearly as possible to the ionic close order proper to the salt structure. Ions hydrated to a varying degree, and close order consisting of ions and water molecules jointly coordinated around the ion, may be referred to structural groups of the second type.

The solubility of salts is determined more or less by the change in the structural state of the solution on change of its concentration. Structural changes in aqueous electrolyte solutions are considered on the basis of ideas on the dynamic equilibrium change of ion hydration on diluting the solution [7, 10]. The principle of this approach may be extended also to characterizing interchanges of the predominant forms of close order of particles in anhydrous-salt solutions on change of concentration.

In a dilute anhydrous-salt solution, as in the case of a hydrated salt, a tetrahedral water structure is maintained, in which ions dynamically displace water molecules in equilibrium positions. In the case of tetrahedral hydration there are no bonds between ions, since every ion is surrounded by water molecules. The predominance of the close order of water in the solution structure applies to various salts in different concentration regions at the given temperature. As the concentration increases, the solution structure goes over to denser packing, and other forms of close order, whose rise is determined by bonds between ions and dehydration of ions, become predominant in it. As the solution concentration increases, each ion is surrounded by an ever-increasing number of oppositely charged ions and an ever-decreasing number of water molecules. In a homogeneous liquid phase the dynamic equilibrium continually shifts toward the ionic close order proper to the salt structure. In a saturated solution, this order becomes effective, determines crystallization, and coexists with the solid phase and the liquid-phase close order consisting of ions and water molecules.

The attainment of equilibrium concentrations on solution of uni-univalent salts with large ions is determined by change in the structural state of the solution to a greater degree than on solution of salts of other groups. This follows if only from the fact that since water molecules do not take part in crystallization, they have a more or less inhibiting effect on the formation of an effective structure in the liquid phase. In the case of solubility under consideration, apparently, the concentrations of solutions with any given predominant form of close order are determined to a considerable extent by the action of ions on the water structure, and water molecules on the ionic close order.

The action of large, singly charged ions on the water structure may be characterized by their negative hydration [7], to the manifestation of which we also relate the weakening of order in the original tetrahedral cell of water, caused by the very entrance of the ion into it. It must be noted that when the ions have slight negative hydration, regions of displacement or intrusion structures apparently may noticeably predominate even in moderately concentrated solutions. A strong manifestation of negative hydration by the ions facilitates the attainment of that state of solution structure in which crystallization of salts becomes possible at a relatively diminished ion concentration.

The transition of the solution structure at the given temperature to denser packing changes the role of water as solvent. In the case of tetrahedral hydration the solvent power of water is manifested mainly in the weakening of interionic attractive forces by the aqueous environment. In concentrated solutions, water molecules disturb the ionic close order and thus inhibit to some extent the formation of the effective structure. Hence the attainment of equilibrium concentrations on solution of uni-univalent salts with large ions is determined also by the relative stability of the structural ion groups arising in the solutions, which determine crystallization.

An approximate and purely qualitative estimate of the relative stability of ionic close order in liquid solutions may be given, based on crystallochemical data on ions and salts.

Solubility in the System $NH_4NO_3 - NH_4I - H_2O$

The results of our investigation of this system, which had not been studied before, are given in Table 1 and Fig. 1. In general, the component salts have high, but appreciably different equilibrium concentrations: the molality of a saturated NH_4NO_3 solution at 25° is more than twice that of a saturated NH_4I solution. The noncommon anions of the salts, which differ structurally, strongly and to about the same degree disrupt the water structure of the solution [11, 12]. The ammonium ion can form hydrogen bonds [13], the conditions of formation of the hydrogen bond NH . . . O being similar to those of the bond OH . . . O [14]. Bearing in mind certain peculiarities of the crystal structures of NH_4NO_3 and NH_4I, it is logical to assume that the high individual solubilities of the named salts are directly connected with the relatively diminished stability of the structural ion groups arising in their solutions, which take part in crystallization.

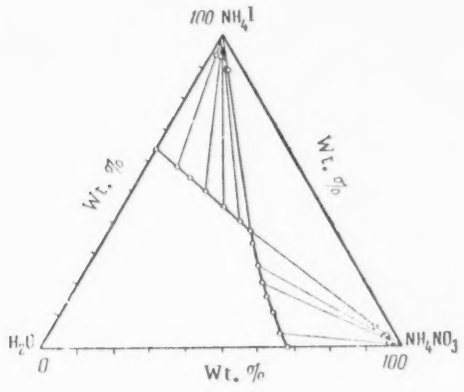

Fig. 1.

The low-temperature crystalline modification of NH_4NO_3 – IV, existing at 25°, has the lowest symmetry (rhombic) in comparison with other forms [15]. In a crystal of this modification the mutual coordination and packing of the tetrahedral and triangular ions NH_4^+ and NO_3^-, which have the coordination number eight relative to one another, lead to an unstable and unsymmetrical configuration of the coordination sphere. Crystals of NH_4I with cubic syngony at 25° have the NaCl structure [15], in which each ion is octahedrally surrounded by six ions of opposite sign. The interionic distance in the NH_4I crystal is 3.62 A [16].

From the data given, it follows that the ionic close orders proper to NH_4NO_3 and NH_4I crystals will have increased sensitivity in liquid solutions to thermal motion and the action of water molecules. In connection with this, the rise of the effective structure on solution of these salts is possible only at relatively high concentrations of the saturated solutions. It may also be assumed that the close order of NH_4^+ and NO_3^- ions in the modification of NH_4NO_3 which we considered, as well as all other modifications thereof, is relatively less stable than the close order of NH_4^+ and I^- ions in the NH_4I structure; this is indicated, in particular, by the low-melting point of ammonium nitrate (169.6°) and the variety of crystalline modifications of this salt. The considerable difference in the solubilities of NH_4NO_3 and NH_4I apparently is determined to a substantial extent by the fact that thermal motion and water molecules hinder the formation of the effective structure on solution of NH_4NO_3 to a greater degree than on solution of NH_4I.

The attainment of high equilibrium concentrations on solution of NH_4NO_3 and NH_4I also is determined to a certain extent by the formation of hydrogen bonds between ammonium ions and water molecules in solutions of both salts. The configuration and size of the NH_4^+ ion and its ability to form hydrogen bonds with water molecules determine its greatly diminished action on the water structure [11]. In NH_4NO_3 and NH_4I solutions the ion relatively stabilizes the tetrahedral structure of the solvent and weakens the influence on solubility of negative hydration which is pronounced in the case of NO_3^- and I^- anions. Hydrogen bonds of the ammonium ion with four water molecules or less favor the predominance of joint order of ions and water molecules in a rather large region of concentrations of NH_4NO_3 and NH_4I solutions.

Joint solubility in the system $NH_4NO_3 - NH_4I - H_2O$ is characterized along both univariant curves and at the eutonic point of the isotherm (Fig. 2) by a linear relation between $x_0 - x$ (moles of salted-out salt) and y (moles of dissolved salt) and by approximately constant displacement coefficients, calculated from the data in Table 1. Deviations from average values of K (equal for NH_4NO_3 and NH_4I to 1.44 and 0.37, respectively), lying beyond the limits of analytical error, occur only in the case of solutions in a very short segment of the NH_4NO_3 univariant curve, adjacent to the eutonic point and for the concentration of this salt in the eutonic solution. The manifestation of the noted accuracy must be regarded as proof that in solutions saturated with respect to NH_4NO_3 and NH_4I, a structural order of particles is present, which influences the change of individual solubilities of salts in ternary solutions.

TABLE 1

System $NH_4NO_3 - NH_4I - H_2O$ at 25°

No. of point	Composition of solutions						K	Comp. of residue, wt. %		Solid phase
	wt. %			moles per 1000 g H_2O						
	NH_4I	NH_4NO_3	H_2O	NH_4I	NH_4NO_3	sum		NH_4I	NH_4NO_3	
1	63,86	—	36,14	12,19	—	12,19	—	—	—	NH_4I
2	58,10	9,20	32,70	12,26	3,51	15,77	0,35	97,45	1,28	The same
3	54,50	14,20	31,30	12,01	5,67	17,68	0,37	—	—	" "
4	50,70	20,30	29,00	12,06	8,75	20,81	0,36	95,60	2,50	" "
5	45,25	27,83	26,92	11,60	12,91	24,51	0,37	95,70	2,67	" "
6	40,65	34,57	24,78	11,32	17,43	28,75	0,37	95,34	3,30	" "
7	36,91	40,40	22,69	11,22	22,25	33,47	0,37	—	—	$NH_4I + NH_4NO_3$
							1,36	5,95	90,30	
8	30,50	44,30	25,20	8,35	21,95	30,30	1,41	—	—	NH_4NO_3
9	25,41	48,00	26,59	6,59	22,52	29,11	1,43	3,70	95,10	The same
10	20,76	51,32	27,92	5,13	22,97	28,10	1,46	2,40	96,50	" "
11	15,50	55,30	29,20	3,66	23,66	27,32	1,49	—	—	" "
12	10,07	59,77	30,16	2,30	24,75	27,05	1,48	—	—	" "
13	5,38	63,65	30,97	1,13	25,67	26,80	1,48	0,70	98,04	" "
14	—	68,00	32,00	—	26,56	26,56	—	—	—	" "

As is evident from Table 1, the molalities of NH_4NO_3 and NH_4I in the eutonic solution are only slightly less than in the corresponding saturated binary solutions. This means that ternary solutions on the univariant curves of the given system remain unsaturated with respect to the second salt in a wide range of concentrations. The increase in the solvent power of water in ternary solutions of the system under consideration is directly connected with the transition of the solution structure to denser packing and with the joint presence of NO_3^- and I^- ions therein. The noncommon NO_3^- and I^- anions apparently, to different degrees, strongly inhibit the formation of an effective nonsaturating-salt structure in ternary solutions on each of the univariant curves. Therefore, such structures are formed in the eutonic solution under conditions where its total molality is not substantially different from the sum of molalities of the saturated binary solutions. The peculiarity discussed above, of joint solubility in the system $NH_4NO_3 - NH_4I - H_2O$, supports the idea of diminished stability of structural ion groups determining the crystallization of NH_4NO_3 and NH_4I, and the idea of the substantial influence of this factor on the solubility of these salts.

The rather large difference in the displacement coefficients characterizing the solubility of the saturating salts must be regarded as another peculiarity of joint solubility in the system under consideration. It follows from comparison of the average displacement coefficients on the isotherm curves that the salting-out effect of NH_4I is much greater than that of NH_4NO_3. This means that identical molar quantities of NH_4NO_3 and NH_4I are salted-out from their saturated solutions by far fewer moles of NH_4I than of NH_4NO_3. This peculiarity of joint solubility in the system $NH_4NO_3 - NH_4I - H_2O$, apart from other factors considered in part by us, is determined by the structures of the saturated binary solutions.

Saturated NH_4NO_3 solution contains, on the average, one water molecule per ion. The structure of this solution with respect to close order of particles approaches, as nearly as possible, the structure proper to the salt.

Presumably the greater degree of salting-out of NH_4NO_3 from ternary solutions in comparison with NH_4I is due to the fact that the structure of a saturated solution of this salt contains a relatively large region of ionic close order, capable of crystallization. The greater degree of salting-out of NH_4NO_3 also determines the greater lowering of the individual solubility of NH_4NO_3 in the eutonic solution, although this solubility is more than twice the individual solubility of NH_4I.

The close order of NH_4^+ and I^- ions, being more stable and symmetrical than that of NH_4^+ and NO_3^- ions, becomes effective under conditions where joint order of ions and water molecules predominates in the structure of the saturated solution. Such a structural state of the saturated NH_4I solution favors both little salting-out of the saturating salt from it and considerable solubility of NH_4NO_3 in it. Quite probably, ions of the nonsaturating salt NH_4NO_3 will be preferentially located in a water-rich region of the saturated solution and will not appreciably disturb any part of the structure substantially effective with respect to NH_4I.

Solubility in the System $KNO_3 - KI - H_2O$

This system had not been studied before. The results of our investigation are given in Table 2 and Fig. 3. In contrast to the preceding system the individual solubility of the iodide is far greater than that of the nitrate. The great difference in the solubilities of ammonium and potassium nitrates also merits attention.

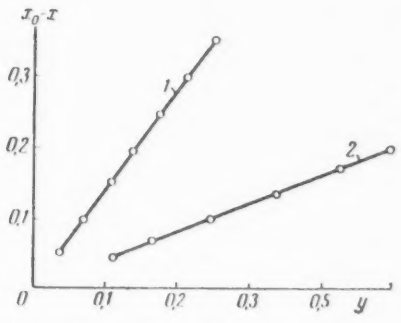

Fig. 2. Relation between $x_0 - x$ and y for ternary solutions of the system $NH_4NO_3 - NH_4I - H_2O$, saturated in NH_4I (1) and NH_4NO_3 (2).

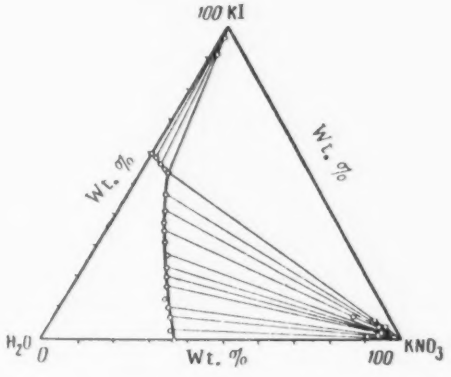

Fig. 3.

The rhombic KNO_3 crystal is made up of K^+ and NO_3^- ions. The manner of packing and coordination (6 :6) of the ions is the same as in the aragonite structure [17], which can be derived from the NiAs structure by substituting potassium for nickel and the nitrate group for arsenic. The six NO_3^- ions are so disposed relative to the K^+ ion, that each K^+ ion is directly adjacent to nine oxygen atoms. The cubic KI crystal has the NaCl structure. The interionic distance is 3.526 A [15].

In order to evaluate the influence of the stability of structural ion groups determining crystallization from solution on the solubility of KNO_3 and KI, the sharply different changes in the solubilities of the salts at temperatures above 25° must be noted: the molality of saturated KNO_3 solution is approximately equal to that of saturated KI solution at 60° but is nearly twice as great at 90° [18]. Apparently, the effect of this factor on the solubility of each salt depends to a substantially different degree on the intensity of thermal motion in the solution. It follows from comparison of the solubilities at 25°, that thermal motion hinders the attainment of effective ionic order on solution of KNO_3 to a lesser degree than on solution of KI, although the close order for the first salt is less stable than that for the second. Hence, the greater solubility of KI in comparison with KNO_3 at 25° may be explained by the fact that under these conditions thermal motion weakens the attractive forces between K^+ and I^- ions in the solution to a greater degree than between K^+ and NO_3^- ions. It may be further presumed that as the temperature rises, the sensitivity of the less stable close order of K^+ and NO_3^- ions to thermal motion increases more than that of the close order of K^+ and I^- ions. This hypothesis is confirmed by comparison of the solubilities of KNO_3 and KI at temperatures above 60°, from which it follows that the effect of the stability of structural groups on the solubility of KNO_3 is most distinctly manifested at relatively high temperatures.

It must also be noted that the greater solubility of KI in comparison with KNO_3 at 25° is explained by the diminished negative hydration of the I^- ion in comparison with the NO_3^- ion. Possibly the pronounced disruption of the solvent–water structure by the NO_3^- anion at relatively low temperatures facilitates crystallization of KNO_3 from solution, to a substantial degree. The great difference in the solubilities of ammonium and potassium nitrates at 25° and other temperatures is directly determined by the difference in stability of close order of the ions. Undoubtedly the grouping of NH_4^+ and NO_3^- ions in aqueous solution is less stable than that of K^+ and NO_3^- ions not only because it is less symmetrical, but also because its central ion has a higher coordination number.

TABLE 2

System $KNO_3 - KI - H_2O$ at 25°

No. of point	Composition of solutions, wt. %			moles per 1000 g H_2O			K	Comp. of residue, wt. %		Solid phase
	KI	KNO_3	H_2O	KI	KNO_3	sum		KI	KNO_3	
1	59,88	—	40,12	8,99	—	8,99	—	100	—	KI
2	58,60	2,56	38,84	9,09	0,65	9,74	0,32	98,20	0,40	same
3	57,10	4,97	37,93	9,07	1,30	10,37	0,35	97,36	0,99	"
4	56,03	6,40	37,57	8,98	1,69	10,67	0,36	94,50	1,80	"
5	55,06	7,80	37,14	8,93	2,08	11,01	0,38	4,80	91,43	KI + KNO_3
							0,57	—	—	KNO_3
6	48,08	9,60	42,32	6,84	2,24	9,08	0,59	3,60	95,34	same
7	43,93	9,90	46,17	5,73	2,12	7,85	0,64	5,80	86,29	"
8	39,20	10,76	50,04	4,72	2,33	6,85	0,68	—	—	"
9	36,79	12,08	51,13	4,34	2,34	6,68	0,66	2,50	94,40	"
10	31,53	13,80	54,67	3,47	2,50	5,97	0,69	—	—	"
11	28,36	14,80	56,84	3,00	2,58	5,58	0,71	0,18	97,80	"
12	24,42	16,12	59,46	2,48	2,68	5,16	0,73	0,60	97,93	"
13	21,53	16,76	61,71	2,10	2,68	4,78	0,78	0,66	94,36	"
14	17,70	18,30	64,00	1,67	2,83	4,50	0,81	0,90	91,67	"
15	14,56	19,82	65,62	1,34	2,99	4,33	0,81	—	—	"
16	11,62	21,40	66,98	1,05	3,16	4,21	0,79	0,50	95,97	"
17	8,52	22,80	68,68	0,75	3,29	4,04	0,80	0,16	98,56	"
18	3,50	25,32	71,18	0,30	3,52	3,82	0,81	0,40	96,73	"
19	—	27,16	72,84	—	3,69	3,69	—	—	100	"

Joint solubility in the system $KNO_3 - KI - H_2O$ is characterized by a linear relation between $x_0 - x$ and y, this relation being represented, in the case of ternary solutions saturated with respect to KNO_3, by two straight lines of different slope, whose intersection gives a break point (Fig. 4). The lower and upper straight lines of the graph for KNO_3 are drawn through points calculated on the basis of ternary-solution compositions corresponding to points 13-18 and 5-12, respectively, in Table 2.

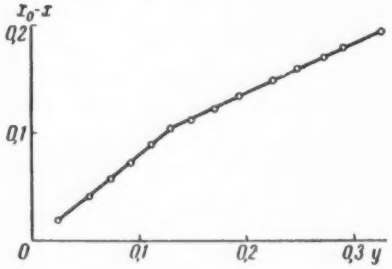

Fig. 4. Relation between $x_0 - x$ and y for ternary solutions of the system $KNO_3 - KI - H_2O$, saturated in KNO_3.

The average value of K in ternary solutions saturated in KI is 0.35, whereas that in ternary solutions saturated in KNO_3 is 0.80 for the lower straight line and 0.66 for the upper one. In the region of ternary-solution concentrations, corresponding to the upper straight line, deviations of calculated values of K from the average value lie beyond the limits of analytical error in most cases.

With respect to the mutual influence of salts, joint solubility in the system $KNO_3 - KI - H_2O$ is generally similar to that in the system $NH_4NO_3 - NH_4I - H_2O$. In the eutonic solutions of both isotherms the molality of the nitrates is far lower than that of the iodides despite the opposite difference in the individual solubilities of the component salts of the system. It follows from the given comparison, that NO_3^- ions have a greater inhibiting effect on the crystallization of iodides from ternary solutions than I^- ions have on the crystallization of nitrates.

The presence of a break on the curve of $x_0 - x$ and y for KNO_3 indicates that joint solubility is determined to a certain extent by the change in the structure of the saturated KNO_3 solution in ternary solutions with a predominant concentration of the nonsaturating salt KI. Presumably, in a KNO_3 solution saturated at 25° (moderate concentration) the close order proper to water is retained to a considerable degree. The transition of this "eutectic" structure to a more densely packed one leads to a change in the conditions of joint solubility and a decrease in the region of effective structure, which also is reflected in a decrease in the average value of K in ternary solutions corresponding in concentration to the upper segment of the curve $x_0 - x = f(y)$.

It follows from comparison of the average values of K along both isotherms, that the less symmetrical (in comparison with iodides) ionic close order in nitrates has greater capacity for crystallization from ternary solutions.

SUMMARY

1. Solubility in the systems $NH_4NO_3 - NH_4I - H_2O$ and $KNO_3 - KI - H_2O$ at 25° was studied.

2. Solubility in the systems named was compared with the structures of the component salts and their saturated solutions.

3. The varying solubility of salts in the studied systems is determined to a certain degree by the relative stability of the ionic close order taking part in the crystallization of salts from saturated solutions: the more stable this order is, the less soluble is the salt.

4. Joint solubility in both systems is characterized by a linear relation between $x_0 - x$ (moles of salted-out salt) and y (moles of dissolved salt).

5. The linear relation between $x_0 - x$ and y, its representation for KNO_3 by two straight lines of different slope, and the difference in displacement coefficients indicate with one accord, that joint solubility is determined by the structural state of saturated solutions.

LITERATURE CITED

1. P. S. Bogoyavlenskii, Doklady Akad. Nauk SSSR 101, 865 (1955).
2. P. S. Bogoyavlenskii, Uchenye Zapiski Shankhaiskogo Univ. Futan 2, 387 (1957).
3. P. S. Bogoyavlenskii, Zhur. Fiz. Khim. 32, 2035 (1958).
4. P. S. Bogoyavlenskii, et al., Uchenye Zapiski Shankhaiskogo Univ. Futan 1, 92 (1958).
5. J. Bernall and R. Fowler, J. Chem. Phys. 1, 515 (1933).
6. A. F. Kapustinskii and O. Ya. Samoilov, Zhur. Fiz. Khim. 26, 918 (1952).
7. O. Ya. Samoilov, Structure of Aqueous Electrolyte Solutions and Hydration of Ions [in Russian] (Izd. AN SSSR, Moscow, 1957).
8. M. I. Shakhparonov, Zhur. Fiz. Khim. 27, 111 (1953).
9. M. A. Klochko, Doklady Akad. Nauk SSSR 82, 261 (1952).
10. A. F. Kapustinskii, Zhur. Fiz. Khim. 32, 1648 (1958).
11. N. K. Voskresenskaya and G. N. Yankovskaya, Izvest. Akad. Nauk SSSR, Otdel. Khim. Nauk 1, No. 3 (1945).
12. N. K. Voskresenskaya and K. S. Ponomareva, Zhur. Fiz. Khim. 20, 433 (1946).
13. A. F. Wells, Structure of Inorganic Substances [Russian translation] (IL, Moscow, 1948).
14. L. Pauling, Nature of the Chemical Bond [Russian translation] (Goskhimizdat, Moscow, 1947) p. 321.
15. B. F. Ormont, Structure of Inorganic Substances [in Russian] (GTTI, Moscow-Leningrad, 1950).
16. O. K. Rice, Electronic Structure and the Chemical Bond [Russian translation] (IL, Moscow, 1949) p. 254.
17. R. Evans, Introduction to Crystal Chemistry [Russian translation] (Goskhimizdat, Moscow, 1948).
18. A. Seidell, Solubilities of Inorganic and Organic Compounds (New York, 1928).

INVESTIGATION OF THE STRUCTURE OF CERTAIN UNSATURATED COMPOUNDS BY THE METHOD OF COMBINATION SCATTERING OF LIGHT

Ya. S. Bobovich and V. V. Perekalin

S. I. Vavilov State Optical Institute, Leningrad
Translated from Zhurnal Struktornoi Khimii, Vol. 1, No. 3, pp. 313-318,
September-October, 1960
Original article submitted February 4, 1959

The intensity and, in part, degree of depolarization of the Raman lines of styrene and 21 nitro compounds were investigated. It was shown that these spectral parameters make it possible to reach conclusions on certain structural details of the molecules and on the connection with the properties of their electron shells.

INTRODUCTION

One of the important parameters of the individual chemical bond and the molecule as a whole is the polarizability α. Being a tensor quantity, the molecular polarizability is usually expressed in the form of an ellipsoid. In the course of vibratory motion of nuclei the ellipsoids of polarizability α undergo periodic deformations. The character of these deformations is represented in turn by the ellipsoid of the derivative of polarizability $\frac{d\alpha}{dq}$ with respect to the normal vibration coordinate q. The form of this ellipsoid often can be estimated directly through a simultaneous study of the intensity and state of polarization of Raman lines. Since the ellipsoids of α and $\frac{d\alpha}{dq}$ coincide in orientation in some cases [1], indirect evidence on the relative polarizabilities of molecules and individual bonds and groups can be obtained from Raman spectral data [2].

Conjugated multiple bonds occupy a special place in Raman spectroscopy. As experiment shows, conjugation has an extremely marked effect on the intensity of Raman lines owing to the great polarizability of π electrons. Hence, intensities in Raman spectra may be used for objective characterization of the degree of conjugation in such systems. Information of this kind is especially valuable because Raman lines, being characteristic in contrast, for instance, to ultraviolet absorption bands, make it possible to draw conclusions on local variations in the electron cloud, and not only on the behavior of the molecule as a whole.

Extensive experimental investigations of the effect of different structural factors (in particular, conjugation) on the intensity of Raman lines of various compounds were conducted by Shorygin and his co-workers [3].

In the present work a new class of substances important in practical synthesis – unsaturated nitro compounds – was investigated in the aspects noted above, apparently for the first time.

In this case, in order to obtain the fullest possible information on the behavior of different parts of the molecule, we studied the intensity and state of polarization of lines corresponding to vibrations of the nitro group, the double carbon-carbon bond, and the benzene ring.

Wave Numbers (in cm^{-1}), Intensities (on a scale of arbitrary units), and Degrees of Depolarization of Certain Raman Lines in the Spectra of Styrene and Unsaturated Nitro Compounds

Compound	Symmetrical vibration of the NO_2 group	Antisymmetrical vibration		Vibration of the C=C double bond
		NO_2 group	benzene ring	
I CH_3NO_2	1380 — 1400 (0,02, ρ = = 0,32)	1555 (0,005, ρ = = 0,74)	—	—
II $CH_3CH_2CH_2CH{=}CH{-}NO_2$	1340 (0,36)	1510 (0,054)	—	1650 (0,187)
III $CH_3CHCH{=}CH{-}NO_2$ (CH$_3$ branch)	1340 (0,38)	1510 (0,042)	—	1650 (0,183)
IV 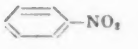	1345 (0,75, ρ = = 0,22)	1510 (0,04, ρ = = 0,72)	1610 (0,16, ρ = = 0,55)	—
V 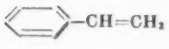	—	—	1610 (0,30, ρ = = 0,55)	1640 (0,42, ρ = = 0,28)
VI 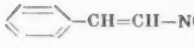	1320 (9, ρ = = 0,32)	?	1600 (2,4, ρ = = 0,43)	1630 (4,3, ρ = = 0,35)
VII 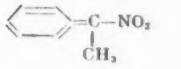	1325 (4,3)	?	1600 (1,3)	1660 (2,3)
VIII 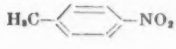	1340 (1,5 ρ = = 0,32)	?	1600 (0,41)	—
IX 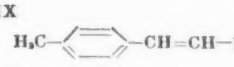	1335 (10,6)	1510 (0,9)	1620 (4,1)	1640 (4,2)
X 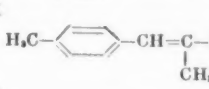	1320 (7,3)	?	1615 (2,6)	1660 (3,7)
XI 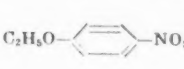	1340 (5, ρ = 0,42)	1500 (0,2, ρ = = 0,50)	1600 (1, ρ = 0,50)	—
XII 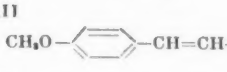	1325 (40, ρ = = 0,39)	1500 (3,7)	1600 (19, ρ = = 0,38)	1625 (10, ρ = = 0,30)
XIII	1305 (26)	?	1590 (10)	1640 (10)
XIV 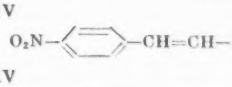	1335 (3,4)	1510 (0,45)	1590 (4,1)	1630 (4,8)
XV 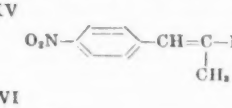	1345 (2,8)	?	1600 (3)	1665 (3)
XVI	1340 (30)	?	1590 (39)	1630 (27)
XVII 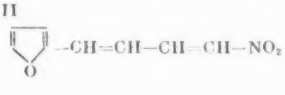	1335 (255)	?	—	1620 (95)

Table (Continued)

Compound	Symmetrical vibration of the NO_2 group	Antisymmetrical vibration		Vibration of the C=C double bond
		NO_2 group	benzene ring	
XVIII	1335 (16, ρ = = 0,36)	1510 (2,8)	1610 (50, ρ = = 0,41)	1625 (18, ρ = = 0,39)
XIX	1325 (14, ρ = = 0,43)	1515 (0,7)	1610 (25, ρ = =0,49)	1660 (11, ρ = = 0,43)
XX	1340 (0,4)	1520 (0,13)	1595 (0,14)	—
XXI 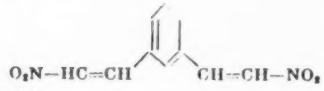	1340 (8)	1510 (1,0)	1595 (3,56)	1630 (5,4)
XXII 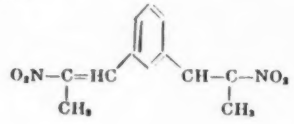	1325 (3,5)	1510 (0,20)	1610 (1,3)	1665 (2,8)

Experimental

The investigation was conducted by means of a photoelectric instrument [4]. The solvent was acetone in all cases. The intensity of nitro-group vibration lines was measured with respect to the 1430 cm^{-1} line, whereas that of benzene-ring and C=C bond vibration lines was measured with respect to the 1710 cm^{-1} line of acetone. The spectral aperture width was about 16 cm^{-1}. In this case, no appreciable differences in the half-width of the measured lines were observed. The choice of wider apertures was limited by the requirement that benzene-ring and C=C bond vibration lines having nearly the same wave number be resolved.

The spectra were excited by the 4358 A line of a low-pressure mercury spectrum tube [5]. In this case the conditions of the investigation were very close to resonance for many substances. The concentration of the great majority of substances varied from 10^{-1} to 10^{-3} M, which practically excluded the possibility of molecules of these substances interacting among themselves. The reproducibility of results was ± 3-4 % for intensities, ± 0.01-0.03 for degrees of depolarization, and ± 5 cm^{-1} for wave numbers.

Discussion of Results

A clear idea as to how strongly the molecular structure and character of conjugation affect the intensity of Raman lines may be obtained from a comparison of the data given in the table. For the simplest nitro compound – nitromethane (I) – the intensity of the symmetrical valence vibration of the nitro group is equal to 0.02 in the chosen units. In the case of the paramethoxy derivative of nitrostyrene (XII) the intensity of this vibration is 40, and for a nitro compound containing two double carbon-carbon bonds and a five-membered furan ring, all conjugated (XVII), the intensity reaches 255.

Being very sensitive to conjugation, the lines of different vibrations vary differently in intensity, depending on the molecular structure. The intensity of the antisymmetrical benzene-ring vibration is the most strongly affected. This may be illustrated by the example of compounds VI, XII, XVI, and XVIII. It is evident from comparison of these data, that the intensity of the NO_2-group vibration changes at least 4.5-fold, whereas the intensities of the ring and C=C bond vibrations change about 20- and 6-fold, respectively. The absence of "covariance" in the intensities of different vibrations also merits attention: the intensity of the ring vibration

is greatest for the symmetrical dinitro derivative (XVIII), that of the C=C bond vibration is greatest for another dinitro derivative (XVI), and that of the nitro-group vibration is greatest for the paramethoxy derivative of nitrostyrene (XII). Thus, the effect of conjugation apparently depends on the inductive influence of the groups. The pronounced influence of nucleophilic substituents in the para-position of the benzene ring on the nitro group vibration intensity has been observed many times in the case of aromatic nitro compounds [3].

If the spectra of substances VI and XVIII are compared, it is evident that the presence of symmetrically oriented groups and bonds in conjugated systems not only does not diminish, but on the contrary, quite sharply increases the intensity of every vibration.* This is observed also in the spectra of analogous compounds in which however, hydrogen on an ethylenic carbon atom is replaced by a methyl group (XII) and (XIX). For unsymmetrical dinitro derivatives (XIV and XV) the intensities of benzene-ring and double-bond vibrations are increased, whereas the intensity of the nitro-group vibration, on the contrary, is diminished in comparison with compounds VI and VII. Since the table contains intensity data referred to a single NO_2 group on the basis of their assumed equivalence, the latter result – relative weakening of the nitro-group vibration – is nothing other than evidence that this hypothesis is incorrect. Obviously, it is more correct to regard the two NO_2 groups in compounds XIV and XV as nonequivalent. The NO_2 group attached directly to the ring probably makes a smaller contribution to the measured intensity. This means that the position of groups has a substantial influence on conjugation. It may be presumed that the vibration frequencies of each nitro group also differ. This is subject to experimental verification.

The facts regarding the influence of symmetrically oriented groups and bonds in conjugated systems may be qualitatively explained on the basis of quantum-mechanical concepts where a molecule with conjugated bonds is regarded as a potential box in which the boundary conditions are represented by infinitely high barriers, and the presence of single bonds is represented by finite barriers within the box. According to Vol'kenshtein and Yazykova [6], the intensity of the symmetrical valence vibration of the polyene chain must depend to an extremely great extent on the length L of the "box" ($I \sim L^6$). Presumably, the dependence of I on L will also be very pronounced for any other vibrations. On the other hand, according to the data of Veselov and Rekasheva, the form of the barrier at the boundaries is nearly independent of α, $d\alpha/dq$, and the intensity of the Raman line [7]. The influence of certain end groups in the molecules, in particular, obviously affects the change of form of the barrier at the boundaries. Hence, it is conceivable that in symmetrical dinitro derivatives the factor of increase in the length L of the "box," which determines the observed effects, predominates to a considerable degree.

Comparison of para- and meta- derivatives between themselves (XVIII, XIX, and XXI, XXII) shows that the intensities of all lines in the latter group of compounds, especially benzene-ring vibration lines, are greatly diminished. From Shorygin's works [3] it is known that a similar picture is observed in the spectra of aromatic compounds. Clearly, differences in the conditions of conjugation are manifested here. In this case the benzene-ring vibration is changed most of all. Here, as in the examples considered earlier, the special position of the benzene ring is evidently explained by the fact that the corresponding vibration encompasses the whole system of conjugated bonds at once and is not localized in one bond. In the given case, therefore, the summary effect of conjugation is observed.

The data given in the table are of some interest if one compares compounds VI, IX, XII, and XIV among themselves on the one hand and compounds VII, X, XIII, and XV on the other. Evidently, the replacement of hydrogen on the ethylenic carbon atom by a methyl group invariably leads to appreciable weakening of the entire spectrum. It may be assumed that the introduction of methyl groups in the indicated position disturbs the planarity of the molecule; this results in weakening of the conjugation and hence the intensity of the Raman lines. Thus, these results of the investigation indicate that the nitro groups in molecules VII, X, XIII, and XV and, at least, the benzene rings do not lie in the same plane.

Let us turn now to the description and discussion of the results of polarization measurements. The degree of depolarization ρ of the C=C bond vibration line, according to the tabular data, lies in the interval 0.28 to 0.43. The more favorable the conditions for conjugation are, the greater is the degree of depolarization. For

* The vibration intensities in the table relate to the same number of NO_2 groups and C=C bonds.

the characteristic bond vibration, as well as the diatomic molecule, the degree of depolarization may assume a maximum value of 0.5. This corresponds to maximum anisotropy of the ellipsoid $d\alpha/dq$ [1]. This means that in the case under consideration the ellipsoid $d\alpha/dq$ extends further and further along the axis connecting the carbon atoms, as the effect of conjugation increases. Obviously, the polarizability α of the C=C bond also increases along this axis, together with the stated effect. Our data on the behavior of the C=C bond on conjugation agree with literature data for other molecules [8, 9].

Earlier one of us, together with Vol'kenshtein, measured the degree of depolarization of the symmetrical valence vibration line of the nitro group in certain aromatic nitro compounds [2]. In this case, it was shown that the introduction of nucleophilic substituents in the para-position of the benzene ring causes systematic elongation of the ellipsoid $d\alpha/dq$ oriented along the symmetry axis of the nitro group and retaining this orientation. It is of definite interest to follow the influence of a double carbon-carbon bond in the side-chain on the degree of depolarization of this vibration. For this purpose, we compare nitrobenzene (IV) ($I_1 = 0.75$, $\rho_1 = 0.22$) and nitrostyrene (VI) ($I_2 = 9$, $\rho_2 = 0.32$). Both the intensity and the degree of depolarization of the line are greater for VI than for IV. Hence, it may be considered that for the given molecules ellipsoid $d\alpha/dq$ and, quite probably, ellipsoid α simply extend in one direction – along the symmetry axis of the nitro group.

Apparently, a different picture is observed in the case of para-ethoxynitrobenzene (XI) ($I_1 = 5$, $\rho_1 = 0.42$) and para-methoxynitrostyrene (XII) ($I_2 = 40$, $\rho_2 = 0.39$). Since the intensity and the degree of depolarization of the line vary in opposite directions on passing from the first compound to the second, this should be attributed to simultaneous elongation of all axes of the nitro-group ellipsoid $d\alpha/dq$. It may be assumed on the preceding grounds, that a change of molecular structure entails a change in the polarizability of the nitro group in all directions • in the case under consideration.

The behavior of the degree of depolarization of the benzene-ring vibration line is also interesting. As is evident from the tabular data, this line is distinctly polarized in the spectra of molecules distinguished by favorable conditions for conjugation. Thus, for instance, in the case of para-methoxynitrostyrene (XII) the degree of depolarization of this line is 0.38. The latter fact, it would seem, indicates a change in the form of the "antisymmetrical" ring vibration as a result of bond conjugation (see also [9]).

The ~ 1600 cm^{-1} benzene-ring line under consideration belongs to the doubly degenerate vibration E(A + B). It may be assumed in principle that in molecules with good conjugation the first component is strengthened as a result of optical resonance, only if it corresponds to a longer-wave band. Thereby the systematic decrease in the degree of depolarization of this line (the first component is polarized, in contrast to the second) is also explained. This explanation, however, is contradicted by the fact that for the antisymmetric nitro-group vibration, which is not degenerate, the degree of depolarization apparently varies in a similar manner with respect to the conditions of conjugation (see IV and XI). As yet we have available no data on the behavior of this vibration of the nitro group in other compounds. Nevertheless, on the basis of all the measurements already carried out, it is suggested that the increase and decrease in the degree of depolarization of lines that are polarized and depolarized, respectively, in the absence of conjugation, is a general consequence of the proximity of the exciting line to the actual absorption band; i.e., it is due to the phenomenon of optical resonance. The correctness of this generalization can be verified by measuring the state of polarization of Raman lines excited in a given substance by different lines of the mercury tube.

The authors thank P. P. Shorygin for a fruitful discussion of the results.

LITERATURE CITED

1. M. V. Vol'kenshtein, M. A. El'yashevich, and B. I. Stepanov, Vibrations of Molecules [in Russian] (GITTL, 1949) Vol. II.
2. Ya. S. Bobovich and M. V. Vol'kenshtein, Doklady Akad. Nauk SSSR 71, 1045 (1950).
3. P. P. Shorygin, Doctoral Dissertation (Fiz.-Khim. Inst. im L. Ya. Karpov, Moscow, 1949).

• The accuracy of measurement of ρ is compatible in principle with these considerations.

4. Ya. S. Bobovich and D. B. Gurevich, Zhur. Eksp. i Teoret. Fiz. 27, 318 (1954).
5. Ya. S. Bobovich and V. M. Pivovarov, Uspekhi Fiz. Nauk 60, 689 (1956).
6. M. V. Vol'kenshtein and S. M. Yazykova, Doklady Akad. Nauk SSSR 104, 834 (1955).
7. M. G. Veselov, Doctoral Dissertation (Izd. LGU, 1952); T. N. Rekasheva, Master's Thesis (Izd. LGU, 1954).
8. M. M. Sushchinskii and V. I. Tyulin, Doklady Akad. Nauk SSSR 95, 505 (1954).
9. T. V. Yakovleva, Author's Abstract, Master's Thesis (Vysokomolek. Soed. AN SSSR, Leningrad, 1953).
10. K. Kohlrausch, Raman Spectra [Russian translation] (IL, Moscow, 1952).

ACCEPTOR-DONOR CONCEPTS APPLIED TO EXTRACTION*

A. V. Nikolaev, N. M. Sinitsyn, and S. M. Shubina

Institute of Organic Chemistry, Siberian Branch of the Academy of Sciences of the USSR

Translated from Zhurnal Strukturnoi Khimii, Vol. 1, No. 3, pp. 319-323, September-October, 1960
Original article submitted December 16, 1959

On the basis of acceptor-donor concepts and the inductive effect, and also experimental data (infrared spectroscopy, effectiveness of extraction, stability of molecular compounds, etc.) a definition is given of the special features of organic extraction agents which give them the ability to extract inorganic substances from aqueous solutions. Special attention is paid to the polarity of the organic molecules, to methods of changing this parameter, and also to the availability of extraction agents with higher and lower boundary values of polarity. Certain classes of compounds for further investigation as extraction agents are discussed.

Recently a series of organic derivatives of phosphoric acid have been suggested as extraction agents for inorganic substances [1, 2, 3]. Tributyl phosphate or TBP, $(C_4H_9O)_3PO$, has been especially widely used and has attained industrial importance [4]. The aim of the present article is to discuss the structure of this group of extraction agents on the basis of acceptor-donor concepts and the inductive effect in order to establish an optimal region of composition both for extraction and for purification. Our previous paper contained the basic ideas of this investigation and below we shall use them and, if this is successful, generalize them.

The starting point for the discussion is the important experimental fact (established by us [3] and also by foreign workers [1]) that in extraction the basic interaction between the extraction agent and the substance extracted proceeds through the oxidic oxygen on the phosphorus, and not the ester oxygen. This is shown on the one hand by the change in the P=O vibration frequency in the infrared spectrum and on the other hand by the sharp rise in extraction as the ester groups are changed into alkyl groups in compounds of the tributyl phosphate type. The partition coefficients rise a hundred- or a thousand-fold. In other words, not only does the ester group not facilitate extraction, it actually makes it more difficult.

In the previous report [2] two circumstances were noted: displacement of the electron cloud of the extraction agent toward the oxidic oxygen increased the polarity and the extraction power when an increase in the inductive power of the organic substituent occurred, in particular when the ester group was changed into an alkyl substituent. Hence, it was concluded that in the series below, which represents the growth of positive inductive effect

$$CH_3 < C_2H_5 < CH(CH_3)_2 < n\text{-}C_3H_7 < C(CH_3)_3 \quad \text{etc.},$$

there should be an increase in extraction power of the corresponding derivatives; this conclusion has undoubted practical interest in the selection of extraction agents.

* Reported at the symposium on extraction in Moscow, December, 1959.

Several authors have shown that the electron cloud is displaced toward the oxidic oxygen in compounds of the tributyl phosphate type [5]. However, the polarity of the molecule will be determined not only by this displacement but also by evident movement of electrons to the ester oxygens, though this is far less than that to the oxidic oxygen. As a result of this the positive charge on phosphorus is somewhat increased $O^- - P^+ \rightleftharpoons O^-$ which leads to a decrease in the polarity of the group as a whole. From this point of view the change of the ester oxygen into a substituent with a more positive inductive effect decreases this secondary negative charge and increases the polarity of the acidic oxygen:

Such an effect would be the clearer the larger the inductive properties of the alkyl R'. This explains the widespread use of tributyl phosphate and not trimethyl, triethyl or tripropyl phosphates which have substituents with smaller inductive effects. Further increase in the chain length of the alkyl substituent should be discussed, but the increased inductive effect dies out by degrees. All octyl derivatives for example should clearly be more effective than the corresponding butyl derivatives.

Similar conclusions can be drawn based on the negative inductive effect, the value of which for different substituents generally follows the series

$$F > Cl > Br > I > OCH_3 > C_6H_5 \ldots$$

Thus, halogen substituted alkyls, just like the OR group, reduce the polarity of the oxide group because of their negative inductive effect according to the scheme.

This has already been mentioned above in another connection. Aromatic substituents with various inductive properties can change the polarity of the whole molecule within wide limits.

Thus, using two routes to the solution of the problem the conclusion is reached that the introduction of an alkyl substituent (without polar groups) leads only to an increase in positive inductive effect and to an increase in the polarity of the oxidic oxygen and of the molecule as a whole. Using the series which gives the value of the positive inductive effect many useful results can be obtained. For example, by changing all the ester groups into the corresponding alkyl groups one can achieve the maximum positive inductive effect, the maximum polarity and in fact the maximum extraction. In fact, as our experiments have shown [3], tributylphosphine oxide gives maximum extraction; a very stable molecular compound of tributylphosphine oxide with uranyl nitrate was successfully separated. This compound must be considered to be more polar than the extraction agent because it precipitates from nonpolar solvents (limiting high-boiling hydrocarbons – LHH) in which the oxide itself is very soluble. Such compounds possess basic properties which are connected with their great polarity.

Substitution of two alkyl groups for two ester groups in TBP* leads to a polarity greater than that of the starting material, but less than that of the alkylphosphine oxide. Strongly polar addition products are not formed in this case, and the normal effect of an increased partition coefficient is observed; for uranyl, plutonium (IV) and others it is increased one-hundred fold whereas for ruthenium nitrosonitrate it only increases some 8-10 times [2].

A similar change of only one ester group leads, for example, to the dibutyl ester of butylphosphonic acid (DEBP). This has greater polarity than TBP, but less polarity than the butyl ester of dibutylphosphonic acid

* For example, the butyl ester of dibutylphosphorus acid, BEDP.

(BEDP). The partition coefficient is correspondingly increased by comparison with TBP–15-20 times as great for uranyl and plutonium, but only twice as great for ruthenium.

As can be seen extraction with BEDP and DEBP of the two groups of substances discussed is increased in such a way that the purification of such difficult substances as ruthenium is increased ten-fold by comparison with extractions using TBP.

Interesting results can be obtained by changing the butoxy-groups in TBP into other radicals such as methyl, ethyl, propyl, phenyl, etc. Increased polarity could be expected and therefore increased extraction and purification; for example the ethyl ester of diethylphosphonic acid would be more polar than TBP and perhaps also than DEBP. Besides the various substituents of the type discussed (alkyl, phenyl, etc.,) the amino-group should be especially effective – it is a typical group with a large positive inductive effect. In this case one could avoid the original change in polarity found in the phosphine oxides (see above).

The esters of sulfuric acid

and the sulfones

are too polar for use as extraction agents but one could expect extraction properties to appear in derivatives of sulfonic acids.

In practical organic chemistry dimethylsulfoxide $(CH_3)_2S \rightarrow O$ has obtained recognition. The molecule of this compound fits in well with the interpretation used for the view point under discussion. Dimethylformamide, $(CH_3)_2N-CH=O$, also has the properties now recommended for a solvent for organic compounds as can be easily understood. This molecule contains an amido-group with a large inductive effect and an oxygen with a negative charge. The amido-group reinforces this charge and a polarity as great as that in aqueous solutions is attained [6].

These two examples show that the statements discussed above have general value, and it further appears possible to approach the definition of extraction agents with optimal extracting power (for inorganic and certain organic compounds) starting from the structure of these molecules. Extraction agents may be substances containing: a) polar or semipolar groups (oxygen, sulfidic sulfur, etc.) attached to multivalent atoms (P, S, C, etc.) capable of carrying a positive charge, and b) groups with an inductive effect sufficient to promote the attainment of polarity by the whole molecule. The polarity should not rise to such an extent that the extraction agent begins to be soluble in water or that it gives strongly polar molecular compounds which are insoluble in the extraction agent and in nonpolar solvents. At the same time extraction agents of small polarity may not cause extraction because they are unable to form molecular compounds.

The upper and lower limits of polarity should be further defined experimentally; within this polarity range will be included the true extraction agents of varying types.

Some ideas on the mechanism of addition of the extracted substance to the extraction agent are now appended. The molecular compound of phosphorus oxychloride with stannic chloride (m. p. 54°, b. p. 118°) has been known for a relatively long time. Thus substance is nonpolar since it dissolves in nonpolar solvents and its conductivity in the molten state is very small. A clear analogy in composition with this is observed in the compound $2(C_4H_9O)_3PO \cdot UO_2(NO_3)_2$ found in the study of the extraction equilibrium with tributyl phosphate

---

* Our attention was drawn to these two compounds by corresponding Member of the Academy of Sciences of the USSR, N. N. Vorozhtsov.

[8]. This is unstable in comparison, for example, with the sulfate complex of uranyl ($K_{inst} = 0.2$) and an aqueous solution of sulfate re-extracts uranyl nitrate from TBP. We have isolated [3] the strongly polar compound with tributylphosphine oxide which is very stable. The composition of this is analogous to those discussed above: $2(C_4H_9)_3PO \cdot UO_2(NO_3)_2$. This compound is insoluble in nonpolar solvents (IHH).

Kuznetsov [9] later on correctly turned his attention to oxygen-containing compounds which are used in the extraction of a large number of inorganic compounds. For example, the compound of uranyl nitrate with diethyl ether [10] is well known. From a different point of view aryldiazonium salts of the type $ArN_2Cl \cdot MCl_3$ (where M = Fe^{3+}, Sb^{3+}, As^{3+}, Bi^{3+}, and Hg^{2+}) are also of interest. These separate from organic solvents; the salt molecules in these compounds can be substituted.

In Vosnesenskii's book [7] published twenty-two years ago it was noted that the bonds in inner complex compounds with stannic chloride were weakened on the introduction of negative substituents:

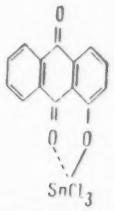

Typical inner complex salt with a red color

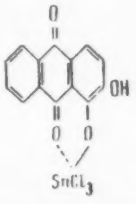

A more soluble and dissociable salt with a dark violet color

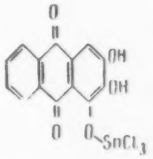

Unstable easily hydrolyzed salt

It was also noted that meta- and para-hydroxyketones formed addition compounds with $SnCl_4$, whereas ortho-hydroxyketones initially gave addition products which then eliminated hydrogen chloride and were transformed into inner-complex compounds.

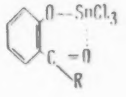

If instead of a hydroxy group a methoxy-group was placed in the position ortho to the carbonyl group then a more stable addition product was obtained, which was only transformed into an inner complex salt on heating.

These few examples are sufficient to show clearly the different possibilities for weakening and strengthening the bonds in addition compounds of salts with organic substances. Many more similar examples could be cited.

It should be noted that the large field of investigation concerned with the structure of extraction agents and their ability to extract inorganic compounds which is being opened up is little understood and any advance in it will be very useful and important in practice.

In conclusion attention should be paid to one particular circumstance that interests us, namely that alkyl derivatives should be relatively more stable to hydrolysis and irradiation than esters.

LITERATURE CITED

1. L. Burger, J. Phys. Chem. 5, 62, 520 (1958); C. A. Blake, et al., Second International Conference on the Peaceful Uses of Atomic Energy, Geneva, 1958, No. 1550; I Byrke, et al., Second International Conference on the Peaceful Uses of Atomic Energy, Geneva, 1958, No. 497; P. Brow, et al., Second International Conference on the Peaceful Uses of Atomic Energy, Geneva, 1958, 15/P/31 IK, 1958; V. B. Shevchenko and V. S. Smelov, Atomnaya Energ. 6, 2, 140 (1959).*

* Original Russian pagination. See C. B. translation.

2. A. V. Nikolaev and N. M. Sinitsyn, Doklady Akad. Nauk SSSR 127, 1, 117 (1959).*
3. A. V. Nikolaev, S. M. Shubina and N. M. Sinitsyn, Report in the Symposium on Extraction [in Russian] GEOKhI Akad. Nauk SSSR, December, 1959).
4. J. C. Warf, J. Am. Chem. Soc. 71, 3257 (1949).
5. R. Hunter, Electronic Theory in Chemistry [Russian translation] (ONTI, Moscow, 1937); O. A. Reutov, Theoretical Problems in Organic Chemistry [in Russian] (Izd. MGU, 1956) p. 39.
6. A. Weissberger, et al., Organic Solvents [Russian translation] (IL, Moscow, 1958).
7. S. A. Voznesenskii, Inner Complex Compounds and Their Value in Analytical Chemistry [in Russian] (GONTI, Moscow, 1938).
8. A. V. Nikolaev, A. G. Kurnakova, and I. I. Yakovlev, Reports on the Seventh Mendeleev Conference [in Russian] (1959) No. 1, p. 97.
9. V. I. Kuznetsov, Uspekhi Khim. 23, 6, 654 (1954).
10. L. Katzin and U. Sullivan, J. Colloid Chem. 55, 346 (1951).
11. A. V. Nikolaev, Khim. Nauk i Prom. 5, 554 (1956).

* Original Russian pagination. See C. B. translation.

CONDITIONS OF SOLUBILITY OF ORGANIC SUBSTANCES IN THE SOLID STATE

A. I. Kitaigorodskii

Institute of Heteroorganic Compounds, Siberian Branch of the Academy of Sciences of the USSR

Translated from Zhurnal Strukturnoi Khimii, Vol. 1, No. 3, pp. 324-332, September-October, 1960
Original article submitted December 30, 1960

An attempt has been made to establish the connection between the conditions of solubility and the conditions of equilibrium for a solid phase in a binary organic system with, on the one hand, the physical properties of the crystals of the pure components and, on the other hand, of the solid solutions. It is shown that it is possible to draw conclusions about the structure of the solid solutions and the characteristic lattice vibrations from the thermodynamic functions of the organic crystals obtained from the known diagrams of state.

Introduction

In our first paper [1] on this subject the conditions for the formation of a continuous series of solid solutions was principally discussed. The correctness of the ideas put forward in this paper was confirmed experimentally in the structures laboratory of the INÉOS of the Academy of Sciences of the USSR. In fact, such systems as, for example, dibenzyl – stilbene, anthracene – phenanthrene, and acridine – anthracene appeared to be erroneously attributed to systems with continuous solubility.

The present report is concerned with the other side of the question – the conditions of solubility for organic substances when the formation of mixed crystals is a much more advantageous process than crystallization of the components separately. These conditions were not discussed in much detail. Only the conditions for the solubility of an organic substance in the solid state were formulated, and this without substantiation. It was asserted that: if, mentally, one removes a molecule from the crystal and in its place puts the "foreign" molecule then solubility will occur if such a change is possible with the retention of intermolecular distances which differ only negligibly from the normal ones. We believed that these conditions are necessary and sufficient for molecular crystals.

Now we are attempting to establish the thermodynamic basis and a quantitative expression for the conditions of solubility for organic substances in the solid state.

On replacing a molecule in the crystal of A by a molecule of the impurity B the free energy of the A crystal is changed. First, introduction of a foreign molecule leads to a change in the lattice energy which can be called the lattice tension; the free energy is changed by the quantity ΔU_{tens}. In the second place the free energy is decreased by a quantity $\Delta F_{mix} = T|\Delta S_c|$, where $\Delta S_c = R[(1-x)\ln(1-x) + x\ln x]$ is the configuration entropy. Thirdly, the substitution of a molecule leads to a change in the free energy of the vibration spectrum by a value ΔF_{vib}. Fourthly and finally, one should take into account the possibility of a change in the conformation of the impurity molecule on introducing it into a solid solution. If the difference in the conformation energies is ΔE, then by comparison with the pure substance, the free energy of the solution changes by $x\Delta E$, where x is the impurity concentration.

Thus, if a solid solution of B in A is formed then its free energy will be

$$F_A + \Delta U_{tens} + \Delta F_{mix} + \Delta F_{vib} + x\Delta E.$$

At a given temperature, it is possible either to form a mixture with free energy $xF_B + (1 - x)F_A$, or to form a solid solution. If the solution is to be formed, it is necessary that its energy should be the smaller, i.e.,

$$F_A + \Delta U_{tens} - T|\Delta S_c| + \Delta F_{vib} + x\Delta E < xF_B + (1-x)F_A.$$

Since the free intramolecular energy (interaction between molecules does not affect the intramolecular energy) is in the same form in both halves of the inequality, then

$$\Delta U_{tens} - T|\Delta S_c| + \Delta F_{vib}^{cr} + x\Delta E < x(F_B^{cr} - F_A^{cr}),$$

where F^{cr} is the "crystalline" part of the free energy. Similarly,

$$T|\Delta S_c| > \Delta U_{tens} + \Delta F_{vib}^{cr} + x(F_A^{cr} - F_B^{cr} + x\Delta E),$$

i.e., the configuration effect of mixing should exceed the sum of four terms: 1) the strain energy, 2) the change in free energy due to the change in vibration spectrum of the crystal lattice, 3) an additive change in the crystal part of the free energy, and 4) the energy due to the change in conformation of the impurity molecules. These four factors determine the solubility conditions.

Thus the following factors can be obstacles to solubility: 1) an increase in the high strain due to the impossibility of placing the foreign molecules in the normal lattice; 2) an increase in free energy of the molecular lattice vibrations which can lead to an increase in the characteristic temperature of the crystal if the substitution of the foreign molecule leads to a growth in the vibration frequency of the molecule; 3) the crystal B (the dissolved substance) possesses a considerably lower crystal part of the free energy than the crystal A; 4) the energy ΔE due to the change in conformation, which is necessary to make the dissolved molecule correspond geometrically to the solvent molecules, is very large.

As we shall show below, the free energies of organic crystals which do not contain hydrogen bonds and which are made up of molecules containing the same number of atoms differ very little from one another, i.e., $(F_A^{cr} - F_B^{cr})$ is small. Moreover, the parameter ΔF_{vib}^{cr} for weak solutions is negligible and in most cases negative. Therefore, if ΔU_{tens} is small, i.e., if the substitution does not lead to a large deviation from the normal intermolecular distances, then solubility is possible. These are our basic conditions of solubility which were put forward in [1].

However, one must take into account the influence of all three factors to explain the limits of solubility. The configuration entropy rises slowly and the inequality which is fulfilled for small concentrations x is transposed for large x if the tension becomes large or if the characteristic temperature rises considerably. However, if $F_B^{cr} < F_A^{cr}$, then it is possible for the solubility limit to fall. In an exactly similar way one can anticipate a limit to the solubility when ΔE is large for the solute.

Recently, we have only had available a few trustworthy values of the equilibrium interaction values for atoms of different sorts. These values differ by negligible amounts, as is shown by an analysis of the heats of sublimation of organic crystals, and we shall not discuss them. Leaving this we return to the question which we took for the present investigation, that the energy effects of mixing can lead only to an increase in energy since the presence of a foreign molecule in a crystal disturbs the equilibrium distances.

Factors which Determine Solubility

1. Strain energy. An estimate of ΔU_{tens} can be obtained by using the curve of interactions between atoms not linked by valence bonds. We shall assume that the foreign molecule does not distort the regularity of the basic crystal lattice. The distances between some atoms of the foreign molecule and the atoms of its immediate neighbors are changed: r_1 to $r_1 + \Delta r_1$, r_2 to $r_2 + \Delta r_2$, etc. From the interaction curve, we find the differences between $U(r_1)$ and $U(r_1 + \Delta r_1)$, between $U(r_2)$ and $U(r_2 + \Delta r_2)$, etc. The differences are summed and in this way we obtain the contribution U_{mol} of one foreign molecule to the total strain energy. In fact this estimate gives a limiting value of U_{mol} because dispersion of the tension will lower the energy.

By estimating U_{mol} and neglecting the possibility of tension between two molecules which are not nearest neighbors, we obtain for the strain energy:

$$\Delta U_{tens} = xU_{mol}.$$

If the limit of solubility is determined only by ΔU_{tens}, then a solubility greater than 1% is impossible when $xU_{mol} > T\,|\Delta S_c|$, i.e., at room temperature $T = 293°$ K when $U_{mol} > 3$ kcal/mole, because for a 1% solution at room temperature $T\Delta S \approx 0.03$ kcal/mole. In agreement with this the curve of interaction between nonbonded atoms, which we set up [2] for hydrocarbons by investigating the conformational tension in the molecule, gave two or three short interatomic distances within 20-30% of each other which lead us to the same limit.

Thus the geometric condition for the solubility of large molecules in a medium of small ones leads to a quantitative expression. It has been shown by us elsewhere [3] that the solubility of small molecules in a medium of large ones is in general greater than in the reverse case. This is quite natural if account is taken of the asymmetry of the interaction. In fact, one can get an estimate of the "open" part of the molecular surface. Taking into account our earlier paper [4] in which it was shown that the heat of sublimation L is proportional to the surface area of the molecule we can assume that the lattice energy increases in proportion to this part of the surface. Thus, if σ_A is the surface of the molecule A and intrusion of a molecule B "opened" to the neighboring molecule a surface $\Delta\sigma$, then the increase in energy will be $U_{tens} = Lx\ \Delta\sigma/\sigma_A$. For example, the solution of naphthalene in anthracene is connected with the exposure of six phenyl nuclei, i.e., a surface equivalent to two anthracene molecules. Thus (L = 20 kcal/mole) for 1% of impurity we have $\Delta U_{tens} \approx$ $\approx 0.02\ L \approx 0.4$ kcal/mole, i.e., larger than the configuration energy; consequently, solution is impossible.

A solubility greater than 1% is impossible with $0.01\ L\ \Delta\sigma/\sigma_A > 0.03$ kcal/mole (other factors being excluded). Since L oscillates between the limits 10-30 kcal/mole for most organic crystals, the solubility condition has the form $\Delta\sigma/\sigma_A < 0.2$, i.e., small molecules going into solution must not expose more than approximately 20% of the solvent molecule surfaces.

2. Difference in Free Energy of the Components. The crystalline part of the free energy of a molecular crystal can be put in the form

$$F = \epsilon + F_{trans} + F_{osc},$$

where ϵ is the lattice energy, F_{trans} and F_{osc} are the free energies of translational and oscillatory vibration of the molecule (all these parameters are negative).

Both the acoustic and optical energy of translational vibration can be estimated by Debye's formula

$$F_{trans} = -3RT \ln (T/\theta) - RT.$$

For each basic frequency of oscillatory vibration there is a contribution to the free energy equal to

$$F_{osc} = h\nu/2 + kT \ln [1 - e^{-(h\nu/kT)}].$$

Thus, in this simplified model the free energy of vibration is the sum of the energy of a point lattice (the points are the centers of gravity of the molecules) and of the energy of oscillatory vibration of the molecule.

All the parameters necessary for the calculations of F can be found experimentally. The lattice energy ϵ is found from the heat of sublimation F_{osc} from the infrared frequencies (30-130 cm^{-1} region). To calculate F_{trans} it is necessary to know the characteristic temperature θ of the crystal. The parameter θ for $T > \theta$ can be connected to the mean squared translational vibration.

$$\theta = \sqrt{\frac{3h^2T}{4\pi^2 mk\bar{u}^2_{trans}}}$$

The parameter $\bar{u}^2_{trans}$ is found from the temperature factor of x-ray dispersion in the following way. After constructing a series of electron densities, $\bar{u}^2_{trans}$ is estimated from the form of the peaks. In this way $\bar{u}^2_{trans}$ is estimated for the atoms of molecules close to the center of gravity and consequently only translational vibration is concerned.

The value of the characteristic temperature is estimated from Cruickshank's formula [5] for benzene, naphthalene and anthracene. For all three crystals the value of θ was shown to be close to 90° K. Hence, the corresponding part of the free energy at T = 300° K is $F_{trans} \approx -3$ kcal/mole. It is unlikely that this part of the free energy for crystals of the same type (i.e., without hydrogen bonds, of about the same molecular weight, and without especially heavy atoms) will differ from this value by more than 10-20%, since it is known from x-ray experiments that $\bar{u}^2$ and θ for very different organic crystals differ little from one another (with a relative value of $\bar{u}^2$ equal to $^3/_4$, the corresponding relative value of θ will be 0.87, which leads to an approximate 10% change in F_{trans}).

Gross and his co-workers and also some French workers [6] have presented data on the oscillatory frequency in various organic crystals. Below are given only those frequencies (cm^{-1}) which have been identified as due to oscillations:

Benzene	105 and 63	p-Dichlorobenzene	27, 46 and 54
Diphenyl ether	100 and 30	p-Dibromobenzene	20, 38 and 93
Diphenyl	88 and 50	p-Diiodobenzene	15, 25 and 93
Naphthalene	118, 75 and 50	m-Diiodobenzene	24, 79 and 101
p-Diphenylbenzene	85 and 42	o-Diiodobenzene	23, 74 and 127
Anthracene	120, 68 and 48		

At a temperature of 300° K the contribution to the free energy of a frequency of 100 cm^{-1} equals 0.27 kcal/mole, 50 cm^{-1} equals 0.76 kcal/mole, and 25 cm^{-1} equals 120 kcal/mole. Thus, in organic crystals without heavy atoms this part of the free energy lies within the limits -1 to -2 kcal/mole, which in the presence of heavy atoms is lowered to -3 or -4 kcal/mole.

The differences between the lattice energy and the heat of sublimation L in the cases which are of interest to us are small and are easily calculated to an accuracy of a few tenths of a kilocalorie per mole. In fact,

$$L = \varepsilon + A + (E_{tr} + E_{vr} + E_{vib})^{gas} - (E_{vib.\,lat} + E_{vib.\,mol}),$$

where A is the work of expanding a gas which is approximately equal to RT. The energies of motion of gaseous molecules are $E_{tr} \approx 3RT/2$ and $E_{vr} \approx 3RT/2$. It is assumed that the energy of intramolecular vibration changes negligibly and E_{vib} for a molecule in a gas or a crystal can be excluded.

With regard to the lattice vibration energy, in those cases which interest us $kT > h\nu$ and we have

$$E_{vib.\,lat} = N\bar{h\nu}/2 + 3RT,$$

where $\bar{h\nu}$ is the mean zero point energy. Since lattice vibration occurs at a limiting frequency of about 100 cm^{-1} which corresponds to an effective temperature of the order of 100° K, then the first term will equal 0.1 to 0.2 RT, i.e., it will not exceed 0.1 kcal/mole.

After simplification, we obtain

$$L \approx \varepsilon + RT,$$

i.e., at room temperature the lattice energy is less than the heat of sublimation by 0.6 kcal/mole. The precision of similar estimates of ϵ in organic compounds at 300-400° K is not lower than 0.2-0.3 kcal/mole, i.e., it corresponds to the precision of the measurements. Below are cited the heats of sublimation of some organic crystals (in kcal/mole):

Benzene	9.2	Tolane	21.2
Naphthalene	15.9	Stilbene	21.7
Dibenzyl	17.5	Anthracene	22.3
Phenanthrene	20.1		

In such crystals as anthracene or stilbene the contribution of the vibrational energy of the molecule is not large (about 1.5 kcal/mole), and the whole crystalline part of the free energy approaches 20 kcal/mole.

Now we can confirm the estimate of the parameter x $(F_1 - F_2)$ carried out above. The free energies of crystals constructed from organic molecules of similar shape do not differ by more than 4-5 kcal/mole. Corresponding to this the value of x $(F_1 - F_2)$ for a 1% solution will be of the order of 0.01 kcal/mole and in any case will be less than 0.1 kcal/mole.

3. Changes in the Vibrational Spectra of Crystals. The introduction of impurity molecules changes the vibrational spectrum of a crystal. These changes have been discussed theoretically by Lifshits and his co-workers [7]. In particular, at low concentrations, it is possible for small local vibrations to arise, which are not spread through the whole crystal. However, in the case of molecules which are similar in mass, its value is not large and the change in the mean square of the atomic motion $\bar{u}^2$ (measured directly by x-ray diffraction) can be taken as a measure of ΔF_{vib}. This method is widely used for metallic alloys. Only further investigation can show to what extent it can be applied successfully to molecular crystals. We believe that by this method the correct order of parameters can be obtained.

Let us assume that

$$\sqrt{\frac{\bar{u}_p^2}{\bar{u}^2}} = \frac{\theta}{\theta_p}$$

then using the Debye approximation, we get

$$\Delta F_{vib} = \frac{3}{2} RT \ln \frac{\bar{u}_p^2}{\bar{u}^2}.$$

Here it is supposed that the introduction of a foreign molecule principally affects the translational vibrations. The ratio of u^2_{tot} to u^2_{trans} is close to one, and for our rough estimate the ratio $\bar{u}_r^2/\bar{u}^2$ may be substituted for the ratio of the heat factors of x-ray dispersion shown, if this does not introduce complications.

In forming a solid solution the lattice is distorted. In x-ray experiments the values of $\bar{u}^2 = \bar{u}^2_{heat} + \bar{u}^2_{stat}$ are measured. At the same time the change in ΔF_{vib} defines only $\bar{u}^2_{heat}$. Thus, for the heat dispersion factor it is necessary to take measurements at least two temperatures in order to separate $\bar{u}^2_{heat}$. Thus,

$$\Delta F_{vib} = \frac{3}{2} RT \ln \frac{w_p^2}{w^2},$$

where $\bar{w}^2$ is the mean square of the heat of translational vibration in the molecules.

Guided by some indirect considerations, it can be assumed that on increasing $\bar{u}^2$ the larger part of the change would be transferred to the disturbance of the lattice and only 10-30% of the change would occur as a result of the increased intensity of thermal vibration. However, cases are met in which $\bar{u}^2$ falls instead of rising. Such a change in $\bar{u}^2$ has been detected by us when p-dibromobenzene or p-dichlorobenzene is dissolved in p-diiodobenzene. The assumption that the introduction of impurity molecules into a crystal improves its lattice seems absurd to us. In cases of decreasing $\bar{u}^2$ the intensity of thermal vibration is also decreased (the spectra are displaced to larger frequencies) which can lead to the limit of solubility.

In the absence of other factors it is necessary that $\Delta F_{vib} > 0.035$ kcal/mole, i.e., $\ln w_p^2/w^2$ should be ≈ 0.017, i.e., $\bar{u}^2$ should fall by about 4% in order that the limit of solubility should occur at a 1% solution.

4. Conformational change. The energies of different conformations of molecules have been calculated in many papers. Thus, for example the difference in energy of the boat-and-chair-conformations of cyclohexane has been estimated as about 10 kcal/mole, and the difference in energy of the trans- and the unstable cis-conformations of ethane is also some kilocalories per mole.

Thus, the introduction of a foreign molecule into a crystal, leading to a change in the conformation of the former is not an absolute obstacle to solubility, since the order of the parameter 0.01 ΔE is a gain in

configurational energy (0.035 kcal/mole in a 1% solution) which is essentially a value of the first order.

In the formation of solid solutions, it is frequently possible to change the conformation which is linked with the disturbance of the planarity of aromatic systems, for example rotation of the benzene ring around a C-phenyl bond. The loss in resonance energy in these cases is in large measure compensated for by the decrease in intramolecular steric strain. It seems to us, however, that the theoretical calculations relatively overstated the value of the resonance energy. In any case, the parameter ΔE, which is of the order of several kilocalories, cannot prevent the latter from changing its configuration and going into solid solution.

Conditions of Equilibrium for the Two Solid Solutions

If the components form a system with limited solubility, then at the lower eutectic or peritectic temperature we find two crystals of equal composition which are in equilibrium. We shall draw up the equilibrium conditions for these two mixed crystals at set external conditions of p and T. We shall call the free energies of the crystal components F_A and F_B. It may be assumed that the change in free energy for the substitution of a molecule B for a molecule of A and the reverse will be relatively small (of the order of a few percent of F). We shall therefore write down the first phase (with the crystal structure of A)

$$F_1 = (n_A + n_B) F_A + \varphi(n_B) + kT \left(n_A \ln \frac{n_A}{n_A + n_B} + n_B \ln \frac{n_B}{n_A + n_B} \right)$$

and for a crystal of the second phase

$$F_2 = (n'_A + n'_B) F_B + \psi(n'_A) + kT \left(n'_A \ln \frac{n'_A}{n'_A + n'_B} + n'_B \ln \frac{n'_B}{n'_A + n'_B} \right).$$

Here n_A, n_B, n'_A and n'_B are the variable numbers of moles of the components, and $\varphi(n_B)$ and $\psi(n'_A)$ are the changes in crystal free energies on substitution (allowing it to be written in a form which is obviously that of a free energy of mixing).

The equilibrium conditions have the form:

$$\left(\frac{\partial F_1}{\partial n_A} \right)_{n_B = \text{const}} = \left(\frac{\partial F_2}{\partial n'_A} \right)_{n'_B = \text{const}},$$

$$\left(\frac{\partial F_1}{\partial n_B} \right)_{n_B = \text{const}} = \left(\frac{\partial F_2}{\partial n'_B} \right)_{n'_A = \text{const}},$$

i.e.,

$$F_A + RT \ln (1 - x) = F_B + \frac{\partial \psi}{\partial n'_A} + RT \ln (1 - x'),$$

$$F_A + \frac{\partial \varphi}{\partial n_B} + RT \ln x = F_B + RT \ln x'.$$

Here, $x = \frac{n_B}{n_A + n_B}$, $1 - x = \frac{n_A}{n_A + n_B}$ (and similarly for x'); x and x' are the concentrations of molecules of B in the equilibrium mixed crystals (x – concentration of molecules of B in crystals of A, x' – concentration of molecules of B in crystals of B, therefore $x < x'$).

Calling $F_B - F_A = \Delta F$, we can write the equilibrium conditions in the following form:

$$\frac{1 - x}{1 - x'} = e^{\frac{\Delta F + \frac{\partial \psi}{\partial n'_A}}{RT}}, \qquad \frac{x}{x'} = e^{\frac{\Delta F + \frac{\partial \varphi}{\partial n_B}}{RT}}.$$

Thus, the equilibrium concentration allows some thermodynamic functions which characterize the mixture to be found. Because $\frac{x}{x'} < 1$ the following inequalities are always correct

$$\Delta F < \frac{\partial \varphi}{\partial n_B} \quad \text{and} \quad \Delta F + \frac{\partial \psi}{\partial n'_A} > 0.$$

In further discussion, we shall take the equations we used in discussing solubility, and we shall use them for the changes in free energy, φ and ψ which occur on substitution. These equations are:

$$\varphi(n_B) = \Delta U_B + n_B \Delta E_B + \Delta F_B^{vib},$$
$$\psi(n'_A) = \Delta U_A + n'_A \Delta E_A + \Delta F_A^{vib}.$$

It is true the strain energy is additive for many mixed crystals, and in any case for small concentrations, i.e.,

$$\Delta U = n \Delta U_{mol.}$$

In these cases the values which interest us are basically the simple limits of solubility which are expressed by the equations:

$$RT \ln \frac{1-x}{1-x'} = \Delta F + \Delta U_A + \Delta E_A + \frac{\partial \Delta F^{vib}}{\partial n'_A},$$
$$RT \ln \frac{x}{x'} = \Delta F - \Delta U_B - \Delta E_B - \frac{\partial \Delta F^{vib}}{\partial n_B}.$$

Using these last equations, we shall proceed to analyze some concrete examples.

Analysis of the Solubility in Systems Studied Experimentally

The investigation of the structure of solid solutions, without which it is impossible to analyze the conditions of solubility, were begun some years ago in our laboratory. Until this investigation was started no studies of solid solutions of organic substances lrad been carried out; the examples given below include all the data of this type.

The system stilbene – dibenzyl was studied by N. Ya. Kolosov, acridine – anthracene and β-chloronaphthalene – naphthalene by R. M. Myasnikov, anthracene – phenanthrene by V. M. Kozhin, and p-dibromobenzene–p-diiodobenzene by Liang Tung-ch'a. We shall illustrate the suggested method of analysis in the two simplest examples.

System stilbene – dibenzyl [8]. In agreement with the geometric analysis, the substitution of a molecule in this system was not connected with noticeable increase in strain. Nor did we find a change in $\bar{u}^2$ which retained its value for the dibenzyl and stilbene phases at all concentrations. Therefore, we assume that the parameters ΔU_{tens} and ΔF_{vib} can be neglected for both phases.

On being introduced into a crystal of stilbene a molecule of dibenzyl retains its trans-configuration and the energy of conformation does not change. Consequently, $\Delta E = 0$ for the stilbene phase. The case is somewhat different for the dibenzyl phase. On being introduced into the dibenzyl lattice the stilbene molecule loses its planarity. The rotation of the rings is connected with a somewhat increased energy, ΔE.

Thus, the conditions of solubility acquire the form (x – stilbene content):

stilbene phase $\quad |T\Delta S| > (1-x)(F_{st} - F_{dib});$
dibenzyl phase $\quad |T\Delta S| > x[(F_{dib} - F_{st}) + \Delta E].$

From the conditions of stability of the stilbene phase it follows that ($F_{st} - F_{dib}$) cannot be greater than 0.83 kcal/mole because the composition x = 0.5 at which the configuration energy has its greatest value (0.415 kcal/mole at room temperature) belongs to the stilbene phase.

At x = 0.1 the dibenzyl phase is still important. From the conditions for the stability of the dibenzyl phase it also follows that $0{,}22 > 0{,}1\,[\Delta E - (F_{st} - F_{dib})]$. Thus ΔE exceeds the difference ($F_{st} - F_{dib}$) by not more than 2.2 kcal/mole.

Let us now discuss the investigations which lead to the equilibrium conditions for the two phases. Using our simplified expressions, we obtain:

$$RT \ln \frac{1-x}{1-x'} = \Delta F \text{ and } RT \ln \frac{x}{x'} = \Delta F - \Delta E,$$

where $\Delta F = F_{st} - F_{dib}$, and x and x' are the quantities of stilbene in the dibenzyl stilbene phases.

At T = 325° equilibrium occurs at x = 0.1 and x' = 0.3, and at T = 295° at x = 0.1 and x' = 0.5. We find for ΔF and ΔE 0.16 and 0.88 and 0.35, 1.3 kcal/mole, respectively. Thus, F_{st} is not much bigger than F_{dib}, and the energy due to the change of conformation of stilbene is close to 1 kcal/mole which is given in the theoretical paper by Adrian (we assume that the energy curve used by this author is strongly overstated). The conclusions from the conditions of solubility are in agreement with the conclusions from the equilibrium conditions.

System acridine-anthracene. The phase diagram for this system and the curve of the cell volume change has been established by Myasnikova [9]. Substitution of anthracene by acridine takes place without strain; on the other hand, as has been shown by geometric analysis, substitution in the acridine crystal proceeds with the rapid accumulation of strain which leads to a solubility limit at x ≈ 6% anthracene.

It is interesting that the values of $\overline{u}^2$ for the anthracene and acridine phases remain practically unchanged; consequently $\Delta F^{vib} = 0$. Neither molecule loses its conformation, so ΔE = 0. Thus, the conditions of solubility acquire the form:

$$\text{acridine phase} \quad T\Delta S > \Delta T_{tens} + x(F_{acr} - F_{anth});$$
$$\text{anthracene phase} \quad T\Delta S' > (1-x)(F_{anth} - F_{acr}).$$

At equilibrium solutions are found which contain x = 0.06 and x' = 0.3 for anthracene (x = content in the acridine phase).

Consequently:

$$RT \ln \frac{0{,}94}{0{,}7} = \Delta F \text{ and } RT \ln \frac{0{,}06}{0{,}3} = \Delta F - \Delta U,$$

from which ΔF = 0.2 kcal/mole and ΔU = 1.8 kcal/mole.

Thus, F_{anth} is not much greater than F_{acr}. Again we see that these conditions are in agreement with the conclusions from the conditions of solubility.

The value of ΔU can be independently estimated from geometric analysis of the substitution, if only the curve for the interaction of nonbonded atoms is known. On introducing anthracene molecules into an acridine crystal the principal change is a shortening of the distances by about 0.6 A from the normal. Using the interaction curve mentioned above, we find that U_{mol} equals 1.0 kcal/mole. Taking into account the approximations in the theory and particularly in the interaction curve the agreement should be considered satisfactory.

LITERATURE CITED

1. A. I. Kitaigorodskii, Doklady Akad. Nauk SSSR 113, 604 (1957).*
2. A. I. Kitaigorodskii, Tetrahedron 9, 183 (1960).
3. A. I. Kitaigorodskii, Yu. V. Mnyukh, and N. A. Nechitailo, Kristallografiya 3, 298 (1958).
4. A. I. Kitaigorodskii, Acta Physicochim. URSS 22, 309 (1947).
5. D. W. J. Cruickshank, Acta Cryst. 9, 1005 (1956).
6. A. Frühling, Ann. Phys. (Paris) 6, 401 (1951).
7. I. M. Lifshits and G. I. Stepanova, Zhur. Éksp. i Teoret. Fiz. 30, 938 (1956).
8. N. Ya. Kolosov, Kristallografiya 3, 700 (1958).
9. R. M. Myasnikova and A. I. Kitaigorodskii, Kristallografiya 3, 160 (1958).

* Original Russian pagination. See C. B. translation.

THE STRUCTURE OF $K_2[RuCl_5H_2O]$

T. S. Khodashova

The N. S. Kurnakov Institute of General and Inorganic Chemistry,
Academy of Sciences of the USSR
Translated from Zhurnal Strukturnoi Khimii, Vol. 1, No. 3, pp. 333-336,
September-October, 1960
Original article submitted March 3, 1960

An x-ray structural investigation of $K_2[RuCl_5H_2O]$ has been carried out which was of interest because of the absence of published structural data for compounds of trivalent ruthenium. The distances found were: $Ru^{III} - Cl$ 2.33 ± 0.02, $Ru - OH_2$ 2.12 ± 0.05 A. In complexes of Ru^{III} and Ru^{IV} (including a number of nitroso-compounds) the Ru-Cl distances are the same and do not depend on the valence state of the metal.

The value 2.12 A for the $Ru-OH_2$ distance agrees with the postulate discussed earlier about the regular increase in the $M-O$ distance on changing from O to OH and H_2O for osmium and ruthenium compounds.

By scanning the literature data on complex compounds of ruthenium and osmium and comparing these facts with structural data obtained in the crystal chemistry laboratory of the Institute of General and Inorganic Chemistry, Academy of Sciences, USSR, an assumption was stated about important definite regularities in a series of oxygen- and nitrogen-containing compounds [1]. In particular, it was shown that the $M-O$ distance increased regularly in the series $M-O < M-OH < M-OH_2$. For ruthenium compounds this series is incomplete: there are structural data only for $Ru-OH$ and $Ru-O$ distances (Table 3). The structural investigation of potassium aquopentachlororuthenate was intended to determine the $Ru-OH_2$ distance and to test the truth of the rule for ruthenium compounds discussed above.

In the second place, we were concerned with the determination of the Ru-Cl distance for a complex compound of trivalent ruthenium, because all the known structural data are either for chloro-complexes of tetravalent ruthenium or nitroso-compounds (Table 3). By structural analysis of $K_2[RuNOCl_5]$ [2] it was established that it was isomorphous with the aquocomplexes of the type $M_2^I[M^{III}Cl_5H_2O]$ (where M^{III} = Fe, In). Thus, it would be expected that $K_2[RuCl_5H_2O]$ would belong to this structural type (a rhombic deformation of the K_2PtCl_6 type). Therefore, a model of the structure of $K_2[RuNOCl_5]$ was taken as the basis for this investigation. For both structures, the same method of improving coordinates, locating the electron density maxima and estimating the real error of the coordinates found, was used.

The experimental materials were photographs of $h0l$ and $h1l$ taken with a KFOR camera (Mo-K_α radiation). 94 Reflections of $h0l$ type and 97 of $h1l$ were used. The ratio $F^2_{max} : F^2_{min}$ were equal respectively to 538 : 1 and 2130 : 1. Intensities were estimated visually, taking into account the Lorents factor and the polarization. A survey about other crystallographic directions was difficult because of the insufficiently high quality of the crystals. The basic structural parameters are as follows: space group D^{16}_{2h} – Pnma; a = 13.53 ± 0.05; b = 9.55 ± 0.05, c = 6.96 ± 0.03 A; N = 4; d_{calc} = 2.76 g/cm^3. The parameters a and c were determined in the KFOR camera with NaCl as standards.

The atoms Ru, Cl_1, Cl_2, and Cl_3 and the molecule H_2O are situated on a plane of mirror symmetry at heights of $y = {}^1/_4$ and $y = {}^3/_4$ [position 4 (c)]; the Cl_4 atoms (the fifth and sixth vertices of the ruthenium coordination octahedron) and the K^+ ions are found in the general positions 8 (d). Therefore, for our purposes (i.e., the estimation of Ru-OH_2 and Ru-Cl distances) it is quite sufficient to determine the x and z coordinates only, using the h0l and h1l reflections. The coordinates y_{Cl_4} and y_K, which are not of the utmost importance, were not found exactly because of the difficulty of obtaining the corresponding experimental data. The x and z coordinates were found more precisely by the method of weighted projections of the electron density. As was shown in the analysis of the $K_2[RuNOCl_5]$ structure [2], this method is very satisfactory for the given structural type: the distribution

$$\sigma_0(xz) + \sigma_1(xz)/\varkappa_1 \text{ where } \varkappa_1 = \overline{f(h0l)/f(h1l)},$$

which appears to be superimposed in the sections $y = {}^1/_4$ and $y = 0$ makes it possible to separate the atoms of a single complex. Two cycles of successive approximation were carried out for $\sigma_0(x,z)$ and $\sigma_1(x, z)$. To determine the sign of the structure amplitudes, F (h0l) and F (h1l), in the construction of the projection of the first approximation, the coordinates of the atoms in the $K_2[RuNOCl_5]$ structure were used. In Figs. 1 and 2 are presented the distributions $\sigma_0(x, z)$ and $\sigma_1(x, z)$ for the second approximation.

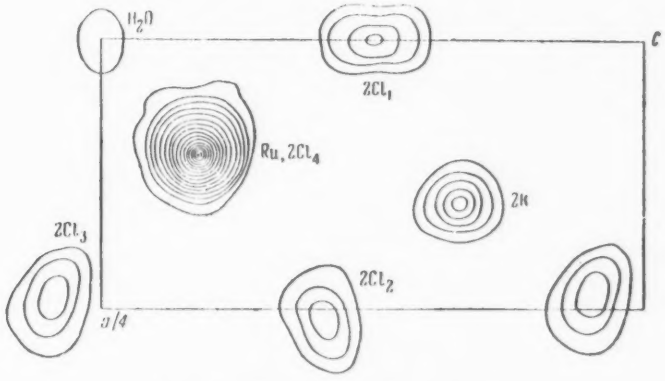

Fig. 1. The distribution $\sigma_0(x, z)$.

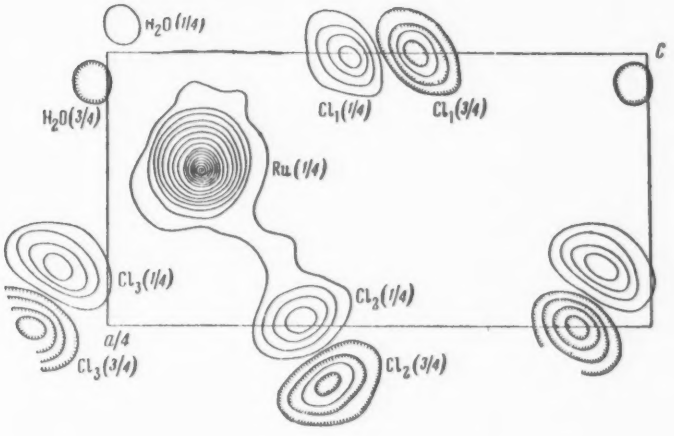

Fig. 2. The distribution $\sigma_1(x, z)$.

In Table 1 the values F_{meas} (h0l) and F_{calc} (h1l) are compared after converting to an absolute scale. The temperature correction constant B = 4.3 A^2. The coordinates were found from the distribution $\sigma_0(x, z)$ and $\sigma_1(x, z)/\kappa_1$; the final values are given in Table 2.

TABLE 1

Measured and Calculated Structure Amplitudes for h0l

h0l	F_{meas}	F_{calc}	h0l	F_{meas}	F_{calc}	h0l	F_{meas}	F_{calc}
400	36,6	—41,0	17,02	5,0	4,0	505	21,7	—20,2
600	9,2	—8,6	103	26,4	—22,3	805	7,8	—12,5
800	45,9	39,6	203	32,0	29,1	905	12,0	12,0
1000	16,6	14,2	503	26,5	29,2	1105	3,6	3,4
1400	7,5	—4,8	603	7,0	—8,8	1205	4,9	6,2
1800	5,5	4,1	703	5,0	8,0	1305	5,1	—5,4
2000	4,5	3,4	803	6,5	—6,7	1505	6,8	—4,7
101	4,2	3,7	903	26,9	—22,9	006	11,1	15,0
201	33,2	—33,3	1003	3,4	6,1	106	6,7	—6,6
301	7,2	—6,4	1103	9,3	—13,2	206	5,9	5,3
401	34,2	—35,0	1303	12,4	10,6	306	6,6	—7,0
501	14,1	—16,0	1503	5,1	4,2	406	18,2	—17,2
601	25,5	24,2	1703	5,9	—5,0	706	15,9	13,7
701	18,5	—19,9	1903	5,9	—2,7	806	7,1	6,9
801	34,8	31,9	0004	14,3	—16,3	1006	2,6	1,6
901	12,8	9,6	104	41,1	36,8	1106	5,1	—5,1
1001	7,8	—8,9	204	19,9	17,4	1306	5,7	—4,3
1201	20,8	—22,2	304	35,1	26,0	107	6,6	—7,0
1301	10,7	—11,7	404	4,3	6,3	207	10,9	—12,5
1601	10,6	10,0	504	6,2	—9,4	307	7,4	11,2
002	21,9	—25,2	704	26,0	—21,7	507	5,1	4,4
102	24,9	—24,6	804	2,7	—3,8	607	7,1	7,8
302	59,9	—56,0	1004	9,7	9,9	807	5,4	6,3
402	47,2	52,5	1104	12,7	12,0	1207	5,8	—4,6
502	36,2	37,2	1304	4,5	3,6	808	7,6	—9,2
602	20,0	20,6	1404	3,3	—1,8	108	4,0	—5,3
702	14,1	14,2	1504	4,0	—2,1	408	7,2	6,0
802	8,8	—9,4	1704	6,0	—8,5	608	4,4	3,9
1002	6,8	—6,2	105	20,2	20,3	1008	7,9	—6,8
1102	9,1	—6,1	305	6,9	—8,9	209	6,4	7,4
1202	6,3	4,2	405	3,0	6,7	609	6,2	—5,5
1402	7,7	8,8						

The precision in localizing the maxima is: Ru 0.003; K 0.014; Cl 0.010; O 0.020 A. The error factor R (h0l) equals 0.14 (without including the zero reflections). The true errors in the coordinates determined $\varepsilon(x)_{Ru} = 0{,}005$, $\varepsilon(x)_K = 0{,}016$, $\varepsilon(x)_{Cl} = 0{,}014$, $\varepsilon(x)_O = 0{,}039$ A.

TABLE 2

Coordinates of the Atoms

Atom	Position	x	y	z	Atom	Position	x	y	z
Ru	4 (c)	0,108	0,250	0,189	H_2O	4 (c)	—0,022	0,250	0,019
Cl_1	4 (c)	0,002	0,250	0,454	K	8 (d)	0,148	~0	0,646
Cl_2	4 (c)	0,245	0,250	0,386	Cl_4	8 (d)	0,108	~0	0,189
Cl_3	4 (c)	0,212	0,250	—0,077					

The interatomic distances in the square section of the complex have the following values (A):

$Ru - Cl_1$ 2,34, $Ru - Cl_3$ 2,33,
$Ru - Cl_2$ 2,31. $Ru - OH_2$ 2,12.

Thus, the mean value of the Ru^{III} - Cl distance, 2.33 A (real error 0.02 A), coincides within the limits of experimental error with the Ru-Cl distances in other ruthenium compounds recently studied (Table 3) and it is evident that it does not depend on the valence state of the metal. The maximum divergence (2.29 A in K_2RuCl_6) coincides with the least exactly determined coordinate: the authors [3] got an error of 0.04 A for this distance.

TABLE 3

The Structures of Ru Complex Containing Cl and O

Compound	Distance, A		Reference
	Ru–Cl	Ru–O	
K_2RuCl_6	2,29		[3]
$K_4[RuCl_{10}O]\,H_2O$	2,34	1,80 (O)	[4]
$KRuO_4$	—	1,79 (O)	[5]
$(NH_4)_2[Ru(NO)(OH)Cl_4]$	2,35	2,03 (OH)	[6]
$[Ru(NO)(OH)(NH_3)_4]Cl_2$	—	1,98 (OH)	[7]
$K_2[RuNOCl_5]$	2,35	—	[2]
$K_2[RuCl_5H_2O]$	2,33	2,12 (OH_2)	—

The Ru-OH_2 distance (2.12 ± 0.05 A) is of the same order as the Os-OH_2 distance [1]. It is now possible to follow the change in the Ru-O distance in oxygen-containing complexes of ruthenium for the series O – OH – OH_2. It can be seen from Table 3 that this parameter increases regularly from 1.8 A in the $KRuO_4$ structure and in bridging oxygen to a maximum value of 2.12 A in $K_2[RuCl_5H_2O]$. A complete analogy is observed between the compounds of ruthenium and osmium.

The author extends her sincere thanks to Professor G. B. Bokii for advice in the work and in the interpretation of results and to N. A. Ezerskii for giving us the potassium aquopentachlororuthenate.

LITERATURE CITED

1. G. B. Bokii, L. O. Atovmian, and T. S. Khodashova, Doklady Akad. Nauk SSSR 128, 1, 78 (1959).
2. T. S. Khodashova and G. B. Bokii, Zhur. Strukt. Khim. 1, 2, 151 (1960).*
3. C. S. Adams and D. P. Mellor, Austr. J. Sci. Res., Ser. A 5, 3, 577 (1952).
4. A. Mathieson, Acta Cryst. 5, 185 (1952).
5. M. S. Silverman and H. A. Levy, J. Am. Chem. Soc. 76, 12, 3317 (1954).
6. N. A. Parpiev and G. B. Bokii, Zhur. Neorg. Khim. 2, 8, 1927 (1957).
7. G. B. Bokii and N. A. Parpiev, Kristallografiya 2, 5, 691 (1957).

* Original Russian pagination. See C. B. translation.

THE CRYSTAL STRUCTURE OF THE ISOMORPHOUS DIHALOGENO-DIPYRIDINEATES OF COBALT AND ZINC

(THE PROBLEM OF THE NATURE OF THE ISOMERIC COBALT COMPOUNDS WITH COMPOSITION CoA_2X_2)

M. A. Porai-Koshits, L. O. Atovmyan, and G. N. Tishchenko

N. S. Kurnakov Institute of General and Inorganic Chemistry, Academy of Sciences of the USSR

Translated from Zhurnal Strukturnoi Khimii, Vol. 1, No. 3, pp. 337-341, September-October, 1960
Original article submitted January 15, 1960

A partial structural investigation of $ZnPy_2Cl_2$ and the isostructural $CoPy_2Br_2$ has been carried out. The angle $Cl_I - Zn - Cl_{II}$ is 126°. The angles $N - Zn - Cl_I$ and $N - Zn - Cl_{II}$ are 100-110°. The compound is molecular (monomeric); the complexes have a tetrahedral structure.

The violet α and blue β forms of the compounds CoA_2X_2 are polycoordination isomers; the α forms are polymers with octahedral coordination about Co; the β forms are monomers with tetrahedral coordination.

The transition metals of the fourth period form a large group of compounds with the composition $M^{II}A_2X_2$, where M^{II} = Mn, Fe, Co, Ni, Cu, Zn; X = monovalent acid residue; A = H_2O, NH_3, Py and other organic ligands.

It is particularly interesting that the cobalt compounds with this composition occur in two isomeric series which differ both in the color of the crystals and in the chemical properties; the α series have reddish violet crystals and the β series blue ones. The most characteristic members of these series are the violet and blue crystals of $CoPy_2Cl_2$. The problem of the structures of these isomers has several times attracted the attention of investigators.

Use of Werner's coordination theory led Biltz and Fektenheuer [1] and Hantzsch [2] to the conclusion that the α and β forms were geometric isomers, i.e., trans- and cis-isomers. Cox and his co-workers [3] supported this idea. They carried out the first crystallographic and x-ray measurements of both $CoPy_2Cl_2$ modifications. From the small value of the period c in α-$CoPy_2Cl_2$ crystals they attributed a trans square planar structure to this complex. Correspondingly a cis-structure was attributed to the blue form. In this work it was also shown that β-$CoPy_2Cl_2$ is isomorphous with $CoPy_2Br_2$ and $CoPy_2I_2$. Cox's suggestion of a square structure for $CoPy_2Cl_2$ was refuted by Mellor and Coryell [4] on the basis of the magnetic moments of these compounds. Mellor and Coryell were led to the conclusion that α-$CoPy_2Cl_2$ has a chain structure with octahedral coordination around Co, and that the blue β-form has a tetrahedral structure.

The stereochemical conclusions of Mellor and Coryell concerning the isomeric dichlorodipyridinocobalts were further directly supported by the structural investigations of Vainshtein [5] [$Co(H_2O)_2Cl_2$ with octahedral coordination], Malinovskii [6] [$Co(p\text{-}CH_3C_6H_4NH_2)_2Cl_2$ and $Co(p\text{-}CH_3C_6H_4NH_2)_2I_2$ with tetrahedral coordination] and finally by structural investigations of the crystals of α-$CoPy_2Cl_2$ itself in papers by Porai-Koshits and

Tishchenko [7], Dunitz [8] and Ferroni and Bondi [9] who independently showed that α-$CoPy_2Cl_2$ has a chain structure with octahedral coordination around Co.* However, the final solution of the problem of the nature of the α and β isomers of $CoPy_2Cl_2$ undoubtedly requires that structural data on the second, β form of this compound be obtained. It is true that the instability of β-$CoPy_2Cl_2$ prevents one from obtaining experimental x-ray data directly from samples of this compound. But it has been established convincingly that this compound is isostructural with $CoPy_2Br_2$ and the latter (as the result of our investigations) with $ZnPy_2Cl_2$. This makes it possible to use these compounds as models for determining the structure of β-dichlorodipyridinocobalt.

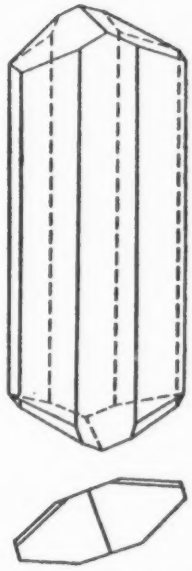

Fig. 1. Crystal habit of $CoPy_2Br_2$ and $ZnPy_2Cl_2$.

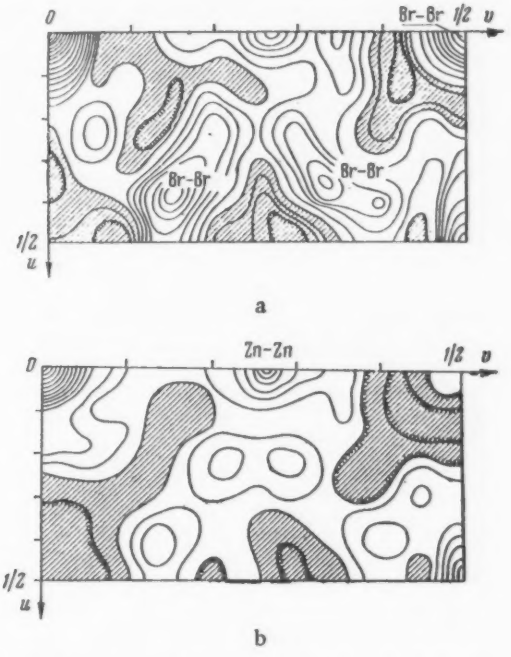

Fig. 2. Patterson Projection P (uv). a) $CoPy_2Br_2$, b) $ZnPy_2Cl_2$.

The discovery by Cox that β-$CoPy_2Cl_2$ and $CoPy_2Br_2$ are isostructural was confirmed by comparing Debye photographs of these compounds. The isostructural nature of $CoPy_2Br_2$ and $ZnPy_2Cl_2$ followed directly from the equality of their crystallographic characteristics and lattice parameters. The crystals of $CoPy_2Br_2$ and $ZnPy_2Cl_2$ have almost identical habits (Fig. 1). Goniometric measurements showed that the crystals belonged to the monoclinic-prismatic symmetry form. The lattice parameters were determined from three oscillating x-ray photographs:

TABLE 1

	a	b	c	β	Space group	d_{meas}	Z
$CoPy_2Br_2$	8,40	18,0	8,52	101°15′	$P2_1/c$	1,87	4
$ZnPy_2Cl_2$	8,44	17,5	8,25	102°	$P2_1/c$	1,64	4

* Our Debye photographs showed that α-$CoPy_2Cl_2$ and $NiPy_2Cl_2$ are isostructural.

The experimental data used for the structural determination (projection method) were obtained from x-ray photographs taken in the KFOR camera using MoK α-radiation. The intensities were estimated visually according to the degree of blackening. In calculating the structural factors the polarization and Lorents factors were taken into account. The basis for the structure solution was the comparison of Patterson projections of the compounds under discussion (Figs. 2 and 3). In the $CoPy_2Br_2$ projection the strongest maximum should correspond to the Br – Br vector and in the $ZnPy_2Cl_2$ projection to the Zn – Zn vector. Comparing the P (uv) projections it is not difficult to see that in the Co-compound the strongest maxima are at (0.40; 0.15), (0.35; 0.33) and (0; 0.49) whereas in the Zn-compound the strongest maximum is at (0; 0.27). The maxima at u = 0 evidently correspond to vectors of the first degree with components 0, $^1/_2$ - 2y: the first of these (u = 0, v = = 0.48) overlies a Br – Br vector, while the second (u = 0, v = 0.27) overlies the Zn – Zn vector.

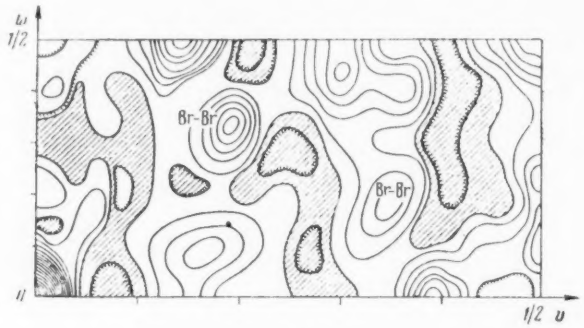

a

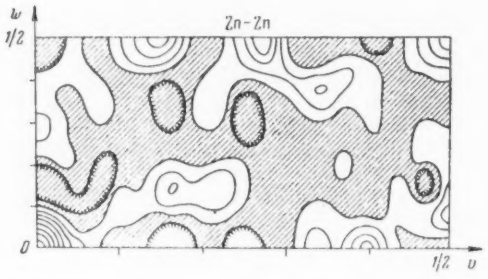

b

Fig. 3. Patterson Projection P(uv): a) $CoPy_2Br_2$; b) $ZnPy_2Cl_2$.

Similarly by a comparison of 3a and 3b, it follows that in the bc projection the Br – Br vector corresponds to maxima at (0.19; 0.32) and (0.35; 0.18) which are the strongest in the Co-compound, while the vector Zn – Zn corresponds to the maximum at (0.27; 0.5) which is the strongest in the Zn-compound.

Although these comparisons are far from exhausting all the Zn-Zn and, especially, the Br – Br vectors they do provide a starting point for the further analysis of the projection of interatomic functions by algebraic correlation between the components of first and second order vectors. This part of the investigation was carried out using the projection of the Zn-compound. The coordinates of the Zn, Cl_I and Cl_{II} atoms were defined more accurately by projections of the electronic density (constructed without taking into account the nitrogen and oxygen atoms when determining the signs of the structural amplitudes). These are shown in Fig. 4. The maxima corresponding to Zn, Cl_I and Cl_{II} which are clearly distinguished in these projections permit no doubt about the correctness of the general structural interpretation. The atomic coordinates obtained from a projection of the first approximation are

	x	y	z
Zn	0,236	0,115	0,286
Cl_I	0,344	0,008	0,225
Cl_{II}	0,017	0,178	0,131

The values found for the distances $Zn-Cl_I$ (2.15 A) and $Zn-Cl_{II}$ (2.25 A) are obviously subject to further increase in precision.

To determine the position of the pyridine groups the difference between the projections $\sigma(xy) - \sigma_{Zn,Cl}(x,y)$ was calculated. This allows the position of one pyridine ring to be found (Fig. 5). It could be expected that on taking into account the N and C atoms of this ring the process of successive approximations would proceed successfully and would expose the positions of the remaining light atoms. The structural determination of $ZnPy_2Cl_2$ is not yet completed. However, the basic stereochemical question, on account of which this investigation was undertaken, can be considered solved.

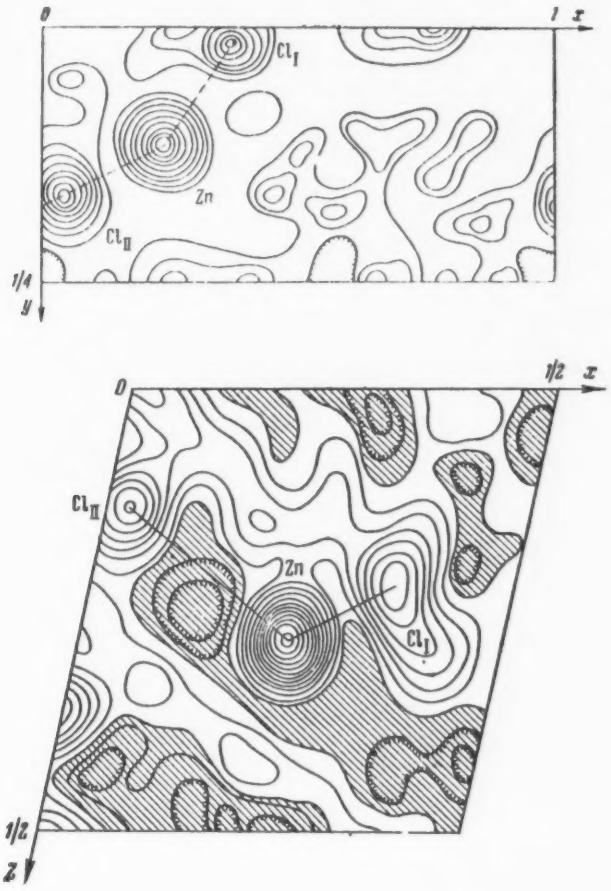

Fig. 4. Projections of the electron density in $ZnPy_2Cl_2$.

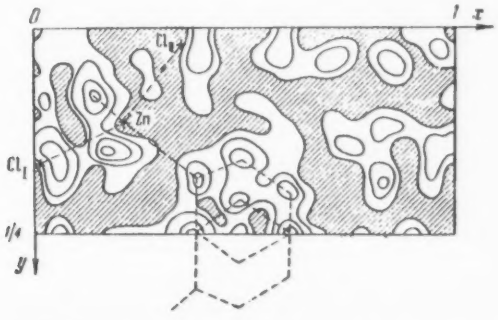

Fig. 5. Difference of the projections $\sigma(xy) - \sigma_{Zn,Cl}(xy)$.

As can be seen from the projection, the valence angle $Cl_I - Zn - Cl_{II}$ is considerably different both from 90° and 180°. Calculations based on the coordinates obtained give a value of 126° for this angle. The valence angles $N_I - Zn - Cl_I$ and $N_I - Zn - Cl_{II}$ are close to 100-110°. Hence, it cannot be doubted that the complexes in the series β-$CoPy_2Cl_2$, $CoPy_2Br_2$ and $ZnPy_2Cl_2$ have a tetrahedral structure.

Thus the two forms (α and β) of $CoPy_2Cl_2$ are polymorphoisomeric modifications: the α form is a polymer and the β form a monomer (polymorphism). In the α-isomer cobalt has octahedral coordination and in the β-isomer tetrahedral. This new type of isomerism can be called polycoordination or configurational isomerism.

LITERATURE CITED

1. W. Biltz and B. Fetkenheuer, Z. anorgan. Chem. 89, 1; 97, 121 (1914).
2. A. Hantzsch, Z. anorgan. Chem. 159, 277 (1927).
3. E. G. Cox, et al., J. Chem. Soc. 1556 (1937).
4. D. P. Mellor and C. D. Coryell, J. Am. Chem. Soc. 60, 1786 (1938).
5. B. K. Vainshtein, Doklady Akad. Nauk SSSR 68, 301 (1949).
6. T. I. Malinovskii, Kristallografiya 2, 734 (1957).
7. M. A. Porai-Koshits and G. N. Tishchenko, Seventh All-Union Conference on the Chemistry of Complex Compounds. Abstract of Papers [in Russian] (Leningrad, 1956) p. 229.
8. J. D. Dunitz, Acta Cryst. 10, 307 (1957).
9. E. Ferroni and E. Bondi, J. Inorg. Nucl. Chem. 8, 458 (1958).

THE STRUCTURAL UNITY OF STRUCTURAL TYPES

N. L. Smirnova

M. V. Lomonosov Moscow State University
Translated from Zhurnal Strukturnoi Khimii, Vol. 1, No. 3, pp. 342-345,
September-October, 1960
Original article submitted September 8, 1959

A series of structural types is considered as the result of positioning atoms at the tetrahedral sites of the structural type β-W.

The structural types obtained by positioning atoms at the octahedral and tetrahedral sites of dense packings are well known and have been thoroughly studied. In addition to these, there are also structural types obtained by positioning atoms at the tetrahedral sites of the structural type β-W, e.g., V_3Si. In the figure, the V atoms are shown as forming icosahedra with the Si atoms inside. The icosahedra and the tetrahedra I fill the space. The icosahedra are formed from two kinds of tetrahedra. One of these (II) is actually a trigonal pyramid, while the other (III) has three equal edges, two different equal edges, and a third edge. The elementary cell of V_3Si contains 6 type I tetrahedra, 16 of type II, and 24 of type III. The center of a tetrahedron may be taken as the point equidistant from its vertices. Then the coordinates of the center of tetrahedron I will be x = 0.25, y = 0.5, z = 0 [position 6 (d) in the Fedorov group Pm3n], those of tetrahedron II will be x = y = z = 0.208 [position 16 (i)], and those of tetrahedron III will be x = 0, y = 0.0938, and z = 0.314 [position 24 (k)]. All the structural types to be considered are compared in Table 1 (the symbol □ denotes an unoccupied site). Tables 2, 3, and 4 show all the compounds belonging to the structural types of Table 1; also shown are $\Delta\alpha, \Delta x, \Delta y, \Delta z$ obtained by subtracting the ideal values from the actual values of $\alpha, \underline{x}, \underline{y}$, and $\underline{z}$. If $\Delta x, \Delta y, \Delta z$, or $\Delta\alpha$ are equal to 0, they are not shown in the tables, and there are dashes if $\underline{x}$, $\underline{y}$, and $\underline{z}$ have not been determined.

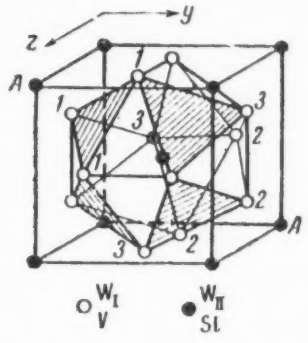

The structural type β-W (V_3Si). One icosahedron is shown. The unhatched faces correspond to type III tetrahedra, and the hatched faces to type II tetrahedra. Type I tetrahedra are not shown.

In the structural type PdS, the Pd atoms form a structure of the V_3Si type, while the S atoms are at type II tetrahedral sites but only occupy half of these. Table 3 shows that there is some displacement from the centers of the sites. In the structure of garnet $Ca_3Al_2(SiO_4)_3$, Al atoms occupy the Si positions and Ca and Si atoms occupy the V positions. The garnet elementary cell consists of 8 cubes with a V_3Si structure. In each cube the Ca atoms occupy positions 1 and 2 (see figure), but the cubes are turned in such a way that the AA axes coincide with the three perpendicular axes. Oxygen atoms occupy 12 of the 24 type III tetrahedra in such a way that the Al atoms are in octahedra of O atoms. In the garnet structure, type III tetrahedra are formed by two Ca atoms, an Al atom, and an Si atom. The Si – O spacing should be a minimum. The O atom is consequently displaced, and the deviation of $\underline{x}$ from its ideal value (Δx in Table 4) is a maximum.

TABLE 1

Structural type	Positions of atoms		Tetrahedral sites		Coupled tetrahedral sites II	No. of compounds with the structural type
	Si	V	II	III		
V_3Si	Si	V_3	—	—	—	29
Ni_3S_2	S_2	Ni_3II_3	—	—	—	1
PdS	Pd^{II}_2	$Pd^{I}_2Pd^{III}_4$	S_8II_8	—	—	1
$Ca_3Al_2(SiO_4)_3$	Al_2	Ca_3Si_3	—	$O_{12}II_{12}$	—	31
$Ca_3Al_2(SiO_4)_2(OH)_4$	Al_2	$Ca_3(Si_2,II)$	—	O_8, $(OH)_4II_{12}$	—	1
$Ca_3[Al(OH)_6]_2$	Al_2	Ca_3II_3	—	$(OH)_{12}II_{12}$	—	1
Bi_4Rh	II_2	Rh_3II_3	—	$Bi_{12}II_{12}$	—	1
$AuZn_3$	Au_2	Au^{II}_6	—	Zn_{24}	—	4
$NaPt_3O_4$	Na_2	Pt_6	—		O_8	1

TABLE 2

Type β-W (V_3Si)								Type $AuZn_3$			
Compound	Lit. ref.	Compound	Lit. ref.	Compound	Lit. ref.	Compound	Lit. ref.	Compound	Δy (Zn)	Δz (Zn)	Lit. ref.
V_3Co	[1]	V_3Sb	[4]	Nb_3Sb	[4]	Mo_3Al	[4]	$AuZn_3$	—0,071	—0,014	[30]
V_3Ni	[2]	Nb_3Os	[7]	Ta_3Sn	[7]	Mo_3Ga	[4]	Cu_6AsSb	—	—	[30]
V_3Au	[3]	Nb_3Ir	[7]	Cr_3Ru	[9]	Mo_3Si	[14]	UH_3	—	—	[31]
V_3Ga	[4]	Nb_3Pt	[7]	Cr_3Os	[10]	Mo_3Ge	[15]	UD_3	—0,061	0,00	[31]
V_3Si	[5]	Nb_3Au	[3]	Cr_3Si	[11]	W_3O	[16]				
V_3Ge	[6]	Nb_3Al	[4]	Cr_3Ge	[6]						
V_3Sn	[7]	Nb_3Ga	[4]	Cr_3O	[12]						
V_3As	[8]	Nb_3Sn	[7]	Mo_3Os	[13]						

TABLE 3

Type Ni_3S_2			Type PdS					
Compound	Δ α	Literature reference	Compound	Δx (Pd^{III})	Δx (S)	Δy (S)	Δ (S)	Literature reference
Ni_3S_2	18°	[17]	PdS	0.02	−0.02	−0.03	0.02	[18]

The structural type of garnet can be obtained by controlled introduction of O atoms into the structural type V_3Si. Now, if atoms are removed from the garnet structure in either a regulated or an unregulated way, we can obtain a series of structural types. Thus, if statistically one-third of the Si atom positions are unfilled, we arrive at a plasolyte $Ca_3Al_2(SiO_4)_2(OH)_4$ structure, and a $Ca_3[Al(OH)_6]_2$ type structure is obtained if none of the Si atom positions are occupied. If both the Si and Al atom positions are empty, then the structure is of the Bi_4Rh type. Belov [28] noted the structural resemblance between the structural types Bi_4Rh and $Ca_3Al_2(SiO_4)_3$. New structural types can also be obtained by "subtracting" atoms from the V_3Si type structure. The Ni_3S_2 structural type is obtained in this way. Thus, the S atoms are in the Si atom positions, but the Ni atoms only occupy half the V atom positions (the Ni atoms only occur at points 1 and 3 in Fig. 1).

In the isostructural compounds UD_3 and $AuZn_3$ it is the U or Au atoms which form the V_3Si type structure. The D or Zn atoms occupy all the type II tetrahedral sites. The tetrahedra are linked by a common face so that the D or Zn atoms tend to move away from each other. Consequently, $\Delta y = -0.061$ for UD_3 and -0.071 for $AuZn_3$.

In the $NaPt_3O_4$ structure the Na and Pt atoms form a structure of the V_3Si type, and the O atoms occur at type II double tetrahedral sites, i.e., at the centers of three faced pyramids [x = y = z = 0.25; Fedorov group Pm3n, position 8 (g)].

TABLE 4

Types $Ca_3Al_2(SiO_4)_3$, $Ca_3Al_2(SiO_4)_2(OH)_4$, $Ca_3[Al(OH)_6]_2$, Bi_4Rh

Compound	Δx (O)	Δy (O)	Δz (O)	Lit. ref.
$Al_2Na_3(LiF_4)_3$	$0,03_5$	$-0,0_6$	—	[19]
$Fe_2Y_3(FeO_4)_3$	$0,027_4$	$0,010_3$	—0,008	[20]
$Fe_2(Y_{0,5}, Nd_{0,5})_3(FeO_4)_3$	—	—	—	[21]
$Fe_2Sm_3(FeO_4)_3$	—	—	—	[21]
$Fe_2Gd_3(FeO_4)_3$	0,038	0,005	—0,015	[22]
$Fe_2Tb_3(FeO_4)_3$	—	—	—	[21]
$Fe_2Dy_3(FeO_4)_3$	—	—	—	[21]
$Fe_2HO_3(FeO_4)_3$	—	—	—	[21]
$Fe_2Er_3(FeO_4)_3$	—	—	—	[21]
$Fe_2Tu_3(FeO_4)_3$	—	—	—	[21]
$Fe_2Yb_3(FeO_4)_3$	—	—	—	[21]
$Fe_2Lu_3(FeO_4)_3$	—	—	—	[21]
$Al_2V_3(AlO_4)_3$	0,04	0,008	—0,017	[23]
$Al_2Cd_3(AlO_4)_3$	—	—	—	[23]
$Al_2Dy_3(AlO_4)_3$	—	—	—	[23]
$Al_2Er_3(AlO_4)_3$	—	—	—	[23]
$Ga_2Y_3(GaO_4)_3$	—	—	—	[23]
$Ga_2Nd_3(GaO_4)_3$	—	—	—	[23]
$Ga_2Sm_3(GaO_4)_3$	—	—	—	[23]
$Ga_2Cd_3(GaO_4)_3$	—	—	—	[23]
$Ga_2Dy_3(GaO_4)_3$	—	—	—	[23]
$Ga_2Er_3(GaO_4)_3$	—	—	—	[23]
$Cr_2Ca_3(SiO_4)_3$	0,035	—0,007	—0,002	[24]
$Fe_2Ca_3(SiO_4)_3$	0,035	—0,007	0,002	[24]
$(Fe, Ti)_2(Ca, Na)_3(SiO_4)_3$	—	—	—	[25]
$Al_2Ca_3(SiO_4)_3$	0,0389	—0,013	—0,0046	[24]
$Al_2(Mg, Fe)_3(SiO_4)_3$	0,04	0,008	—0,017	[24]
$Al_2Mn_3(SiO_4)_3$	0,04	0,008	—0,017	[24]
$Al_2Fe_3(SiO_4)_3$	0,04	0,008	—0,017	[24]
$(Mg, Mn)_2(Ca_2 Na)(AsO_4)_3$	0,0416	0,059	—0,001	[26]
$Al_2Ca_3(SiO_4)_2(OH)_4$	0,035	—0,007	—0,007	[27]
$Ca_3[Al(OH)_6]_2$	0,035	0,008	—0,007	[28]
$Sr_3[Al(OH)_6]_2$	—	—	—	[28]
Bi_4Rh	0,024	0,017	—0,004	[29]

Thus, we see that a number of new structural types can be obtained by adding additional atoms (with or without a superstructure) to the simplest structural types, or by removing atoms from more complex structural types.

SUMMARY

1. Consideration has been given to the structural types obtained by adding atoms to the tetrahedral sites of the β-W structural type.

2. Eight structural types have been found in this way.

3. A method is described for establishing the relations between structural types, i.e., of making their structural unity apparent.

LITERATURE CITED

1. P. Duwez, Trans. Met. Soc. Am. Inst. Min. Metal Eng. 191, 564 (1951).
2. W. Rostoker and A. Yamoto, Trans. Am. Soc. Met. 46, 1136 (1954).

3. E. Wood and B. T. Matthias, Acta Cryst. 9, 534 (1956).
4. E. A. Wood, et al., Acta Cryst. 11, 9, 604 (1958).
5. H. I. Wallbaum, Z. Metallkunde 31, 362 (1939).
6. H. I. Wallbaum, Naturwissenschaften 32, 76 (1944).
7. S. Geller, B. T. Matthias, and R. Goldstein, J. Am. Chem. Soc. 77, 1502 (1955).
8. K. Bachmeyer and H. Novotny, Monatsch. Chem. 86, 741 (1955).
9. E. Raub and W. Mahler, Z. Metallkunde 46, 210 (1955).
10. E. Raub, Z. Metallkunde 48, 53 (1957).
11. B. Boren, Arkiv. kemi mineralogi och geology 11a, No. 1 (1933).
12. N. Schönberg, Acta Chem. Scand. 8, 221 (1954).
13. E. Raub, Z. Metallkunde 45, 23 (1954).
14. D. H. Templeton and C. H. Dauben, Acta Cryst. 3, 261 (1950).
15. A. Searcy, R. Pealver, and H. J. Yearin, J. Am. Chem. Soc. 74, 566 (1952).
16. G. Hagg and N. Schönberg, Acta Cryst. 7, 251 (1954).
17. A. Westgren, Z. anorgan. und allgem. Chemie 239, 82 (1938).
18. T. F. Gaskell, Z. Kristallogr. 96A, 203 (1937).
19. G. Menzer, Z. Kristallogr. 75, 265 (1930).
20. S. Geller and M. A. Gilleo, Phys. and Chem. Solids 3, 1-2, 30 (1957).
21. F. Bertaut and F. Forrat, Compt. rend. Acad. Sci. 244, 1, 96 (1957).
22. F. Bertaut and F. Forrat, Compt. rend. Acad. Sci. 242, 3, 382 (1956).
23. F. Bertaut and F. Forrat, Compt. rend. Acad. Sci. 243, 1219 (1956).
24. G. Menzer, Z. Kristallogr. 69, 300 (1928).
25. O. Zedlitz, Zbl. Mineral. Geol. Paläont., 225 (1933).
26. W. Bubek and F. Machatshci, Z. Kristallogr. 90 A, 44 (1935).
27. A. Pabst, Am. Mineralogist 22, 861 (1937).
28. E. Brandenberger, Schweiz. mineral. und petrogr. Mitt. 13 (1933).
29. V. P. Glagoleva and G. S. Zhdanov, Zhur. Éksp. i Teoret. Fiz. 30, 248 (1956).
30. E. Gunzel and K. Schubert, Z. Metallkunde 49, 234 (1958).
31. R. E. Rundle, J. Am. Chem. Soc. 73, 4172 (1951).

THE DIFFERENT FORMS AND SOME PROPERTIES OF NEUTRAL ZINC SELENITE

L. Ya. Markovskii and Yu. P. Sapozhnikov

State Institute of Applied Chemistry
Translated from Zhurnal Strukturnoi Khimii, Vol. 1, No. 3, pp. 346-352,
September-October, 1960
Original article submitted November 3, 1958

Precise conditions have been determined for obtaining the different forms of neutral zinc selenite, namely $ZnSeO_3 \cdot 2H_2O$, $ZnSeO_3 \cdot H_2O$, and $ZnSeO_3$. It has been found that the anhydrous salt $ZnSeO_3$ exists in two modifications, α and β. Interplanar spacings for these salts are calculated from x-ray powder photographs, and the results of thermographic investigation are described.

The object of this paper was to obtain more precise data on the existence of different forms of zinc selenite. The question arose out of an investigation of chemical affinity in the formation of sulfide-selenide luminophores [1], in which it was established that zinc selenite was formed as an intermediate product according to the reaction:

$$n\,ZnS + 3H_2SeO_3 \rightarrow 2ZnSeO_3 \cdot H_2O + 2S + Se + (n-2)\,ZnS\,. \qquad (1)$$

Zinc selenite was first obtained by Berzelius [2] at the beginning of the 19th century. The neutral and acid zinc selenites were subsequently further investigated by various authors [3-13]. However, the literature data is imprecise and partially contradictory.

According to Nilson [5], Muspratt [6], and Boutzoureano [7], there are three forms of neutral zinc selenite – a dihydrate, a monohydrate, and an anhydrous salt. These authors also describe acid salts – a biselenite $Zn(HSeO_3)_2 \cdot 2H_2O$ and a tetraselenite $ZnSe_4O_9 \cdot 3H_2O$.

Ferrari, Cavalca, and Moretti [12] maintained that neutral zinc selenite did not give hydrated forms containing more than two molecules of water.

Conditions for Obtaining the Different Forms of Neutral Zinc Selenite

It will be shown below that zinc selenite can exist in four forms – a dihydrate $ZnSeO_3 \cdot 2H_2O$, a monohydrate $ZnSeO_3 \cdot H_2O$, and two anhydrous modifications α-$ZnSeO_3$ and β-$ZnSeO_3$. Each of these forms gives its own individual x-ray powder pattern (Fig. 1).

Neutral zinc selenite was synthesized by different methods: a) by interaction of zinc sulfate with potassium or sodium selenite; b) by interaction between selenious acid and freshly prepared basic zinc carbonate; c) by interaction of zinc acetate with selenious acid; d) by boiling an aqueous suspension of zinc oxide with selenious acid.

The results of experiments on the synthesis of zinc selenite are presented in Table 1. The formula of the zinc selenite was established by chemical analysis, x-ray phase analysis, differential thermal analysis, and

TABLE 1

Combined Results of Experiments on the Synthesis of Neutral Zinc Selenite by Different Methods

Experiment No.	Method of preparation	Limits of variation for synthesis conditions in separate experiments				Variation limits for selenite composition in separate experiments by chem. analysis, %			Product composition	Calculated for given composition, %		
		final solution normality	solution temperature, °C	excess reagent above stoichiometric ratio	time for crystallization from mother liquor	ZnO	SeO_2	H_2O		ZnO	SeO_2	H_2O
1	*a*	0,5—2,5	2—40	0—100% K_2SeO_3	18 hr to 52 days	35,5—36,1	47,8—48,7	15,4—15,6	$ZnSeO_3 \cdot 2H_2O$	35,64	48,59	15,78
2	*a*	0,01—2	2—60	0,15% Na_2SeO_3 and K_2SeO_3 and 0—100% H_2SeO_3	0.3 hr to 50 days	38,6—38,8	51,8—52,8	8.54—8,61	$ZnSeO_3 \cdot H_2O$	38,69	52,75	8,56
3	b	0,5	20	70% H_2SeO_3	20 days	38,7	52,5	8,57	$ZnSeO_3 \cdot H_2O$	38,69	52,75	8,56
4	a	0,01—3,5	50—100	0—10% K_2SeO_3 and Na_2SeO_3 and 0—200% H_2SeO_3	0.3 hr to 50 days	41,6—42,4	56,9—57,6	—	β-$ZnSeO_3$	42,31	57,69	—
5	b	~4	100	excess H_2SeO_3	1 day	42,3	57,6	—	β-$ZnSeO_3$	42,31	57,69	—
6	c	~3—4	20	—	1 day	42,2	57,4	—	β-$ZnSeO_3$	42,31	57,69	—
7	d	1,5	100	excess H_2SeO_3	1 hr	42,4	57,5	—	β-$ZnSeO_3$	42,31	57,69	—
8	Heating $ZnSeO_3 \cdot 2H_2O$, $ZnSeO_3 \cdot H_2O$ or α-$ZnSeO_3$ at 300° for 0.5 to 1 hr.					42,3—42,4	56,6—57,4	—	β-$ZnSeO_3$	42,31	57,69	—
9	Heating $ZnSeO_3 \cdot H_2O$ at 200° for 0.5 to 1 hr.					42,3	56,8—57,4	—	α-$ZnSeO_3$	42,31	57,69	—

microscopic investigation. The zinc was determined volumetrically [14, 15] and the selenium iodometrically [16, 17]. All the reagents used were of chemically pure grade.

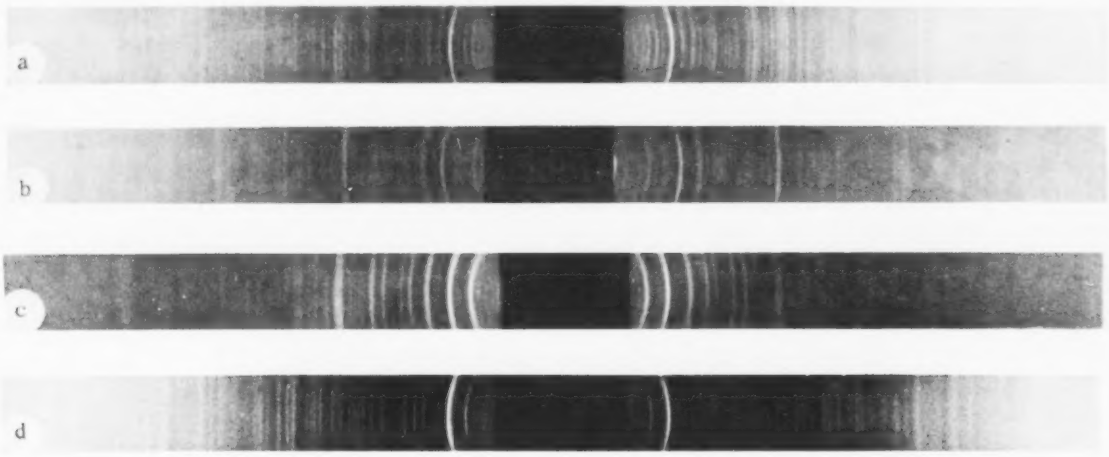

Fig. 1. X-ray powder pattern of different forms of zinc selenite: a) $ZnSeO_3 \cdot 2H_2O$; b) $ZnSeO_3 \cdot H_2O$; c) α-$ZnSeO_3$; d) β-$ZnSeO_3$.

It is evident from Table 1 that by using method a and varying the concentration and temperature of the initial solutions, it is possible to obtain three forms of zinc selenite – dihydrate, monohydrate, and β form of anhydrous salt. Concentrated solutions at room temperature and below precipitate dihydrate; dilute solutions at temperatures from 2 to 60° precipitate monohydrate; the β form of the anhydrous salt is deposited from solutions of any concentration at temperatures from 50 to 100°. In the latter case, with precipitation from concentrated solutions, the β modification sometimes contains a small amount of monohydrate, as is shown by its reduced zinc content.

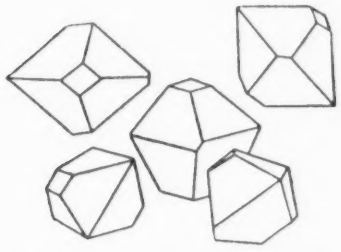

Fig. 2. Diagrammatic representation of $ZnSeO_3 \cdot 2H_2O$ crystals.

Method b gives either monohydrate or β modification; the other methods only give β-$ZnSeO_3$. The α form of anhydrous selenite is not obtained by synthesis from aqueous solution; it can only be obtained by dehydrating the monohydrate at 190-285°.

Characteristics of Neutral Zinc Selenite

Zinc Selenite Dihydrate consists of white, transparent, optically active* rhombic crystals** (Figs. 2 and 3, a) insoluble in water and alcohol, soluble in mineral acids and acetic acid, readily soluble in ammonia and potassium cyanide solution and less so in caustic alkali. The density of $ZnSeO_3 \cdot 2H_2O$ is $d_4^{25} = 3.50 \pm 0.01$ g/ml.***

The dihydrate crystals remained unchanged on standing in air or on exposure for a short time over concentrated sulfuric acid. They were stable to heating at 60-70°, but lost water of crystallization at higher temperatures.

Appreciable loss of water, as shown by change in composition, was already observed at 85°, but was not complete even at 210°. The crystalline dihydrate decomposed to give the monohydrate as an intermediate

* Crystals of all forms of zinc selenite are optically active.
** The crystals obtained were up to 0.4 mm in size.
*** The density was determined using ethyl alcohol in a pyknometer.

product; this was shown by the differential thermal analysis curves and by the x-ray powder patterns of the products. The end product was not α-$ZnSeO_3$ but the more stable β form. It is interesting to note that the dihydrate was also converted to β-$ZnSeO_3$ by boiling with water.

Differential thermal analysis curves [18, 19] for zinc selenite were obtained with an FPK-54 Kurnakov pyrometer. The rate of temperature rise was 4-5° per minute. Transformation temperatures were measured with a chromel-alumel couple to a precision of ± 3°, and were located by marks printed on the photographic paper together with the differential and temperature curves.

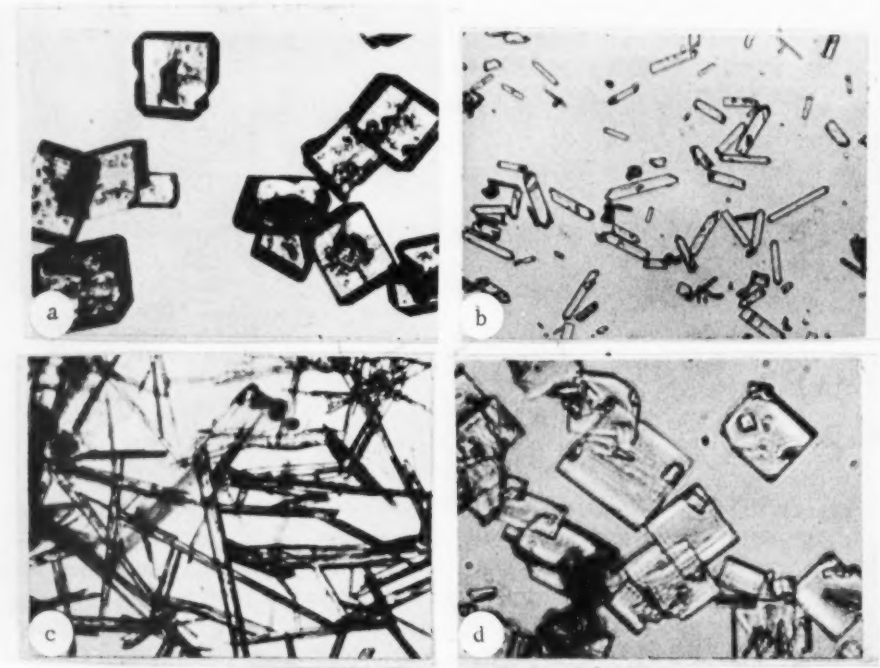

Fig. 3. Photomicrographs of different crystalline forms of zinc selenite: a) $ZnSeO_3 \cdot 2H_2O$, × 72; b) $ZnSeO_3 \cdot H_2O$, × 135; c) $ZnSeO_3 \cdot H_2O$, × 55; d) β-$ZnSeO_3$, × 480.

As a rule the dihydrate gave differential thermal analysis curves as shown in Fig. 4, 1, with an endothermic effect corresponding to the loss of the first molecule of water at 95° and a smaller endothermic effect corresponding to loss of the second water molecule at 190°.

Coarse crystals of $ZnSeO_3 \cdot 2H_2O$ gave differential curves of another shape (Fig. 4, 2). The exothermic effect, observed in this case at 290°, corresponded to the transformation of α-$ZnSeO_3$ to the β form.

Table 2 shows the interplanar spacings calculated from the x-ray patterns for the various forms of zinc selenite.

The x-ray powder patterns were obtained using CuK_α-radiation in a 57.3 mm diameter Debye camera, with rotation of the sample. The intensities were appraised on a five-step scale: vs = very strong, s = strong, m = medium, w = weak, v w = very weak.

The interplanar spacings in Table 2 differ from those presented in Kitaigorodskii's book [20]. The latter are based on American work, and it is clear that the different forms of zinc selenite were not adequately identified in this.

Zinc Selenite Monohydrate is a white crystalline powder of density $d^{25}_4 = 3.830 \pm 0.005$ g/ml. Needle shaped prisms can be seen under the microscope (Fig. 3 b, c). The monohydrate is insoluble in water and in alcohol, but soluble in acids, caustic alkali, and ammonia. There is no loss of crystalline water on standing for a long time in air or over concentrated sulfuric acid, or on heating to 130°.

The dehydration temperature of the monohydrate was determined from the differential thermal analysis curve (Fig. 5); this showed a marked endothermic effect at 190° corresponding to the loss of water and conversion to α-$ZnSeO_3$.

Anhydrous Zinc Selenite is a white crystalline material, sparingly soluble in water [9] and alcohol. Depending on the method of preparation, the anhydrous selenite appears under the microscope to be shapeless, corresponding to α-$ZnSeO_3$, or in the form of rectangular tablets of varying sizes, corresponding to β-$ZnSeO_3$ (Fig. 3, d).

Anhydrous zinc selenite is quite stable at room temperature, and is not affected by air. In a humid atmosphere it absorbs a small amount of water (up to 4-5%), which it readily loses on drying.

The anhydrous salt usually has a slight rose color, which becomes more intense on heating. The color is due to dissemination of a very small amount of dispersed elementary selenium, formed by reduction of the selenite.

TABLE 2

Table of Interplanar Spacings (kX) and Relative Intensities of the X-Ray Powder Pattern Lines of Different Forms of Zinc Selenite

$ZnSeO_3 \cdot 2H_2O$			$ZnSeO_3 \cdot H_2O$			α-$ZnSeO_3$			β-$ZnSeO_3$		
Line No.	I	d	Line No.	I	d	Line No.	I	d	Line No.	I	d
1	medium	4,15	1	medium	3,90	1	strong	3,85	1	weak	4,69
2	strong	3,90	2	weak	3,30	2	weak	3,60	2	very weak	4,03
3	strong	3,45	3	weak	3,17	3	very strong	3,03	3	strong	3,60
4	weak	3,30	4	very strong	2,82	4	strong	2,54	4	very weak	3,33
5	very weak	3,19	5	strong	2,45	5	strong	2,47	5	medium	3,12
6	very strong	3,05	6	strong	2,38	6	weak	2,32	6	very strong	3,03
7	medium	2,99	7	medium	2,30	7	medium	2,22	7	medium	2,79
8	strong	2,75	8	weak	2,20	8	medium	2,11	8	very weak	2,54
9	medium	2,69	9	weak	2,15	9	strong	1,90	9	medium	2,46
10	strong	2,58	10	weak	2,09	10	strong	1,78	10	medium	2,32
11	strong	2,52	11	weak	2,04	11	very weak	1,72	11	medium	2,17
12	strong	2,40	12	weak	1,78	12	very weak	1,69	12	weak	2,11
13	medium	2,26	13	weak	1,69	13	very weak	1,65	13	very weak	2,05
14	strong	2,21	14	weak	1,65	14	weak	1,62	14	very weak	2,00
15	medium	2,17	15	weak	1,63	15	medium	1,56	15	weak	1,97
16	weak	2,09	16	strong	1,57	16	medium	1,53	16	medium	1,90
17	medium	2,04	17	weak	1,50	17	weak	1,46	17	weak	1,89
18	medium	1,98	18	very weak	1,42	18	weak	1,44	18	weak	1,83
19	weak	1,93	19	very weak	1,39	19	weak	1,40	19	weak	1,80
20	weak	1,89	20	very weak	1,35	20	weak	1,36	20	weak	1,79
21	medium	1,79	21	very weak	1,31	21	medium	1,32	21	weak	1,72
22	very strong	1,74	22	very weak	1,28	22	medium	1,29	22	weak	1,69
23	medium	1,73	23	medium	1,25	23	medium	1,27	23	weak	1,67
24	medium	1,69	24	very weak	1,24				24	medium	1,65
25	strong	1,65	25	weak	1,10				25	medium	1,62
26	strong	1,61	26	weak	1,07				26	very weak	1,60
27	medium	1,58									
28	very strong	1,55									
29	strong	1,53									
30	very strong	1,51									
31	medium	1,48									
32	strong	1,44									
33	weak	1,42									
34	medium	1,39									
35	weak	1,37									
36	weak	1,34									

The Dimorphism of Anhydrous Zinc Selenite. It has already been explained that anhydrous zinc selenite exists in two modifications, as revealed by x-ray and thermographic data. The α modification is stable up to 285°; only the β modification exists at higher temperatures. Data from chemical analysis, x-ray phase analysis, differential thermal analysis, and microscopic investigation shows that conversion of the α modification to the β form occurs at 285-290°. The densities of the α and β modifications are $d_4^{25} = 3.94 \pm 0.01$ and $4.71 \pm \pm 0.02$ g/ml, respectively.

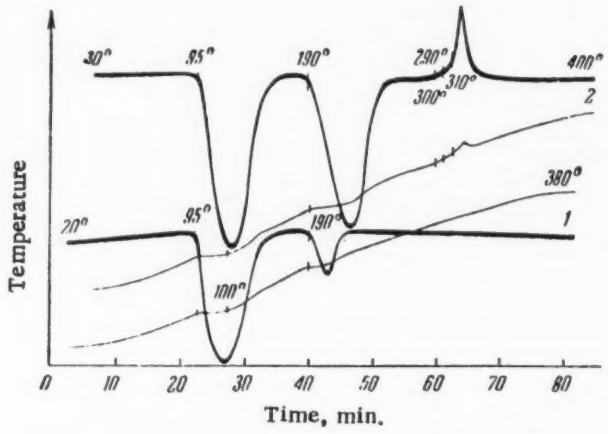

Fig. 4. Differential thermal analysis curves for $ZnSeO_3 \cdot 2H_2O$.

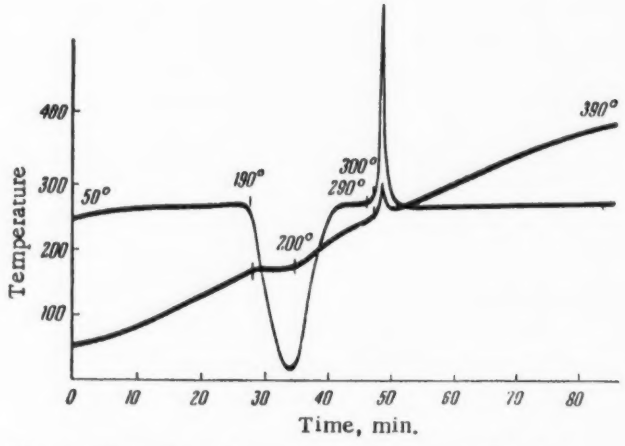

Fig. 5. Differential thermal analysis curve of $ZnSeO_3 \cdot H_2O$.

The differential thermal analysis curves of α-$ZnSeO_3$ (Fig. 6, 1) and of $ZnSeO_3 \cdot H_2O$ (Fig. 5 and Fig. 4, 2) show a marked exothermic effect at 290° corresponding to the conversion of α-$ZnSeO_3$ to the β form. There is no such effect in the curve for β-$ZnSeO_3$ (Fig. 6, 2 and Fig. 4, 1).

The α modification is thermodynamically less stable than the β form. This is shown by the following data:

a) α-$ZnSeO_3$ in solution in selenious acid is converted into the β form at room temperature; the monohydrate is produced on prolonged contact with water.

b) α-$ZnSeO_3$ is not precipitated from solution in the synthesis of zinc selenite by any of the four methods shown in Table 1.

c) Conversion of α-$ZnSeO_3$ to the β form is accompanied by a considerable exothermic effect.

Composition Diagrams for Neutral Zinc Selenite are shown in Fig. 7. It is evident that up to 95° three forms of zinc selenite can exist, namely the dihydrate, the monohydrate, and α-$ZnSeO_3$; up to 190° the monohydrate and α-$ZnSeO_3$; up to 285° α-$ZnSeO_3$; and above 290° only β-$ZnSeO_3$. On further heating, β-$ZnSeO_3$ dissociates into selenium dioxide and zinc oxide.

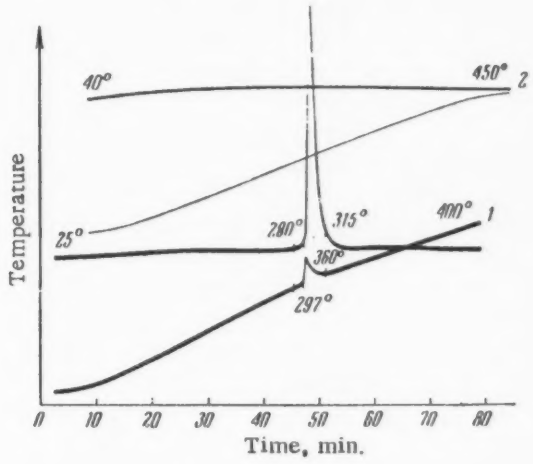

Fig. 6. Differential thermal analysis curves for anhydrous zinc selenite: 1) α-$ZnSeO_3$; 2) β-$ZnSeO_3$.

It is evident from Fig. 7 that dissociation becomes appreciable above 450° at atmospheric pressure. However, the degree of dissociation depends considerably on the experimental conditions, particularly on the possibility of escape of gaseous SeO_2. Curves were obtained showing the effects of heating a thin layer (layer density ~ 0.14 g/cm², total weight 1-5 g) of anhydrous zinc selenite for one hour in a crucible furnace. Under these conditions complete dissociation was only achieved at 600°.

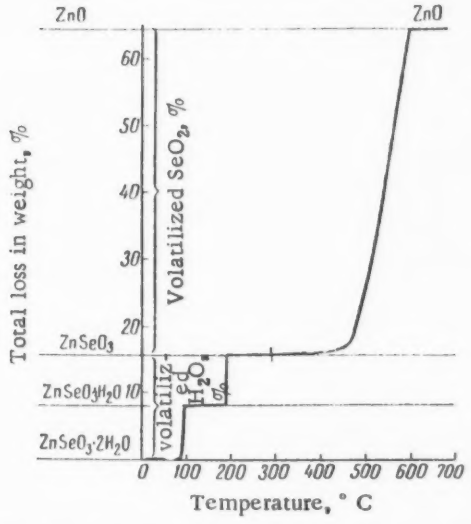

Fig. 7. Composition diagram for neutral zinc selenite.

The results obtained for the dissociation of anhydrous $ZnSeO_3$ do not agree with literature data [10, 11]. The difference is probably due to the experimental conditions, which greatly affect the kinetics of the process.

In conclusion, we would like to thank Yu. D. Kondrashev for assistance with the recording and interpretation of the x-ray patterns and for useful advice, and also to thank T. P. Vorokhobinaya for assistance with the experimental work.

SUMMARY

1. The formation conditions and composition of neutral zinc selenite have been investigated. The existence of two crystalline hydrate forms has been confirmed.

2. It has been shown that anhydrous zinc selenite is dimorphous.

3. The temperature limits for the existence of different forms of zinc selenite have been established by chemical analysis, x-ray analysis, differential thermal analysis, and microscopic studies.

4. Some new data is presented on the physical and chemical properties of zinc selenite.

LITERATURE CITED

1. L. Ya. Markovskii and R. I. Smirnova, Zhur. Neorg. Khim. 2, 2752 (1957).
2. J. J. Berzelius, Ann. Chim. Phys. 9, 160, 225, 337 (1818).
3. J. J. Berzelius, Liebigs Ann. Chem. 49, 253 (1844).
4. Fr. Wöhler, Liebigs Ann. Chem. 63, 279 (1847).
5. L. F. Nilson, Bull. Soc. Chim. France 23, 357 (1875).
6. J. S. Muspratt, Liebigs Ann. Chem. 70, 275 (1849).
7. M. Boutzoureano, Ann. Chim. Phys. 18, 291, 304, 350 (1889).
8. J. W. Mellor, A Comprehensive Treatise on Inorganic and Theoretical Chemistry (1930) Vol. 10, p. 826.
9. V. G. Chukhlantsev, Zhur. Neorg. Khim. 1, 2300 (1956).
10. W. Hirsch and A. Dietzel, Sprechsaal 68, 244 (1935).
11. J. B. Krak, J. Am. Ceram. Soc. Bull. 12, 530 (1929).
12. A. Ferrari, L. Cavalca, and M. Moretti, Gazz. chim. Ital. 80, 151 (1950); Chem. Abstr. 44, 10,438 (1950).
13. M. Prasad, S. S. Dharmatti, and H. V. Amin, Proc. Indian Acad. Sci. Bombey 26-a, 312 (1947); Chem. Abs. 42, 4410 (1948).
14. R. Pribil, Complexones in Chemical Analysis [Russian translation] (IL, Moscow, 1955).
15. S. I. Sinyakova, Zhur. Anal. Khim. 10, 139 (1955).*
16. W. F. Hillebrand, et al., Applied Inorganic Analysis [Russian translation] (GNTKhI, Moscow, 1957) p. 358.
17. V. M. Barshchevskaya and V. N. Vasil'eva, Zavodskaya Lab. 23, 304 (1957).
18. L. G. Berg, A. V. Nikolaev, and E. Ya. Rode, Thermography [in Russian] (Izd. AN SSSR, Kazan, 1944).
19. G. G. Tsurinov, The N. S. Kurnakov Pyrometer; Its Use at Low Temperatures [in Russian] (Izd. AN SSSR, Moscow, 1953).
20. A. I. Kitaigorodskii, X-Ray Structural Analysis of Finely Crystalline and Amorphous Materials [in Russian] (Gostekhteoretizdat, Moscow-Leningrad, 1952) p. 571.

* Original Russian pagination. See C. B. translation.

THE USE OF OVERLAP INTEGRALS FOR THE DETERMINATION OF THE IONIC CHARACTER OF BONDS IN MOLECULES

S. S. Batsanov and V. I. Durakov

Institute of Inorganic Chemistry, Academy of Sciences of the USSR
Translated from Zhurnal Strukturnoi Khimii, Vol. 1, No. 3, pp. 353-359, September-October, 1960
Original article submitted January 14, 1960

We have evaluated the overlap integrals for 32 covalent hydrides and halides; integrals for both the real and the hypothetical purely covalent bonds (with the bond distance equal to the sum of covalent radii and t = 0) were set up. The ratios between these two types of integrals give the deviations of the actual bond types from the idealized covalent state and they are used for the determination of the ionic character of various bonds. The results were in close agreement with Pauling's data, which were based on dipole moment measurements. The ionic character of a bond can be related to the electronegativity by the equation $i = 1 - e^{-0,2\Delta X^2}$

The polarity of bonds constitutes one of the fundamental problems in the theory of chemical structure, since polar bonds are found in a very great number of chemical compounds. The known experimental methods for the determination of the ionic character of bonds from dipole and quadrupole moments yield conflicting results, while at the same time there has obviously not been enough detailed theoretical work done in the field. An intensive study of this problem would constitute, in our opinion, a very far-sighted project, since it will quite obviously lead to a unified quantitative treatment for all the various chemical compounds. The primary purpose of this work is to show how overlap integrals can be used for the determination of the ionic character of chemical bonds in covalent hydrides and halides.

As has already been demonstrated in several papers [1-3] a chemical bond can be represented by integrals of the type $S = \int \chi_A \chi_B dV$, where χ_A and χ_B are the respective atomic orbitals of atoms A and B. Such integrals constitute a one-electron approximation and are evaluated over the entire space. Atomic orbitals can be represented by the following simplified expression (derived by Ziner and Slater [4, 5]):

$$r^{n^*-1} e^{-\frac{Z^*}{n^* a_H}} Y(\theta, \Phi),$$

where Z^* is the effective nuclear charge and n^* the effective principal quantum number (these can be evaluated by using rules derived by Slater [5] and Angus [6]); a_H is the first Bohr radius; $Y(\theta, \Phi)$ is the angular component of the orbital function.

A number of overlap integrals have been evaluated and tabulated [7-11] as functions of $\underline{p}$ and $\underline{t}$:

$$p = (M_A + M_B) R/2a_H \text{ and } t = (M_A - M_B)/(M_A + M_B),$$

where $M = Z^*/n^*$, and R is the interatomic distance. Overlap integrals have previously been used for the determination of energies of homopolar and heteropolar bonds, and the results were in good agreement with experimental data [12-14]. This good agreement suggested that overlap integrals may be very useful for other studies dealing with the nature of chemical bonds. Thus, Fyfe has already shown [15] that the overlap integrals of Li – E bonds, where E = F, O, N, Cl, S, C, P, and Si, decline monotonically as the electronegativity differences between the respective atoms $\Delta x = x_E - x_{Li}$ increase. Hence, it follows that overlap integrals can be used for the determination of the ionic character of chemical bonds; Fyfe, however, did not derive any quantitative relationship between the two variables. Such a relationship can be established if one first reduces all the overlap integrals to one scale. Our scale was based on the overlap integrals of these same bonds but with the two elements separated by a distance equal to the sum of the two respective covalent radii and t = 0. These criteria are very important in the treatment of covalent bonds.

In this way we are comparing the real bonds with purely covalent hypothetical ones. At the same time the hybridization and bond orders are assumed to be identical in both cases.

The covalent radii used in our work are all listed in Table 1; the tabulated values are based on recent data of Pauling, Sidgwick, Huggins, and Zachariasen [16-19], and on our own calculations (we computed the covalent radii of metals by introducing a correction for the coordination number to the corresponding atomic radii).

In accordance with the currently accepted theory of directed valence bonds we assigned diagonal, trigonal, and tetrahedral hybridizations respectively to the elements of Group II, III, and IV [20]. In compounds containing elements of Group V and VI the hybridization was computed from the equation: $\alpha = \cos\theta/(\cos\theta - 1)$, where θ is the bond angle [21]. According to Gordy [22-24], quadrupole interaction data indicate that there is no more than 5% hybridization in the atomic orbitals of halogens. The energy required to promote the transition $s^2x^2y^2z \rightarrow sx^2y^2z^2$ in fluorine was estimated by Pritchard and Skinner [25]; the results confirmed the fact that the hybridization of halogen orbitals is very small. However, since for the majority of halides the exact extent of hybridization is not known anyway, considering the small value of the effect we felt justified in neglecting this hybridization in most of our calculations.

We computed the ionic character $\underline{i}$ of bonds by using the following general equation:

$$i = 1 - \frac{\sum A_j S_j - \frac{1}{2}\sum A_{j'}(S_{j'})^2 + 0{,}82\sum S_k}{\sum A_j S'_j - \frac{1}{2}\sum A_{j'}(S'_{j'})^2 + 0{,}82\sum S'_k},$$

where $A_j = 1$ for S_{ss}, $A_j = 1.732$ for S_{sp}; S_{pp} and $A_k = 0.82$ for $S_\pi S_\pi$.

In this equation the summation over $\underline{j}$ and $\underline{k}$ takes care of the bonding electrons while summation over j' takes into account the repelling electrons. The coefficient A stands for "the specific electron density" of a given type of integral. The numerator represents the actual bond while the denominator represents the reference bond.

Pauling [20] derived the coefficient A = 1.732 for p-bonds by postulating that A = 1 for S – S bonds. Since the corresponding coefficient for the π-π bonds is not found in the literature, we determined it by following Pauling's procedure and assuming a 17% ionic character for the HCl bond; our value is in good agreement with the results obtained by several independent methods [27-30]. The calculated value of $A_k = 0.82$ was used in subsequent calculations.

Hydrides

For the hydrides of elements belonging to the first four groups of the periodic system in which the number of hydrogen atoms is equal to the number of electrons in the valence shell the ionic character of bonds can be evaluated by means of the following simplified equations:

$$i = 1 - \frac{S_{ss}}{S'_{ss}} \qquad \text{for Group I hydrides,}$$

TABLE 1

Covalent Radii (A)

Periods \ Groups	1a	2a	3a	4a	5a	6a	7a	8a	1в	2в	3в	4в	5в	6в	7в
I															H 0,37
II	Li 1,32	Be 0,96									B 0,84	C 0,77	N 0,74	O 0,74	F 0,72
III	Na 1,58	Mg 1,38									Al 1,16	Si 1,17	P 1,10	S 1,04	Cl 1,00
IV	K 2,02	Ca 1,74	Sc 1,44	Ti 1,32	V 1,21	Cr 1,19	Mn 1,19	Fe 1,20	Co 1,18	Ni 1,17	Cu 1,25	Zn 1,27	Ga 1,25	Ge 1,22	As 1,22	Se 1,17	Br 1,14
V	Rb 2,15	Sr 1,91	Y 1,61	Zn 1,45	Nb 1,32	Mo 1,20	Tc 1,26	Ru 1,26	Rh 1,27	Pd 1,30	Ag 1,42	Cd 1,43	In 1,46	Sn 1,40	Sb 1,41	Te 1,37	I 1,33
VI	Cs 2,33	Ba 1,97	La 1,68	Hf 1,44	Ta 1,32	W 1,30	Re 1,25	Os 1,27	Ir 1,28	Pt 1,30	Au 1,43	Hg 1,45	Tl 1,50	Pb 1,50	Bi 1,49	Po —	At —
VII	Fr 2,46	Ra 2,07	Ac 1,79														

Lanthanides	Ce 1,62	Pr 1,62	Nd 1,62	Pm 1,67	Sm 1,64	Eu 1,82	Gd 1,60	Tb 1,59	Dy 1,58	Ho 1,57	Er 1,56	Tu 1,55	Yb 1,70	Lu 1,55
Actinides	Th 1,58	Pa 1,43	U 1,35	Np 1,24	Pu 1,50	Am 1,49								

$$i = 1 - \frac{S_{\text{hybr. sp}}}{S'_{\text{hybr. sp}}} \quad \text{for Group II-IV hydrides.}$$

However, we were unable to determine the ionic character of bonds in Group II hydrides due to the lack of appropriate data on the interatomic distances in these molecules.

When determining the ionic character of bonds in hydrides of Group V - VII, it is also important to take into account the interaction between the free np^2 electron pairs on the central element and the free 2p π - orbitals of the hydrogen atoms, and consequently the numerical formula assumes the form:

$$i = 1 - \frac{1{,}732S_{\text{hybr.}sp} + 0{,}82S_{\pi\pi}/n}{1{,}732S'_{\text{hybr.}sp} + 0{,}82S'_{\pi\pi}/n},$$

where 1/n is the ratio of the number of free electron pairs to the number of free orbitals: 1/n = $^1/_3$ for Group V elements, $^1/_2$ for Group VI, and 1 for Group VII.

We determined the percent ionic character of the bonds in covalent hydrides, and the results are presented in Table 2.

TABLE 2

Percent Ionic Character of Bonds in Hydrides

Molecule	R_{exp}, A*	ΣR_c, A**	$\theta°_{exp}$	Real molecule						Reference molecule				i, %
				i	p	S_j	i	p	S_k/n	p	S'_j	p	S'_k/n	
LiH	1,60	1,69	—	0,21	2,50	0,46	—	—	—	2,64	0,54	—	—	12
NaH	1,89	1,95	—	0,15	3,10	0,39	—	—	—	3,13	0,48	—	—	18
RbH	2,37	2,52	—	0,29	3,47	0,21	—	—	—	3,71	0,40	—	—	47
BH_3	1,27	1,21	120°	—0,13	2,61	0,76	—	—	—	2,63	0,77	—	—	1
CH_4	1,094	1,14	109°28′	—0,24	2,71	0,68	—	—	—	2,83	0,72	—	—	5
NH_3	1,014	1,11	106°47′	—0,32	2,83	0,48	0,59	2,35	0,08	3,10	0,56	2,57	0,19	17
PH_3	1,42	1,47	95°46′	—0,23	3,49	0,56	—0,52	2,82	0,14	3,61	0,57	2,92	0,56	5
H_2O	0,957	1,11	105°3′	—0,39	2,96	0,44	—0,64	2,51	0,07	3,43	0,54	2,91	0,24	27
H_2S	1,334	1,41	92° 16′	—0,29	3,55	0,51	—0,57	2,92	0,18	3,75	0,53	3,08	0,21	6
HF	0,92	1,09	—	—0,44	3,91	0,29	0,67	2,70	0,15	3,71	0,42	3,20	0,43	42
HCl	1,27	1,37	—	—0,34	3,73	0,45	—0,60	3,04	0,32	3,93	0,50	3,28	0,49	17
HI	1,615	1,70	—	—0,31	4,38	0,50	—0,58	3,63	0,30	4,66	0,47	3,86	0,42	4

* These values are reproduced from [33].

** This is the sum of the covalent radii given in Table 1.

As has already been shown by Cotton and Leto, who investigated boron and aluminum halides, the overlap integrals of polyatomic molecules can be determined in the same way as can those of diatomic molecules [14].

Fluorides and Chlorides

In dealing with fluorides and chlorides one has to consider the repulsion between the inner shell electrons of the halogen and those of the other element. In the case of halides of Group III-VII elements one must also take into account the partial double bond character in both the real molecule and the reference model, since multiple bonding has a pronounced effect on the interatomic distances. Due to the lack of direct experimental methods, we have to use overlap integrals at the present time to estimate the percent double-bond character. This last one is determined from the ratio of the overlap integral for the π-bonds in the real molecule to the corresponding integral for a reference molecule in which the interatomic distance is equal to the sum of the double-bond covalent radii of the two elements. Multiple-bond covalent radii were taken from Pauling [34]

and are listed in Table 3. The percent double-bond character is 31 in BF_3, 31 in BCl_3, 59 in FCl, 16 in CF_4, 21 in CCl_4, 25 in SiF_4, 30 in PF_3, 23 in OF_2, and 19 in NF_3. Assuming a linear relationship between the lengths of double and single bonds and using the double-bond percentages derived above one can readily compute the interatomic distance in a reference molecule with the same bond-type as the real compound.

TABLE 3

Multiple-Bond Covalent Radii

Radii, A	Element				
	B	C	N	O	F
Single bond	0,88	0,77	0,70	0,66	0,64
Double bond	0,76	0,66	0,60	0,55	0,64
		Si	P	S	Cl
Single bond		1,17	1,10	1,06	1,00
Double bond		1,07	1,00	0,94	0,89

In Table 4, we have compiled our calculated percent ionic characters of the bonds in covalent halides. The experimental interatomic distances are reproduced from Rittner [35], Cottrell [33], Mulliken [1], and Akishin and Spiridonov [36]. The bond-lengths in reference molecules were all corrected for multiple bonding.

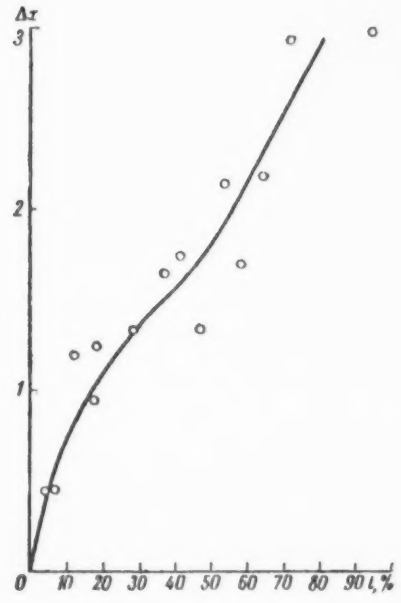

The relationship between the percent ionic character and the electronegativity difference.

The calculated percent ionic characters of the bonds in covalent halides and hydrides are, on the whole, in good agreement with Pauling's data [26]. We have therefore decided to find an analytical function, similar to Pauling's equation, which would connect the ionic character of bonds with the electronegativity difference between the bonded atoms. In our Figure, we have plotted the percent ionic character of bonds in binary molecules against the electronegativity differences (the electronegativities were taken out of a recent paper by Batsanov [37]). It is obvious that the ionic character of bonds increases as the electronegativity difference between the corresponding atoms is increased. The analytical form of the function which fits this curve is: $i = 1 - e^{-0.2\Delta X^2}$. It is interesting to note that in the original form of Pauling's curve the coefficient of ΔX^2 was 0.25 [36] but subsequently it was changed to 0.18 [38]. We can therefore see that our results practically reproduce the percent ionic character data based on dipole moment measurements.

One cannot regard the present form of our method as final. There is no doubt that a more rigorous treatment is required to take into account the effects of hybridization and multiple bonding on the electron density in molecules. In principle, it also seems essential that only orthogonal wave functions be used, but the appropriate data are practically nonexistent at the present time. Mulliken has shown [1] that in certain cases overlap integrals composed of orthogonal functions differ very little from those made up of nonorthogonal functions.

TABLE 4

Percent Ionic Character of Bonds in Halides

Molecule	R_{exp}, A	ΣR_c, A	θ_{exp}	Real molecule									Reference molecule						i, %
				t	p	S_j	t	p	S_k	t	p	S_j	p	S_j	p	S_j	p	S_j	
LiF	1,53	2,04	—	—0,60	4,70	0,06	—	—	—	—0,43	6,6	0,10	6,27	0,20	—	—	9,07	0,01	72
LiCl	1,97	2,32	—	—0,51	5,00	0,17	—	—	—	—0,32	7,08	0,10	5,98	0,36	—	—	8,51	0,04	54
LiI	2,37	2,65	—	—0,49	5,70	0,25	—	—	—	—0,27	7,95	0,09	6,43	0,41	—	—	9,07	0,05	38
NaF	2,00	2,30	—	0,56	6,30	0,03	—	—	—	0,50	8,32	0,09	7,11	0,19	—	—	9,39	0,05	95
NaCl	2,48	2,58	—	—0,47	6,48	0,13	—	—	—	—0,39	8,44	0,19	6,64	0,35	—	—	9,12	0,08	64
NaI	2,87	2,90	—	—0,44	7,14	0,18	—	—	—	—0,34	9,09	0,19	7,15	0,41	—	—	9,10	0,11	58
BeF_2	1,40	1,68	180°	—0,45	4,73	0,21	—	—	—	—0,14	6,02	0,10	5,46	0,41	—	—	7,22	0,05	49
$BeCl_2$	1,75	1,96	180°	—0,35	4,98	0,41	—	—	—	—0,02	6,59	0,12	5,40	0,54	—	—	7,38	0,08	25
BeI_2	2,10	2,29	180°	—0,32	5,71	0,47	—	—	—	0,03	7,64	0,11	6,22	0,49	—	—	8,33	0,08	5
MgF_2	1,77	2,10	180°	0,46	5,94	0,13	—	—	—	0,29	7,12	0,20	6,97	0,32	—	—	7,99	0,08	66
$MgCl_2$	2,18	2,38	180°	—0,36	6,15	0,35	—	—	—	—0,18	7,54	0,195	6,65	0,51	—	—	8,23	0,12	34
BF_3	1,29	1,45	120°	0,33	4,76	0,29	0,33	4,76	0,17	0,00	6,34	0,08	5,34	0,42	5,34	0,13	7,13	0,05	25
BCl_3	1,74	1,81	120°	—0,22	5,48	0,47	—0,22	5,48	0,20	0,12	7,62	0,13	5,70	0,49	5,70	0,17	7,93	0,06	13
CF_4	1,36	1,38	109°28′	—0,23	5,43	0,33	0,23	5,43	0,17	0,11	7,52	0,04	5,51	0,39	5,51	0,12	7,63	0,04	8
CCl_4	1,77	1,72	109°28′	—0,11	6,09	0,44	—0,11	6,09	0,14	0,23	8,84	0,05	5,95	0,46	5,95	0,15	8,59	0,04	5
SiF_4	1,54	1,76	109°28′	0,30	5,80	0,23	0,30	5,80	0,14	0,11	6,80	0,18	6,62	0,35	6,62	0,10	7,78	0,09	33
PF_3	1,54	1,75	104°	0,24	6,11	0,26	0,24	6,11	0,12	0,24	6,11	0,27	6,95	0,29	6,95	0,08	8,25	0,10	10
NF_3	1,37	1,30	102°9′	0,14	5,89	0,28	0,14	5,89	0,10	0,14	5,89	0,205	5,59	0,32	5,59	0,11	5,59	0,23	11
OF_2	1,41	1,25	100°	0,07	6,50	0,23	0,07	6,50	0,11	0,07	6,50	0,15	5,76	0,30	5,76	0,11	5,76	0,21	19
FCl	1,63	1,51	—	0,12	7,14	0,22	0,12	7,14	0,07	0,12	7,14	0,17	6,61	0,28	6,61	0,10	6,61	0,21	21

SUMMARY

1. A new method has been developed for the determination of the percent ionic character of bonds; the method involves a comparison between the overlap integral for the real bond and that for a hypothetical covalent bond.

2. An equation has been derived relating the percent ionic character to the difference between the electronegativities of the corresponding atoms $i = 1 - e^{-0.2\Delta X^2}$.

LITERATURE CITED

1. R. Mulliken, J. Am. Chem. Soc. 72, 4493 (1950).
2. D. Craig, et al., J. Chem. Soc. 332 (1954).
3. H. Jaffe, J. Phys. Chem. 58, 185 (1954).
4. C. Ziner, Phys. Rev. 36, 51 (1930).
5. J. Slater, Phys. Rev. 36, 57 (1930).
6. W. Angus, Proc. Roy. Soc. A136, 529 (1932).
7. R. Mulliken, et al., J. Chem. Phys. 17, 1248 (1949).
8. H. Jaffe, J. Chem. Phys. 21, 258 (1953).
9. H. Jaffe and G. Doak, J. Chem. Phys. 21, 196 (1953).
10. D. Craig, et al., J. Chem. Soc. 354 (1954).
11. L. Leifer, E. Cotton, and J. Leto, J. Chem. Phys. 28, 364 (1958).
12. R. Mulliken, J. Phys. Chem. 56, 295 (1952).
13. V. Aoku, J. Phys. Soc. Japan 10, 503 (1955).
14. E. Cotton and J. Leto, J. Chem. Phys. 30, 993 (1959).
15. W. Fyfe, Am. Mineralogist 39, 991 (1954).
16. L. Pauling, J. Am. Chem. Soc. 69, 542 (1947).
17. N. Sidgwick, Chemical Elements and Their Compounds (1951), Vol. I, p. 29.
18. M. Huggins, J. Am. Chem. Soc. 75, 4126 (1953).
19. W. Zachariasen, Coll: Actinides [Russian translation], (IL, Moscow, 1955).
20. S. Glasstone, Theoretical Chemistry [Russian translation] (IL, Moscow, 1950).
21. C. Townes and A. Schanlow, Microwave Spectroscopy (New York, 1955).
22. W. Gordy, J. Chem. Phys. 19, 722 (1951).
23. W. Gordy, Discuss. Faraday Soc. 19, 14 (1955).
24. W. Gordy, Chemical Applications of Spectroscopy [Russian translation] (IL, Moscow, 1959).
25. H. Pritchard and H. Skinner, Chem. Revs. 55, 745 (1955).
26. L. Pauling and J. Sherman, J. Am. Chem. Soc. 54, 1450 (1937).
27. N. Hannay and C. Smyth, J. Am. Chem. Soc. 68, 171 (1946).
28. R. Sanderson, J. Chem. Educat. 31, No. 2 (1954).
29. G. Burrow, J. Chem. Phys. 28, 485 (1958).
30. R. Ferreira, J. Phys. Chem. 63, 745 (1959).
31. B. Dailey and C. Townes, J. Chem. Phys. 23, 118 (1955).
32. R. L. Barinskii, Zhur. Strukt. Khim. 1, 2, 200 (1960).*
33. T. Cottrell, The Strengths of Chemical Bonds [Russian translation] (IL, Moscow, 1956).
34. L. Pauling, The Nature of the Chemical Bond [Russian translation] (Goskhimizdat, Moscow, 1947).
35. E. Rittner, J. Chem. Phys. 19, 1030 (1951).
36. P. A. Akishin and V. P. Spiridonov, Kristallografiya 2, 475 (1957).
37. S. S. Batsanov, Izvest. Sibir. Otdel. Akad. Nauk SSSR 1, 68 (1960).
38. L. Pauling, J. Phys. Chem. 56, 361 (1952).

* Original Russian pagination. See C. B. translation.

REVIEWS

CONTEMPORARY X-RAY SPECTRAL ANALYSIS*

É. E. Vainshtein

Institute of Inorganic Chemistry, Siberian Division, Academy of Sciences of the USSR
Translated from Zhurnal Strukturnoi Khimii, Vol. 1, No. 3, pp. 360-369,
September-October, 1960
Original article submitted December 25, 1959

This is a review of contemporary methods, apparatus, and theory of x-ray spectral analysis. The possibilities for further development of this method of investigation are also considered.

X-ray spectroscopy as a method of analyzing the chemical composition of substances or as a method of investigation of atomic interactions in compounds is a relatively new method of investigation. Khaddin, Kheveshi, and Noddaki made the first contributions in this area between 1922 and 1925. Their investigations led to the discovery of two new chemical elements: hafnium (Kheveshi, 1923), and rhenium (Noddaki, 1925). Since then x-ray spectral analysis has been increasingly applied for the solution of various problems in chemistry and chemical technology, geology, geochemistry, solid state chemistry, and for the study of metals. The use of x-ray analysis has also been increasing in industry, particularly during the past ten years. On one hand, this has been the result of considerable theoretical development, which has widened the area of application of x-ray spectroscopy in chemistry. On the other hand, the improvement of methods of investigation, particularly the method of counting elementary particles and photons (possible as a result of the intensive development of nuclear physics), has contributed even more to the development of the method. In recent years all this has made possible an intense development of apparatus and methods of fluorescent x-ray spectroscopic analysis and other special methods which have become more and more important, replacing older methods of investigation in chemistry and metallurgy, and indicating the direction of further developments in x-ray spectroscopy. In spite of certain difficulties in many of these new applications of x-ray spectral analysis – proper apparatus sometimes unavailable, some of the methods not yet completely worked out – it seems to us that they will have the greatest future development, and we shall devote the greater part of this review to them. As for methods of x-ray analysis already developed, tested, and widely applied, they have been described in detail in monographs by M. A. Blokhin [1] which appeared last year, and by this author [2, 3]; they give concrete examples of applications for quantitative analysis of a number of elements which were difficult to measure (TR, Zr, Hf, Nb, Ta, etc.) in samples of complex and variable composition.

Fluorescent X-ray Spectral Analysis

One of the most important characteristics of contemporary x-ray spectral analysis is the increasingly clear tendency to pass from almost exclusive use of spectra of primary excitation to a wider use of secondary emission spectra and to use of the so-called x-ray fluorescence method.

In fluorescent x-ray spectrography the excitation of the characteristic radiation of atoms of the substance being investigated is achieved by irradiation with a powerful beam of primary x-rays. This fluorescent method

* Resume of the meeting on the analysis of rare and semiconducting materials held in Moscow, December 7-11, 1959.

of excitation of spectra has a number of advantages with respect to the ordinary method, in which the x-rays appear at the moment the high-speed electrons coming from the surface of the cathode of the x-ray tube are abruptly stopped by the anticathode. Some of the advantages of the fluorescent method come from the fact that the sample can be placed in air, outside the vacuum of the x-ray tube, or can be introduced into the vacuum through a special lock. This makes it unnecessary to use the dismountable x-ray tube with its complex high vacuum system, and makes it possible to make the analysis without heating or destroying the sample, and on the whole speeds up the analysis considerably. Also, the lack of a continuous spectrum of secondary x-ray radiation, and the consequent sharp decrease of background intensity with respect to that of the primary excitation method, leads to an increase of the sensitivity of fluorescent x-ray spectral analysis.

Unfortunately, the intensities of the secondary emission spectra are a few tens of times weaker than those of the primary spectra, and it is inconvenient to register them by photographic methods. For a long time this fact prevented wide practical application of this method of spectra excitation, which has become possible only relatively recently.

At the present time in the USA and in Europe, and recently in the USSR, several types of fluorescent x-ray spectral analysis apparatus for industrial use are being mass produced. These are being used in many branches of industry, geology, chemistry, and metallurgy. In the United States, for example, it has in many cases replaced other types of analysis, particularly optical spectral analysis. X-ray spectral analysis makes possible a quantitative analysis of all the elements, all the way from sulfur to the end of the periodic table. The sensitivity of modern fluorescent analysis is on the average approximately 10^{-2} %, but it depends largely on the atomic number of the elements and the character of the sample being analyzed. In the most favorable cases, it reaches 10^{-3}% while in the least favorable cases it can decrease by almost three orders [4-17]. The precision of quantitative determination of the element depends to a great extent on the choice of the method of analysis, and in most cases can be pushed to 2-5% of the quantity to be determined. Duration of the analysis varies from a few minutes to 1-2 hours. The greatest difficulties arise in the analysis of elements with small atomic numbers and in the area of long wavelengths. These difficulties are the result of the sharp decrease of the relative yield of the characteristic radiation for these elements and the intense absorption of long wavelength radiation in the space between the source of radiation and the sample.

An important drawback of the method of secondary excitation spectra with respect to the primary excitation spectra is the existence of a relationship between the intensity of the analytic line of the element being investigated and the general composition of the sample, particularly, in the presence of the so-called "hindering elements" in the sample, which induce selective excitation or absorption of the radiation of the element under investigation. This leads to the deformation of the linearity of the calibration curves relating the intensities of the analytic lines of the element to the number of excited atoms in the volume of the sample, and in a certain sense creates a situation analogous to that occurring in optical spectral analysis.

This difference between fluorescent x-ray spectral analysis and primary x-ray spectral analysis is due essentially to the fact that the x-rays penetrate deeper into the sample than electrons. Therefore, the excitation of secondary spectra in the fluorescent method occurs in a relatively large volume of the substance, while with primary x-rays the investigation is confined to a very thin surface layer of the substance, the depth usually not exceeding 10-12 μ.

At the present time, a considerable number of publications [18-22] concern problems of the theory and application of fluorescent x-ray spectral analysis. In some of these investigations there are attempts to take into account in a strictly mathematical manner the effect of interaction between different components in systems of various complexity [6, 23, 24, 25]. The general theory of the analysis of multicomponent substances and practical methods of analysis were developed by Beattie and Brissey, based on the Sherman equation. Unfortunately, practical use of the theoretical results obtained in this manner is difficult in the general case because of the complexity of the final mathematical expressions. It is therefore understandable that some investigators tend to develop concrete methods of analysis of different substances by accounting empirically for the hindering effects of some elements in the substance. For example, Barinskii [7] preferred this method for quantitative determination of individual elements in rare earth minerals. In some cases the effect of interaction of the elements can be weakened by using the comparative method with a proper choice of the reference element [26] or by greatly diluting the substance with starch, sugar, lithium carbonate, or some other light filler [27]. It is true that this dilution reduces the sensitivity of the method, and can be recommended only where the substance

contains a large amount of the element to be measured. Where the substance contains a large amount of the element one can also use very thin layers of the substance (of the order of a few microns) to weaken the hindering effects of selective excitation and absorption. To compensate for the resulting decrease of sensitivity, one should use more powerful beams of primary x-ray radiation [5]. This method should not be used if the concentration of the element is low, since the precision of analysis of thin samples is considerably lower than analyses of "thick" samples, which are usually made in the form of briquettes of the required dimension [28, 29]. The binder (which dilutes the substance at the same time) can be a light filler, as we have said before, such as starch, sugar, graphite, or aluminum powder. If the sample does not contain elements capable of inducing selective excitation of the analytic lines of the element being determined, the effect of the total composition of the sample on the result of fluorescent x-ray analysis can be taken into account easily by the methods developed by Losev. In this method the quantity of the element is determined by the method of external standards with a correction for the difference between the mass coefficients of the analyzed sample and the standards used to draw the calibration curve.

Fluorescent x-ray analysis is sometimes combined with chemical or radiometric methods to increase precision and sensitivity. Campbell and Carl [30] used this system in determining U and Th.

In recent years fluorescent x-ray radiation has found one very important industrial application; it is used to determine the thickness of thin protective layers without injury to the layer or the base, making continuous quality control possible. It is being used to determine the thickness of a layer of tin or zinc in the manufacture of tin plate, a layer of ferromagnetic powder on plastic tapes [31, 32], and the thickness of lacquer films on metallic or glass bases [31-37]. The minimum thickness which can be measured by this method varies with different materials from 1 to 80 μ. The precision of measurement is approximately 3 to 6%.

The precision of fluorescent x-ray analysis depends to a great extent on the constancy of the intensity of the primary beam of x-rays falling on the surface of the sample and the standard. During the early years of the development of this method many attempts were made to solve this problem by stabilizing the emission of the x-ray tube, i.e., the generator of the primary x-ray radiation. However, more precise results have been achieved with the so-called monitor method [38, 39]. This method makes it possible to obtain precise measurements of relative intensity of spectral analysis without stabilizing the radiation source. The radiation is partly or completely directed away from the basic registration apparatus into an auxiliary device (the so-called monitor), and the intensity of spectral lines of the element is measured by the main counter over a period of time in which the monitor counts a certain number of impulses decided upon in advance, usually a few thousand. Under these conditions, the average statistical error is usually of the order of 2-5%, and is independent of the concentration of the element. Some investigators prefer other variations of the monitor system in which either the monitor automatically maintains the intensity of the primary radiation or automatically changes the sensitivity of the main counter [40].

The logical extension of the monitor idea has been the wide development of two-channel and multichannel x-ray spectrometers, the so-called quantometers [41-46]. With these devices one can make very rapid quantitative analyses of several elements simultaneously in a series of samples of the same type. A diagram of the simplest of these apparatus – a two-channel spectrometer – first proposed by Drahokoupil and Maresh [47] is shown in Fig. 1. It consists of two two-crystal spectrometers registering the fluorescent radiation of a sample. Each of these spectrometers measures the intensity of the analytical lines of one of the two elements present in the sample, one of them being the element to be determined and the other the reference element. Apparently, the ratio of the intensity of the lines of the two elements does not depend on the variation of the conditions of the radiation source, and can be determined with great precision. Later, quantameters with a great number of channels were constructed – three, eight, and even twenty-four (ultrameters). Diagrams of some of them are shown in Figs. 2, 3, and 4. In all cases, they are combinations of several spectrometers of the same type in which the fluorescent radiation from the element being measured is directed onto the crystal analyzer. Each of the spectrometers is meant to measure the intensity of the analytical lines of a given element with an electronic counter. Since a greater number of channels can be situated around a radiation source in the vertical plane than in the horizontal plane, the quantameters with the greatest number of channels are usually of a construction similar to those shown in Figs. 3 and 4. When plane crystal-analyzers are used in these apparatus, so-called Soller diaphragms (Fig. 4) are used at the same time. However, in the latest x-ray quantameter, constructed by Gesler, Kemp, and Jones, a bent crystal is used.

In cases where the resolving power of the method can be low, the spectral composition of the x-ray radiation can be studied without the crystal analyzer if one uses proportional counters simultaneously with amplitude analyzers for registering the intensity of x-ray radiation. Such an apparatus was recently described by Gosslet and Duncumb [48].

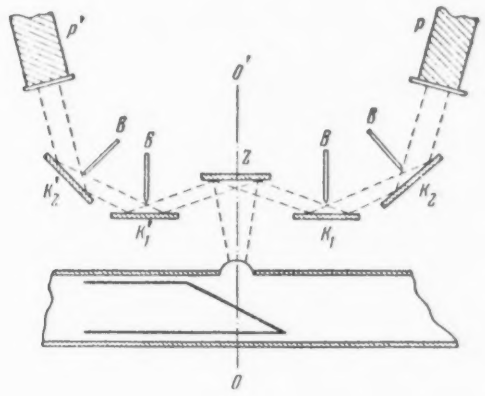

Fig. 1. Diagram of a two-channel x-ray spectrometer. Z) Sample; K_1, K_2, K_1', K_2') crystals; P, P') registering apparatus.

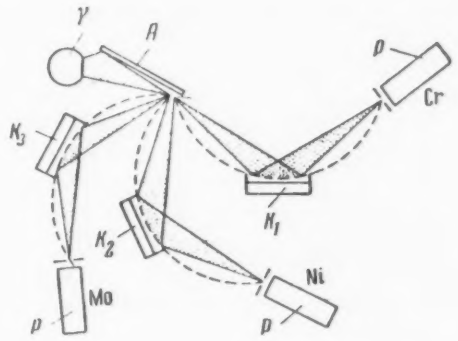

Fig. 2. Diagram of a three-channel x-ray spectrograph. γ) X-ray tube; A) sample; K_1, K_2, K_3) bent crystal-analyzers; P) registering apparatus.

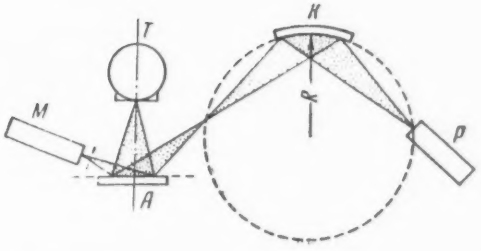

Fig. 3. Diagram of a multichannel x-ray spectrograph. T) X-ray tube; A) sample; M) monitor; K) one of the bent crystal-analyzers; P) registering apparatus.

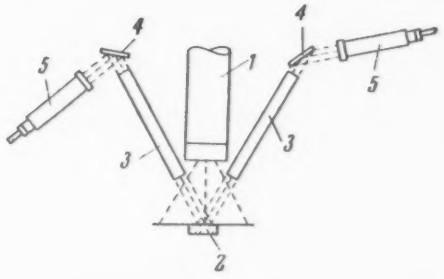

Fig. 4. Diagram of a multichannel x-ray spectrograph with plane crystals. 1) X-ray tube; 2) sample; 3) Soller diaphragm; 4) crystal; 5) registering apparatus.

Absorptional X-ray Spectral Analysis

During recent years, the method of absorptional x-ray spectral analysis has found wide applications in industry, particularly the oil industry [49, 50]. The bases of this method were worked out in the middle twenties by Glocker and Frohmayer [51]. It is particularly useful for determining the concentration of heavy metals in gases, liquids, and plastics. The simplest variation of the absorptional method of analysis – in which the concentration of the element to be measured is determined by the variation of the intensity of a beam of x-rays after they have passed through a standard plane parallel layer of the substance investigated – is useful only to determine the concentration of one heavy metal in a standard medium not containing absorbing impurities. Nevertheless such x-ray photometers are used successfully to measure the concentration of sulfur in carbohydrates [52, 53] and the concentration of lead in oil or gasoline [54]. The sensitivity of this method is approximately 0.2-0.5 %. The relative precision is about 10% where concentrations are 10 times higher than the sensitivity. The precision decreases considerably with decreasing concentrations of the element to be measured. The time

necessary for such an analysis is 5-15 minutes. This method can be used for microscopic investigation of multicomponent alloys or chemical heterogeneities in these alloys [55].

The method of absorptional x-ray spectral analysis based on the use of the values of K or L absorption jumps in the elements to be measured has much greater possibilities of application. With this method, it is possible to determine quantitatively the amount of an element in the presence of other elements. This method, which by analogy with optics could be called the x-ray spectrophotometric method, is characterized by a greater precision (approximately 5%) and greater sensitivity (approximately 0.1%) than the photometric method described previously. There are two variations of the method. In some cases, quantitative determination of an element in a relatively low absorbing medium is made directly with the calibrated curve expressing the relationship between the magnitude of the absorption jump of the element and its concentration in a layer of constant thickness of the sample being investigated. In the other variation one chooses two spectral lines located at each side of the absorption edge of a given element to determine the amount of the element, and for analysis one uses the curve representing the relationship between the relative intensity of the line as a function of the concentration of the element in the absorbing layer. Despuyoles used this method to determine the concentration of zinc in calcium and silicon [56]. Engstrom [57] has determined the concentration of iron in waters of different mineral composition, and Drahokoupil, using an original two-channel apparatus with photographic registration of the radiation, determined the concentration of lead in aqueous solutions which also contained considerable amounts of SiO_2 [58].

The same method has been used in other investigations to determine the diffusion of relatively heavy elements in opaque media [59].

X-Ray Spectral Analysis of Microvolumes of Samples

In recent years a new and quite promising method of x-ray spectral analysis has been developed for determining the chemical composition of microvolumes of substances. This development became possible after Castaing and Guinier [60-62] developed a microanalyzer with high resolving power in 1951-1953. The basis of the apparatus is a microfocusing x-ray tube connected with an optical metallographic microscope. A special electron-optical system forms a thin electronic probe which bombards a small area of the polished sample (of the order of 1 μ in diameter) placed on the anode, and excites x-rays whose spectral composition is analyzed with an ordinary x-ray spectrograph with a bent crystal. A diagram of the Castaing microanalyzer is shown in Fig. 5. Most of the newly developed apparatus for determination of the chemical composition of microvolumes, and in particular the apparatus constructed and used by a group at the IMET of the Academy of Sciences of the USSR and GOI, are constructed on the same principle. In these microanalyzers (Fig. 6) the positioning of the electron probe on a definite point of the sample is controlled with an optical microscope with a magnifying power of 300-400. Such a high power microscope is necessary because of the small size of the area being analyzed. The extreme smallness of this area makes special demands on the design of the electron-optical system of the microanalyzer; various investigators have met these demands in different ways with different degrees of success. The intensity of the diaphragmed x-ray radiation is registered by quantum counters whose types and details of construction depend on the region of the x-ray spectrum being used.

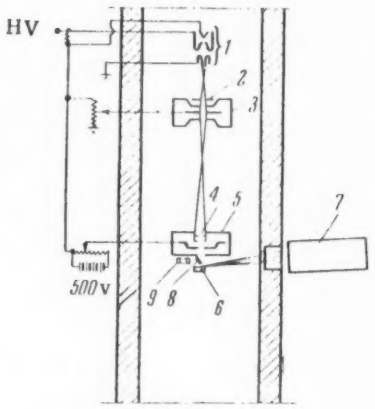

Fig. 5. Diagram of the Castaing and Guinier microanalyzer. 1) Electron gun; 2) diaphragm; 3) first converging electrostatic lens; 4) aperture diaphragm; 5) second converging electrostatic lens; 6) sample; 7) x-ray spectrometer; 8) mirror; 9) objective of the optical metallographic microscope; HV) high voltage.

The microanalyzer may be used either to make a spectral analysis for several elements "at a point" or to determine the distribution of one element in a chosen direction. In the latter case, the sample is moved under the electron beam in a definite direction and the intensity of the analytical line of the element is registered automatically. To determine the absolute concentration of an element at a chosen point of the sample, the intensity of its analytical

line is compared with the intensity of the same line of a standard. The theoretical bases of the method of analysis "at a point" are described in detail by Castaing and Descamps [63, 64]. However, considerable work remains to be done in this area.

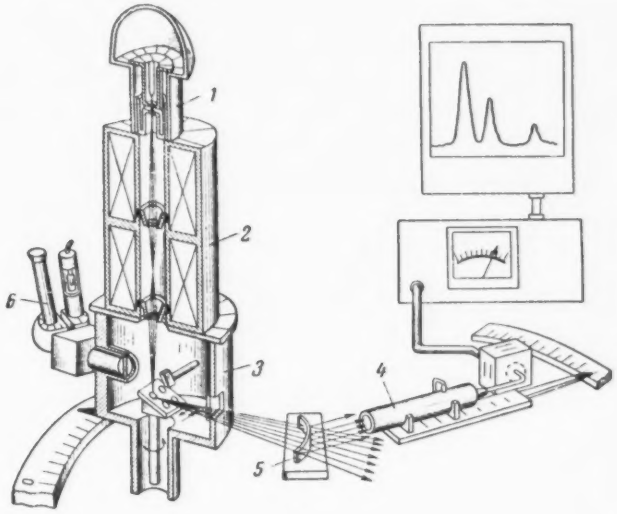

a

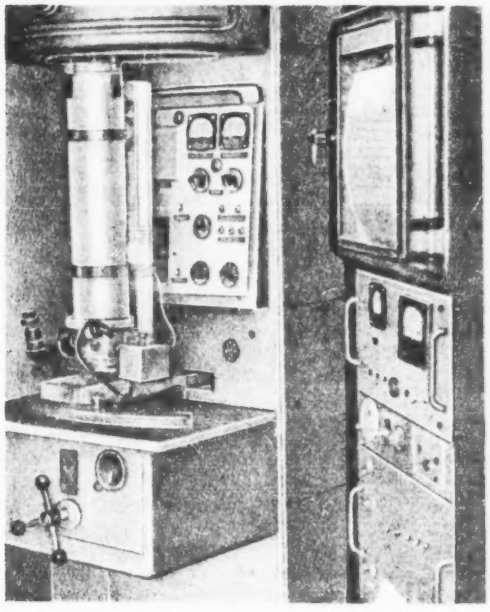

b

Fig. 6. Theoretical diagram (a) and general appearance (b) of the RSASh-2 microanalyzer constructed by Borovskii and Il'in with the beam focused by the Du Mond method.

The construction of microanalyzers sufficiently perfected to investigate different regions of the spectrum and to analyze a large number of elements has been pursued throughout the world ever since Castaing and Guinier published the basic work. The various results of this development have been summarized in recent years

in several national and international symposia and meetings. In the USSR intense work in this direction was first begun in the IMET of the Academy of Sciences of the USSR, and somewhat later in GOI, where several models of microanalyzers are presently being developed and applied for the solution of a number of theoretical and practical problems, both in vacuum and nonvacuum [65-68]. These models are the basis of a considerable amount of work being done in industry to develop mass production of microanalyzers.

These microanalyzers make possible the quantitative determination of elements from Mg to U with a sensitivity of the order of 0.05-0.5%. The concentration curve can be automatically registered when the concentration of the element is between 0.2 and 0.5%. With a suitable choice of the rate of motion of the table holding the sample and of the recorder chart one can obtain concentration curves with a magnification of 400 to 1600 times.

Cosslet and Duncumb's so-called projection microanalyzer [69] was a further development of the idea of the Castaing microanalyzer. In this microanalyzer the electron probe covers a given surface of the sample and makes it possible to observe on a television screen the magnified (more than 10 times) picture of the distribution of chemical elements on the surface of the metallographic sample. Photographs of the area of the screen in which the element is present take the form of white spots on a black background. Analysis of the spectra is made without a crystal by use of a proportional counter and a single-channel amplitude analyzer, which isolates impulses corresponding to the spectral lines of the element.

There are many possibilities in various areas of science for the application of both types of microanalyzers. The high local sensitivity of the microanalyzer (up to 10^{-15} g), the great precision in selection of the area to be examined, and the automatic registration of the concentration curve make it possible to solve a series of important problems very rapidly. Previously, even a statement of the problem was impossible in many cases because of the lack of a quantitative method of investigating microcomposition. Among these problems are the analysis of the phase composition of multicomponent alloys, the degree of homogenization of the alloy, the topology of the distribution of the alloyed elements in the alloy and their redistribution during the process of aging, deformation, or heat treatment, and also the diffusion processes, the determination of diffusion constants, and the study of diffusional and other intermediate layers, particularly the grain boundaries in alloys, the processes occurring at the boundaries, etc. [67, 70]. The new method has been particularly fruitful in investigations of the composition of phases of various metal-ceramic compositions [71] and the investigation of processes accompanying welding of some heat-resistant alloys [72].

The method of analysis of microvolumes can also be applied to the investigation of nonmetallic substances in chemistry, mineralogy, and geochemistry [73, 74]. In this case, it is necessary to condense a thin layer (approximately 0.1 μ) of a light metal – aluminum or beryllium – on the surface of the polished sample (to prevent migration of the beam along the surface). The method can also be used in mineralogy to determine the composition of grains and analyze minerals [75].

Use of X-Ray Spectra for Investigations of the Nature of Chemical Bonds, Particularly Atomic Interactions in Compounds

Up to now, we have examined different methods of applying x-ray spectra to the study of the elementary chemical composition of substances. For this purpose, one usually uses the long wavelength radiation from the K or L series of elements. The wavelength and the shape of the wave are practically independent of the chemical composition of the substance or the type of chemical bond between atoms of the compound, while the intensity is directly proportional to the number of atoms of the element in the volume of the sample investigated. It is one or the other use of this dependence which is the basis of any method of quantitative analysis.

However, there exists in the x-ray spectrum another group of lines, which appear as the result of the transfer of valence electrons of the atoms to the deeper K or L energy levels. The energy state, the relative intensity, and the shape of the line depend on the chemical or physical state of the atoms in the compound, and therefore, they are very sensitive indicators of any change in the character of the chemical bonds between atoms of the substance. Thus, examination of the spectral characteristics of this group of lines of the spectra of the atoms of different elements in the substance, or the investigation of the so-called fine structure of the absorption spectra should, in principle, make it possible to determine experimentally the nature of chemical bonds, and particularly the atomic interactions in different compounds. However, the necessary condition for this study is

a development of the theory of fine structure of x-ray spectra, the development of methods of calculation and correction of various kinds of errors which modify experimental results, and the construction of apparatus with very high dispersional and resolving power which can be conveniently used for such experiments. In recent years a great number of results has been obtained in this area.

A method of interpreting x-ray spectra based on definite physical concepts has been developed [75-82]. Improved methods have been introduced to correct the shape of spectra deformed by imperfections of the apparatus resulting from the finiteness of the width of the internal energy levels of the atoms [1]. And a high power apparatus with adequate resolving power has been constructed [1, 3]. These developments have made the x-ray spectral method into one of the most effective modern tools of investigation of chemical bonds and compounds, particularly solids, and have made it possible to solve many problems which previously could not be studied by any other means. In a number of cases the fine structure of the x-ray spectra of atoms and molecules allows one to calculate their ionization potential and polarization capacity in compounds [77], the charge of the absorbing ion in the molecule [82], and also to check experimentally the type of chemical bonds in compounds and the character of the hydration of atomic functions [83, 84]. Thus, the application of the method of x-ray spectral analysis to investigation of the nature of chemical bonds in hydrides, carbides, nitrides, borides, and silicides of transition metals (which have high resistance at high temperature, hardness, high resistance to activation, and other useful properties), has made it possible to check experimentally many physical concepts in this area of contemporary metallurgy, and has led to the discovery of a series of new facts and relationships [85-88]. The application of x-ray spectral analysis to crystals exhibiting electrooptical activity has also been very effective. In the case of titanates of the elements of the second period, it was shown that the fine structure of the edge of the titanium absorption spectra is very sensitive to changes in the state of polarization of the transition metals in the compounds and to the transfer of material in the electrooptical state. It was also shown that in principle one can determine in this way the value of the internal field in crystals exhibiting electrooptical activity [93]. The relationship between the fine structure of x-ray spectra and the magnetic state of the substance has made it possible to carry out a number of interesting investigations of different magnetic materials – ferro and antiferromagnetics and ferrites [84, 94-100] – and also to investigate the nature of some types of magnetic transformations in metals and alloys [95]. A number of investigators have shown that x-ray spectral analysis can be applied to the investigation of the nature of chemical bonds, particularly of atomic interactions within complexes either in solutions or in solid state [101-109]. Very promising is the application of the method to the investigation of the energy structure of electron spectra in metals and alloys and its relationship to the composition of the alloy, the temperature, and also the chemical nature and concentration of small amounts of impurities (including the alloyed elements) which, as is well known, often drastically change the physical properties of pure metals and alloys [96, 98, 110, 111]. Numerous other examples could be given.

In this review we have only briefly indicated a few basic directions in the development of x-ray spectral analysis in recent years and its state at the present time. This review shows how fast this relatively new method of physicochemical investigation has developed and the extent of the possibilities of its applications in chemistry, physics, geology, and metallurgy at the present time. Further development of the possibilities of the method, its improvement, the industrial production of x-ray apparatus, and new applications of x-ray analysis to the solution of theoretical and practical problems can be expected in the near future.

LITERATURE CITED

1. M. A. Blokhin, Methods of X-Ray Analysis [in Russian] (Gos. Izd. Mat. Lit., Moscow, 1959).
2. É. E. Vainshtein, Methods of Quantitative X-Ray Analysis [in Russian] (Izd. AN SSSR, Moscow, 1956).
3. É. E. Vainshtein, High Power Apparatus for X-Ray Analysis [in Russian] (Izd. AN SSSR, Moscow, 1957).
4. E. N. Danis and R. A. van Nordstrand, Analyt. Chem. 26, 973 (1954).
5. K. I. Narbutt and I. D. Bespalova, Zavodskaya Lab. 24, 617 (1958).
6. I. Scharman, ASTM Spec. Techn. Publ. 157, 27 (1954).
7. R. L. Barinskii, Zavodskaya Lab. 24, 613 (1958).
8. A. S. Ivoilov and N. R. Losev, Izvest. Akad. Nauk SSSR, Ser. Fiz. 21, 1465 (1957).
9. I. Snasta, et al., Collection: Geotechnica, Nakladatelstvi Ceskoslovenske akademie ved. (Prague, 1955).

10. G. T. Kokotillo and G. F. Damon, Analyt. Chem. 25, 1185 (1953).
11. I. M. Axelrod and I. Adler, Analyt. Chem. 27, 1875 (1955).
12. Dorita A. Norton, Am. Mineralogist 42, 7-8 (1957).
13. L. S. Birks and E. I. Brooks, Analyt. Chem. 22, 1017 (1950).
14. C. Lucchesi, Analyt. Chem. 29, 370 (1957).
15. G. Clark and H. Ferford, Analyt. Chem. 26, 1416 (1954).
16. I. Drahokoupil, Hutnicke listy 11, 233 (1956).
17. K. Toyel, Chem. Z. 32, 168 (1958).
18. G. Lang, Z. Mettalkunde 46, 816 (1955).
19. O. Weruer, Arch. Eigenhütenwesen 26, 721 (1955).
20. H. A. Liebhafsky, Analyt. Chem. 26, 26 (1954).
21. A. Liebhafsky and E. H. Winslow, Analyt. Chem. 28, 583 (1956).
22. R. F. Patrick, J. Am. Ceram. Soc. 35, 189 (1952).
23. M. A. Blokhin, Doctoral Dissertation [in Russian] (Rostov Gos. Univ., 1951).
24. I. Sherman, Spectrochim. Acta 7, 283 (1955).
25. H. I. Beattie and R. M. Brissey, Analyt. Chem. 26, 980 (1954).
26. I. Adler and I. M. Axelrod, Spectrochim. Acta 7, 91 (1955).
27. E. L. Gunn, Analyt. Chem. 29, 184 (1957).
28. I. Adler and I. Axelrod, Analyt. Chem. 26, 931 (1954).
29. D. M. Mortimore, P. A. Romans, and I. L. Tews, Appl. Spectroscopy 8, 24 (1954).
30. W. I. Campbell and H. F. Carl, Analyt. Chem. 27, 1884 (1955).
31. C. Legrand and I. I. Trillat, Rev. metallurgie 53, 645 (1956).
32. "Recent advances in x-ray quantometry," Spectrogr. News Letter 7, 1 (1954).
33. "Technical Notes, New x-ray instrument measures metal coating to millionth of an inch," J. Opt. Soc. Am. 46, 1004 (1956).
34. C. Legrand, J. Chim Phys. et Phys-Chem. Biol. 53, 587 (1956).
35. B. Hess, Z. angew. Phys. 6, 19 (1954).
36. H. A. Liebhafsky and P. D. Zemany, Analyt. Chem. 28, 455 (1956).
37. L. S. Birks, E. I. Brooks, and H. Friedman, Analyt. Chem. 25, 692 (1953).
38. E. Gillam and H. T. Heel, Brit. J. Appl. Phys. 3, 353 (1952).
39. E. Gillam and D. G. Cole, J. Scient. Instrum. 30, 429 (1953).
40. A. I. Efremov and A. M. Tyutikov, Izvest. Akad. Nauk SSSR, Ser. Fiz. 20, 794 (1956).
41. L. S. Birks and E. I. Brooks, Analyt. Chem. 27, 437, 1147 (1935).
42. I. Adler and I. M. Axelrod, J. Opt. Soc. Am. 43, 769 (1953).
43. M. F. Hasler, I. W. Kemp, and I. L. Jones, Bull. Pittsburgh Conf. Anal. Chem. (March, 1954).
44. I. W. Kemp, et al., Spectrochim. Acta 7, 141 (1955).
45. E. Löscher, Chem. Rundschau 6, 307 (1953).
46. E. Löscher, Microchim. Acta 2-3, 696 (1955).
47. I. Drahokoupil and I. Mares, Ceskal. casop. fys. 4, 720 (1954).
48. V. E. Cosslet and P. Duncumb, Nature 177, 1172 (1956).
49. H. A. Liebhafsky, Analyt. Chem. 26, 26 (1954).
50. H. A. Liebhafsky and E. H. Winslow, Analyt. Chem. 28, 583 (1956).
51. R. Glocker and W. Frohmayer, Ann. Phys. 76, 369 (1925).
52. H. K. Highes and I. W. Wilszewsky, Analyt. Chem. 26, 1889 (1954).
53. R. W. Cranston, F. W. Matthews, and N. Evans, J. Inst. Petrol. 40, 55 (1954).
54. I. F. Brown and R. I. Weir, J. Sci. Inst. 33, 222 (1956).
55. E. A. Movchan, Zavodskaya Lab. 25, 68 (1959).
56. I. Despuyoles, J. Phys. et radium, Phys. Appl. 13, Suppl. an No. 2, 31A-41A (1952).
57. A. Engström, Rev. Sci. Inst. 18, 681 (1947).
58. J. Drahokoupil, Chekhoslov. Fiz. Zhur. 1, 157 (1952).
59. É. E. Vainshtein, Priroda 8, 48 (1947).
60. R. Castaing, Off. Nat. d'Études et de Rech. Aeronaut 23, 41 (1951).
61. R. Castaing, Off. Nat. d'Études et de Rech. Aeronaut. 55, 1 (1952).
62. R. Castaing and A. Guinier, Analyt. Chem. 25, 5, 724 (1953).

63. R. Castaing and J. Descamps, Compt. rend. 237, 1220 (1953).
64. R. Castaing and J. Descamps, J. Phys. et Radium 16, 304 (1955).
65. I. B. Borovskii and N. P. Il'in, Doklady Akad. Nauk SSSR 106, 654 (1956).*
66. V. N. Vertsner and A. M. Solov'ev, Optika i Spektroskopiya 5, 1, 83 (1958).
67. N. P. Il'in and A. N. Deev, Reports of the Meeting on X-Ray Spectroscopy, IMET** AN SSSR, January, 1960 [in Russian].
68. A. M. Solov'ev and G. G. Dutov, Reports of the Meeting on X-Ray Spectroscopy, IMET AN SSSR, January, 1960 [in Russian].
69. V. E. Cosslet and P. Duncumb, Nature 177, 1177 (1956).
70. I. B. Borovskii, N. P. Il'in, L. E. Loseva, and I. D. Marchukova, Izvest. Akad. Nauk SSSR, Ser. Fiz. 21, 1451 (1957).
71. I. N. Frantsevich and O. K. Teodorovich, Reports of the Meeting on X-Ray Spectroscopy, IMET AN SSSR, January, 1960 [in Russian].
72. V. A. Gorokhov and T. A. Nikitina, Reports of the Meeting on X-Ray Spectroscopy, IMET AN SSSR, January, 1960 [in Russian].
73. A. A. Yavnel', Reports of the Meeting on X-Ray Spectroscopy, IMET AN SSSR, January, 1960 [in Russian].
74. A. D. Genkin, Reports of the Meeting on X-Ray Spectroscopy, IMET AN SSSR, January, 1960 [in Russian].
75. J. Adler and I. M. Axelrod, Econ. Geology 52, 694 (1957).
76. É. E. Vainshtein, R. L. Barinskii and K. I. Narbutt, Doklady Akad. Nauk SSSR 77, 1003 (1951).
77. É. E. Vainshtein, R. L. Barinskii, and K. I. Narbutt, Zhur. Éksp. i Teoret. Fiz. 23, 594 (1952).
78. É. E. Vainshtein, K. I. Narbutt, and R. L. Barinskii, Doklady Akad. Nauk SSSR 87, 381 (1952).
79. É. E. Vainshtein, R. L. Barinskii, and K. I. Narbutt, Doklady Akad. Nauk SSSR 105, 1196 (1955).
80. R. L. Barinskii, Izvest. Akad. Nauk SSSR, Ser. Fiz. 21, 1381 (1957).
81. R. L. Barinskii and É. E. Vainshtein, Izvest. Akad. Nauk SSSR, Ser. Fiz. 23, 585 (1959).
82. É. G. Nadzhakov and R. L. Barinskii, Reports of the All-Union Meeting on X-Ray Spectroscopy, June, 1959 Rostov-on-Don [in Russian].
83. R. L. Barinskii and É. E. Vainshtein, Izvest. Akad. Nauk SSSR, Ser. Fiz. 21, 1387 (1957).
84. É. E. Vainshtein, Roentgen Atom Spectras in Molecular Chemistry and Alloys [in Russian] (Izd. AN SSSR, Moscow, 1951).
85. É. E. Vainshtein and Yu. N. Vasil'ev, Doklady Akad. Nauk SSSR 113, 53, 741 (1957).*
86. É. E. Vainshtein, E. A. Zhurakovskii, and I. B. Staryi, Doklady Akad. Nauk SSSR 122, 365 (1958).*
87. É. E. Vainshtein and E. A. Zhurakovskii, Doklady Akad. Nauk SSSR 128, 695 (1959).*
88. E. A. Zhurakovskii and É. E. Vainshtein, Doklady Akad. Nauk SSSR 127, 634; 129, 86 (1959).*
89. M. A. Blokhin, Doklady Akad. Nauk SSSR 95, 969, 1165 (1954).
90. É. E. Vainshtein, I. B. Staryi, and M. N. Bril,* Doklady Akad. Nauk SSSR 105, 943 (1955).
91. É. E. Vainshtein, M. N. Bril', and I. B. Staryi, Izvest. Akad. Nauk SSSR, Ser. Fiz. 20, 784 (1956).
92. L. T. Shuvaev, Izvest. Akad. Nauk SSSR, Ser. Fiz. 23, 5, 569 (1959).
93. É. E. Vainshtein, M. N. Bril', and Yu. R. Kopelev, Doklady Akad. Nauk SSSR 126, 744 (1959).*
94. É. E. Vainshtein and B. I. Kotlyar, Doklady Akad. Nauk SSSR 110, 44 (1956).*
95. V. A. Kazantsev, Candidate's Dissertation (Rostov Gos. Univ., 1954).
96. S. M. Karal'nik, Candidate's Dissertation (Kiev Gos. Univ., 1952).
97. S. A. Nemnonov and K. M. Kolobova, Fiz. Metal. i Metalloved. 6, 466 (1958).
98. I. B. Borovskii, K. P. Gurov, et al., Izvest. Akad. Nauk SSSR, Ser. Fiz. 21, 1401 (1957).
99. É. E. Vainshtein, B. I. Kotlyar, and A. G. Shapiro, Doklady Akad. Nauk SSSR 124, 65 (1959).*
100. V. A. Trapeznikov, Candidate's Dissertation (Ural Gos. Univ., Sverdlovsk, 1956).
101. W. W. Beenman and I. Bearden, Phys. Rev. 61, 455 (1942).
102. H. Hauson and W. Beeman, Phys. Rev. 76, 118 (1949).
103. É. E. Vainshtein, Doklady Akad. Nauk SSSR 69, 771 (1949).
104. K. I. Narbutt, Zhur. Éksper. i Teoret. Fiz. 26, 208 (1954).
105. B. Kauer, Dissertation (Munich, 1955).
106. K. Bōke, Z. Phys. Chem. Neue Folge 10, 45, 59 (1957); 11, 326 (1957).
107. G. Mitchell and W. Beeman, J. Chem. Phys. 20, 1298 (1952).
108. É. E. Vainshtein and V. S. Kavetskii, Doklady Akad. Nauk SSSR 91, 775 (1953).
109. S. Yoshida, Sci. Papers Inst. Phys. Chem. Res. Tokyo 38, 272 (1941).
110. I. B. Borovskii and K. P. Gurov, Fiz. Metal. i Metalloved. 4, 187 (1957).
111. I. B. Borovskii and K. P. Gurov, Fiz. Metal. i Metalloved. 7, 225 (1959).

* Original Russian pagination. See C. B. translation.

** Institute of Metallurgy.

THE STRUCTURE OF NORMAL PARAFFINS AND OF THEIR SOLID SOLUTIONS

Yu. V. Mnyukh

The Institute of Heteroorganic Compounds, Academy of Sciences of the USSR
Translated from Zhurnal Strukturnoi Khimii, Vol. 1, No. 3, pp. 370-388,
September-October, 1960
Original article submitted December 30, 1959

This review deals with problems of the crystal structure and phase behavior of normal paraffins and their solid solutions, which provide a convenient model for investigating the structure of high polymers. The experimental results are considered on the basis of the theory of dense packing of chain molecules.

I. The Structure of Normal Paraffins

The normal paraffins are a class of substances, the investigation of whose structure and properties is of great interest for various reasons. In the natural state, they provide the main component of petroleum. They are of relatively low molecular weight, but afford an intermediate stage in the transition to high polymers. Paraffins can, with complete accuracy, be considered as polymers of low molecular weight. It is natural that investigation of polymer structure requires a detailed understanding of the simplest members of this class of substance, as provided by the normal paraffins. In considering their structures, the axes of all n-paraffin molecules are always parallel to each other, regardless of the crystal modification under review. It is well known that, in the process of crystallization of polymers, parallel distribution of polymer molecules is generally of great importance [1]. The uniformity of structure of chain substances, such as low and high polymers, is clearly shown in the formation of uniform subunits.*

The investigation of n-paraffins is of great importance in a study of the laws of organic crystal chemistry [2]. It is obvious that, having very simple structures, they are the most suitable for this purpose. However, until recently, linear analysis of the packing of aromatic molecules has played a major role in the development of organic crystal chemistry. Although molecular packing density and molecular symmetry are the two factors which mainly determine the structure of any organic crystal, yet the organic crystal chemistry of linear chain molecules has its own special features.

The n-paraffins are of interest because they exist in different polymorphic forms. Analysis of the molecular packing of the different forms may lead to an understanding of why one crystalline modification is more stable than another. The n-paraffins make it possible to treat polymorphism as a function of temperature and of the number of carbon atoms in the chain.

Investigation of n-paraffin crystal structure began more than 25 years ago, and has not been discontinued in recent years. It may now be considered as essentially complete, although some interesting individual problems still require solution.

* See below for the conception of subunits.

The Configuration of the Aliphatic Chain

In all compounds in which the carbon atom is bonded to four other atoms identical with each other, as for instance CH_4, CCl_4, etc., the ideal tetrahedral angle between the bonds is observed. The case which interests us is a simple aliphatic chain

in which each carbon atom is bonded to two other C atoms and to two H atoms; in spite of the nonidentity with each other of these four atoms, the bond angles are very close to the tetrahedral, although there are some regular deviations described below. However, this fact does still not completely determine the form of the chain, since the various links can rotate about the single bonds. Relying on spectroscopic and thermal data, obtained by investigation of vapors, Pitzer [3] and Taylor [4] concluded that not all rotational positions corresponded to a minimum energy. Thus Taylor, in his thermodynamic calculations, used the following expression for the relation between potential energy, V and angle of rotation, φ, about a single bond:

$$V = V_0 [x (1 - \cos \varphi) + (1 - x)(1 - \cos 3\varphi)],$$

where x is some parameter. Taylor's equation gave the minimum potential energy configuration as a flat zigzag of carbon atoms.

Figure 1 shows the form of the chain, whose axis passes through the centers of the C − C bonds. The hydrogen atoms lie in planes perpendicular to the chain axis. The H − C − H angles are approximately tetrahedral. The minimum potential energy corresponds to the trans configuration ($\varphi = 0$).

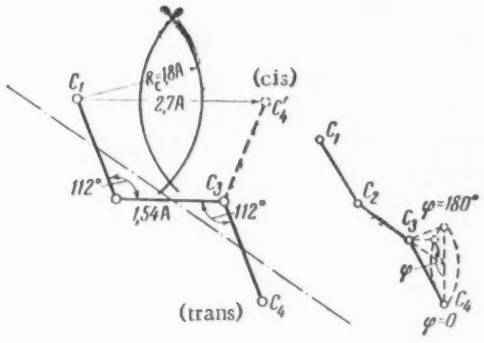

Fig. 1. The form of the aliphatic chain and the interaction of atoms, not connected by valency bonds, which determines it.

A structural basis can be given for the energetic suitability of such a configuration. For this, it is necessary to consider the interaction between atoms not joined by valency bonds, but there is no need to go into its physical nature, which has indeed been little investigated. It is sufficient to note that, for each pair of atoms unlinked by valency bonds, there is an equilibrium separation equal to the sum of intermolecular radii of these atoms, and that the intermolecular attraction curve is steep on the repulsion side and slopes more gradually on the attraction side. The angles between the bonds in an aliphatic chain are the result of mutual interactions between all the four atoms bonded to each particular carbon atom. It is interesting to note that, according to structural data [5, 6], the C − C − C angle is always greater than the ideal tetrahedral angle (approximately 112° instead of 109.5°), and this is readily understandable because the carbon atom intermolecular radius (R_C = 1.8 A) is greater than that of the hydrogen atom (R_H = 1.2 A). It is this feature of the intermolecular interaction which determines the plain zigzag form of the carbon atom chain. It is evident from Fig. 1 that the cis configuration ($\varphi = 180°$) leads to a $C_1 - C'_4$ separation of 2.7 A, which is considerably less than $2R_C$ = 3.6 A. It is therefore natural that the minimum energy should correspond to the trans configuration ($\varphi = 0°$). The plane zigzag form of the molecule is found in all n-paraffin crystals.

The methylene group hydrogen atoms are located in planes passing through the carbon atoms and perpendicular to the chain axes. This was shown well in the electronographic investigation of Vainshtein and Pinsker [7]. The H − C − H angles are approximately 108-109°.

The Difficulty of Experimental Investigation

Investigation of the structure and properties of these simple chain compounds is of great theoretical interest. However, it has developed very slowly because of a number of specific difficulties. There is the difficulty of obtaining individual hydrocarbons in the free state, uncontaminated by homologs, and there is the further difficulty of converting these into monocrystals for x-ray structural analysis. There is also the fact that the n-alkanes can exist in different crystalline modifications, so that the investigator of their physicochemical properties requires a good knowledge of the crystal structure work carried out by other authors. The absence of close contact between the two types of investigators and the use of insufficiently pure samples have been responsible for the appearance of a number of erroneous papers.

The Results of Experimental Structural Investigation

Classification according to crystal modifications. A. Müller was an outstanding investigator of n-paraffin structures, and his main conclusions have been confirmed by later workers. The first of his systematic investigations was carried out by the powder method [8, 19, 23, 29]. However, he also prepared an adequate monocrystal of n-$C_{29}H_{60}$ and completely determined its structure [9]. He showed that the crystal molecules consisted of plane zigzag chains of carbon atoms, and that the molecular axes were parallel to each other. There was a plane perpendicular to the axes, through the terminal groups, which separated one layer of molecules from another. Interchange of the layers gave identical results, so that the structure was built up from two layers. The elementary cell was rhombic with parameters a = 7.45, b = 4.97, and c = 77.2 A. Müller found that the space group was $P_{nam} = V_h^{16}$, with Z = 4; but Smith [10], using purer material, subsequently found a different space group $P_{cam} = V_h^{11}$.

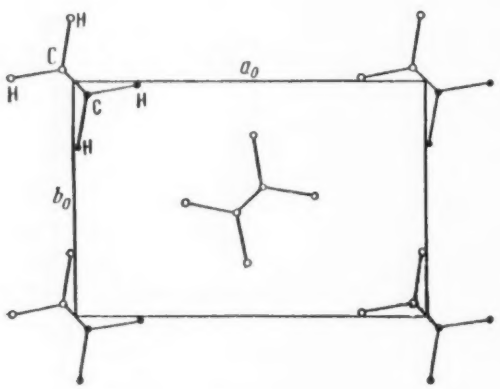

Fig. 2. The ab face of the rhombic cell of paraffin. This shows the mutual distribution of molecules whose axes are perpendicular to the paper. The atoms are denoted by white and black circles, located at different levels in a direction perpendicular to the paper. The distance between these levels is $c_0/2 = 1.27$ A.

Figure 2 shows the ab face of the elementary cell, perpendicular to the chain axes, which Müller showed to be the basic (principal) plane. The cross-sectional distribution of molecular chains, shown in this figure, is very characteristic of most n-paraffins and many other chain compounds, including high polymers. In the latter case there are no complications due to end groups, but other complications can arise associated with the possibility of replacement of carbon atoms by atoms of a different sort, or with the distribution of substituent groups. The simplest case is that of polyethylene, whose structure was investigated by Bunn [11], where there is a limitless plane zigzag of methylene groups. This is the same in practice as the structure of a single layer of paraffin molecules considered above, if it is imagined that the number of carbon atoms in the chain $n \to \infty$, i.e., if no consideration is given to any special packing of the end groups. More complicated structures are possessed by polyethers (Fuller and his coworkers [12-15], Mnyukh [16]), fatty acids (Sydow [17]), and other compounds with aliphatic zigzag chains, but they all have common features.

Vand [18], in order to express the similarity between the different structures of chain molecules, introduced the conception of a subcell with a definite distribution of methylene groups. The most common type of subcell is the rhombic polyethylene cell, with $a_0 = 7.45$, $b_0 = 4.97$, and $c_0 = 2.54$ A (the period of the plane aliphatic zigzag), whose a_0b_0 plane is shown in Fig. 2. But this is not the only type of subcell. Müller [19] noted some differences between even n-paraffins having long and shorter chains. To explain this, Müller suggested that the energy of a crystal should be broken down into two components, one dependent on the lateral interaction of the chain molecules, the other on the interaction of the ends. The relative values of these would alter on changing to a shorter molecule, and this would produce a change in the crystal structure.

In 1948 Müller and Lonsdale [20] published the results of an investigation of the n-$C_{18}H_{38}$ crystal cell, showing that it was triclinic. The monocrystal grown by Muller was imperfect, and the authors only used it for indicating the reflections of the x-ray powder pattern. The n-$C_{18}H_{38}$ structure was based on a different type of subcell, which was not resolved by the authors. The parameters of the actual cell will be shown here in a subsequent diagram. The presence in it of only one molecule was shown by the mutual parallelism of the planes passing through the carbon atoms of the zigzag chains. The triclinic n-$C_{18}H_{38}$ crystals were structurally identical with other members of the homologous series, with an even number of carbon atoms from C_6 to C_{24} [10, 20, 21, 22].

As well as the existence of two crystal modifications in the even n-paraffin series, differences in physical properties have been found between even and odd n-paraffins. In considering the cause of this, Müller [23] correctly stated that it was associated with the structure of the whole chain, bearing in mind the difference in symmetry of the even and odd molecules, although he did not use this terminology. He concluded that, as we move along the c axis, the pattern repeats itself every second molecule in the crystal of an odd n-paraffin, while all the successive molecules are identically situated in the crystal of an even n-paraffin.

A different conclusion resulted from the work of Kohlhaas and Soremba [24], who grew a monocrystal of n-$C_{30}H_{62}$ and investigated it by the x-ray method. They found a rhombic cell, identical with the elementary cell of n-$C_{29}H_{60}$. It later transpired that their result was in error, since their n-$C_{30}H_{62}$ was inadequately purified from traces of homologs [10]. Nevertheless, their work was of interest in showing how small amounts of contaminant could alter the structure.

As well as elucidating the structures of individual members of the n-paraffin homologous series, some authors have investigated the relation between various parameters and the number of carbon atoms in the chain. This work assists in the classification of n-paraffins according to crystal modifications without detailed investigation of all members of the homologous series. Thus, Piper and his coworkers [25, 26] carried on the work begun by Müller [19] on precise measurement of the large period. The "large" or "long" period is the name given to the distance between the planes of the crystal lattice passing through the end groups of chain molecules. A more suitable term, which we shall use, is the "interlayer spacing." This spacing is of the order of magnitude of the chain length of one molecule and can easily be studied, since the corresponding line on the x-ray powder pattern can be separated without difficulty because it lies in the region of relatively low scattering angle θ.

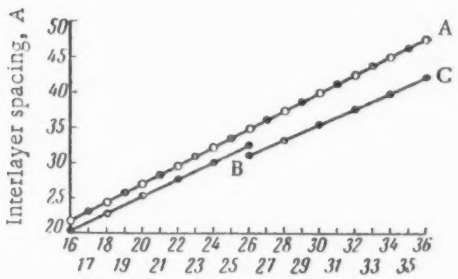

Fig. 3. Relation between interlayer spacing and the number n of carbon atoms in the chain. The symbol ● denotes the corresponding value for the rhombic structure, which exists when the degree of purity is not high enough.

The results of these investigations, partially corrected by taking account of the work of other authors [10, 27] is shown in Fig. 3. This gives a clear picture of how the members of the n-paraffin homologous series belong to different crystalline modifications. The points for all the odd n-paraffins lie on a single straight line A. These have a structure with a rhombic subcell and straight layers, as interpreted by Müller (for $C_{29}H_{60}$) and Smith (for $C_{23}H_{48}$). The triclinic paraffins (even members of the homologous series up to C_{24}) are built up from slanting layers, since the line passing through the corresponding points lies somewhat below. As stated above, the elementary cell was determined for n-$C_{18}H_{38}$ by Müller and Lonsdale: a = 4.28, b = 4.82, c = 23.07 A, α = 91°6', β = 92°4', γ = 107°18', d_{001} = 23.04 A, Z = 1. The subcell type and crystal structure of n-paraffin crystals of this group were determined by Kitaigorodskii and Mnyukh [28] (see below). Even n-paraffins from C_{28} upward have a rhombic subcell and a packing with still more sloping layers, since the line C representing them in Fig. 3 lies still lower. The crystal structure of this group was investigated by Shearer and Vand [5], using n-$C_{36}H_{74}$. The actual cell is monoclinic with two molecules: a = 5.57, b = 7.42, c = 48.35 A, β = 119°6', space group C_{2h}^5 = $P2_1/a$. The rhombic subcell and the coordinates of the carbon atoms in it precisely correspond to Bunn's [11] findings for polyethylene, and also to those of Vainshtein and Pinsker [7] for a paraffin mixture of undetermined composition.

Phase Changes. In addition to the crystalline forms considered above, there is still another stable form in which n-paraffins can exist. At a temperature near the melting point, Müller [29] discovered a reversible phase change in which the angle between the diagonals of the ab face of the rhombic elementary cell, shown in Fig. 2, acquired a value of 60°, and the symmetry was thus increased to the hexagonal state. This form corresponds to a dense packing of cylinders and is a particular case of the gaseous crystalline state, which is characterized by a strict ordering in the distribution of centers (or axes) of molecules and a lack of order in their azimuthal repetitions. This is quite a widespread phenomenon [30, 32].

The most complete representation of the phase behavior of n-paraffins is given in a graph (Fig. 4) constructed by Schaerer and his co-workers [33], which shows melting points and temperatures for reversible phase change in the solid state.* In this, the authors used new data for very pure samples [21]. There is no doubt about the experimental part of the work [33] but the treatment of the results is incorrect.

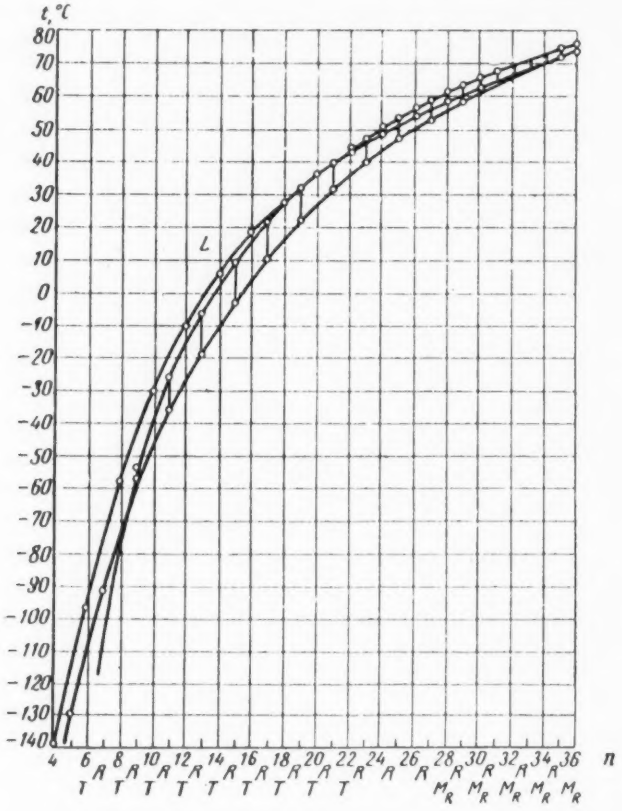

Fig. 4. The graph of Schaerer and his co-workers, incorporating all the reliable information on the phase changes of n-paraffins.

Some corrections have been made in Fig. 4, and a symbol is given to show the nature of the crystalline (low temperature) modification of each member of the homologous series. The range of existence H of the modification is denoted on the graph by a vertical line: T is the n-C_{18} type triclinic structure; R is the n-C_{23} and n-C_{29} type rhombic structure; M_R is the n-C_{36} type monoclinic structure with R type subcell; H is the hexagonal crystalline gas structure.

It is obvious from Fig. 4 (and its authors agree with this view) that there is an alternation in melting point with members of the series below C_{20}, and that there is no alternation in melting point above this, though there is an alternation in the point of phase change in the solid state. In fact, in the range from n-C_6 to n-C_{20}, the melting points of even members of the series lie on a curve which is above that for the odd members; a crystalline gas

* The C_{24} and C_{26} n-paraffins occupy a structurally intermediate position, and, compared with other n-paraffins, show a more complicated phase behavior which has still not been fully investigated.

structure near the melting point is only observed with the odd members. However, with longer chain length, we see that all members show a crystalline gas modification in a corresponding temperature range, and the melting points lie on a single curve, whereas the points for phase change in the solid state lie on different curves for the even and odd members. Schaerer and his co-workers attempted to explain this phenomenon without realizing that n-paraffins could exist in different crystalline modifications. We have spoken above of rhombic, triclinic, monoclinic, and hexagonal cells, but they only considered two crystalline modifications – S_α and S_β. Considering Fig. 4 afresh, it is not difficult to draw the following conclusions. The alternation in physicochemical properties between the even and odd n-paraffins is associated with the alternation in their type of crystal structure: for the shorter chains, R and H of the odd members alternate with T of the even, while, for the longer chains, R alternates with M_R. It is quite natural that there should be no alternation in the existence of an H modification above C_{22}, since for all members of the series, odd or even, the crystalline gas structures can be considered as isomorphous.

The Theory of Packing Density of Chain Molecules

All the information on the structure of n-paraffins was recently reduced to a single system in the theoretical investigation of Kitaigorodskii [34 - 36, 28]. Starting from the general principles of dense packing of molecules in organic crystals, developed by himself [2], he showed that, in the case of chain molecules, it was possible to use geometrical analysis to predict a small number of possible crystal structures, which included all the actual structures found up to the present. Investigation was greatly assisted by the following postulate, which was used as a starting point: The structure always consists of layers of plain zigzag molecules, with their axes parallel. The problem of molecular packing may be split up into two parts – packing of molecules in layers and packing of layers. Let us consider these in general terms.

If the chains are distributed randomly in azimuth (rotating about their axes), then the mean cross section will be circular and there will be a circular (hexagonal) packing. Two types of dense layers are possible in the case of molecules of arbitrary cross section: with oblique angle and with right angle cells. All three types of packing are shown in Fig. 5, where the cross section is represented by an arbitrary contour.

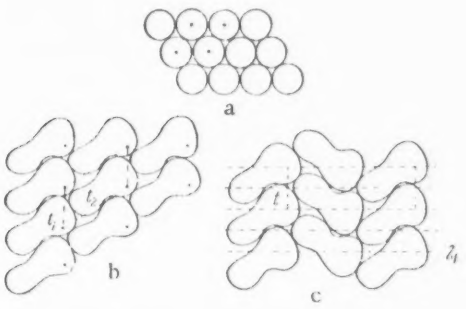

Fig. 5. Three possible types of dense packing of the cross sections of chain molecules: a) hexagonal, b) oblique angled, c) right angled cell.

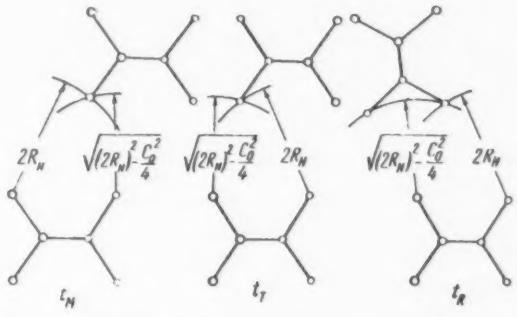

Fig. 6. Types of dense distribution of a pair of aliphatic chains (the chain axes are perpendicular to the plane of the paper).

For geometrical structural analysis, it is first necessary to give a solid form to the aliphatic molecule in accordance with the rules of organic crystal chemistry, i.e., to use the standard intermolecular radii for the carbon and hydrogen atoms (such molecular models are shown in Figs. 7 and 10). Analysis begins with consideration of the densest spacing of two molecular chains of infinite length. This can only happen when a hydrogen atom of one molecule fits into a "recess" between three hydrogen atoms of the accompanying molecule. Two types of such tight contact can exist between parallel molecules, differing by a simple translationary movement. These arrangements, t_M and t_T, are shown in Figs. 6 and 7. Arrangement t_R of Fig. 6 corresponds to case b of Fig. 5, when the planes of the zigzags are not parallel. Each of these three types of chain pair

arrangements gives a separate dense packing. Scheme t_T gives a structure with a triclinic subcell * (T), t_M gives a monoclinic subcell (M), and t_R gives a rhombic subcell (R).

Further use of geometrical analysis soon leads to a derivation of the structure obtained from the arrangement t_T. The two molecules, joined in this way, themselves determine a method of packing an infinite series of molecules in one of the directions (a_0 in Fig. 12) in the crystal. A dense superposition of two such series can be found without difficulty by geometrical construction, or with the aid of molecular models. It is achieved by a translation b_0 perpendicular to the axes of the molecules. We thus find a unique distribution, leading to a coordination of 6 (Fig. 12). This is an ideal structure in which all the intermolecular H − H spacings are the same. If R_H is taken as 1.3 A, we have a cell containing two CH_2 groups and with the following parameters:

$$\begin{array}{ll} a_0 = 4{,}3\text{A} & \alpha = 90^\circ, \\ b_0 = 4{,}45\text{A}, & \beta = 107{,}5^\circ \\ c_0 = 2{,}54\text{A}, & \gamma = 102^\circ \end{array}$$

Ideal parameters can be obtained similarly for the R and M cells. The results are shown in the first column of Table 1. These elementary cells are the actual ones for molecular chains of infinite length. However, a layer of finite length molecules has only a two dimensional periodicity and is not, of course, a crystal. In this case, the cells R, M, and T, formed from a layer of molecules, are subcells, i.e., they characterize the packing of the methylene groups.

TABLE 1

Subcell, A	Layer	Cell of layer, A	φ_a°	φ_b°	φ_c°*
H	$H[00]$	$a = 4{,}8$	90	90	0
R	$R[0, 0]$	$a = 7{,}42$; $b = 4{,}96$; $\gamma = 90^\circ$	90	90	0
	$R[0\pm2]$	$a = 9{,}0$; $b = 4{,}96$; $\gamma = 90^\circ$	90	55,5 124,5	34,5
a_0 7,42	$R[\pm1, 0]$	$a = 7{,}42$; $b = 5{,}57$; $\gamma = 90^\circ$	63 117	90	27
b_0 4,96	$R[0, \pm1]$	$a = 7{,}85$; $b = 4{,}96$; $\gamma = 90^\circ$	90	71 109	19
c_0 2,54	$R[\pm1, \pm1]$	$a = 7{,}85$; $b = 5{,}57$; $\gamma = 81{,}5^\circ$ for $R[1, 1]$ and $R[\bar{1}, \bar{1}]$; $\gamma = 98{,}5^\circ$ for $R[\bar{1}, 1]$ and $R[1, \bar{1}]$	63 117	71 109	31,5
M a_0 4,2	$M[0, 0]$	$a = 4{,}2$; $b = 4{,}4$; $\gamma = 111^\circ$	90	90	0
	$M[\pm1, 0]$	$a = 4{,}9$; $b = 4{,}4$; $\gamma = 107^\circ$	59 121	90	32
b_0 4,4	$M[0, \pm1]$	$a = 4{,}2$; $b = 5{,}1$ $\gamma = 107^\circ$	90	60 120	32
c_0 2,54 γ_0 111°					
T	$T\left[\pm\frac{1}{2}, 0\right]$	$a = 4{,}3$; $b = 4{,}5$; $\gamma = 103^\circ$	[73] 107	[90]	[18]
a_0 4,3 b_0 4,45 c_0 2,54 $\alpha_0 = 90^\circ$, $\beta_0 = 107{,}5^\circ$ $\gamma_0 = 102^\circ$	$T\left[\frac{1}{2}, 1\right]$ $T\left[-\frac{1}{2}, 1\right]$	$a = 4{,}3$; $b = 5{,}2$; $\gamma = 109^\circ$	73 107	120 60	36

* The subcell is constructed from vectors of repetition of methylene groups.

For layers composed of molecules of finite length, there is a new parameter to be considered – the angle between the plane passing through the end groups and the axes of the molecules. If this is 90° then the layer is rectangular, and in other cases, it is oblique angled. The angle cannot have just any value. The point is that a parallel shift along the molecular axis, leading to a different variant of the actual cell without altering the packing of the methylene groups, must be equal to mc_0, where $\underline{m}$ is a whole number. The idea, that all the structural variants for chain molecules could be derived from a single "initial" structure by discrete movements of the molecules, was proposed 20 years ago by Schoon [37], but naturally, could not be substantiated on the basis of the then prevailing structural conceptions. The validity of the idea is now obvious, as may be seen from Fig. 7; if any molecule is shifted along its axis by a whole number of "stages" (one "stage" is one period of the chain = 2.54 A), then the convex parts of one molecule will again fit into depressions in the other molecule, and the nature of the distribution of methylene groups will be unaltered.

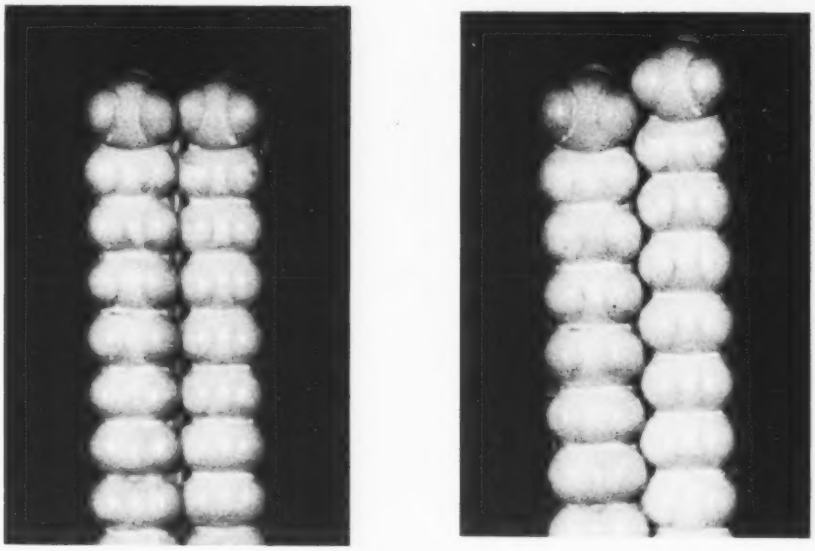

a b

Fig. 7. The arrangement of chain pairs of types t_M (a) and t_T (b), illustrated by models.

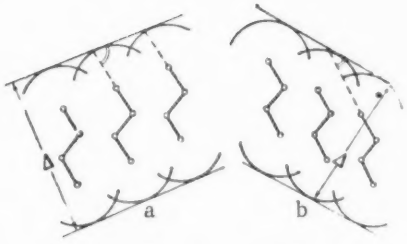

Fig. 8. Layers differing only in the sign of the shift.

Let us denote by $\underline{m}$ the molecular shifts associated with translations a_0, and by $\underline{n}$ the molecular shifts associated with translations b_0. The two-dimensional cell of the layer is determined by the subcell and the numbers $\underline{m}$ and $\underline{n}$. In contrast with the R and M subcells, the T subcell, because of its structure, cannot give rectangular layers, since the methylene groups associated with the a_0 axis are shifted along it by $c_0/2$. It is therefore possible to characterize the two-dimensional subcells by the symbols R[m, n], M[m, n], T[m + ½, n]. It is necessary to appreciate that layers, differing only in the signs of $\underline{m}$ and $\underline{n}$, are not equivalent. Each pair of numbers $\underline{m}$ and $\underline{n}$ gives four layers – $\underline{m}, \underline{n}$; $m, \bar{n}$; $\bar{m}, n$; $m, \bar{n}$. This difference is illustrated in Fig. 8. It is unnecessary to consider all possible shifts of the chains. If the shift of two adjacent chains exceeds one period c_0, then there will be contact between end groups and methylene groups, which will cause a reduction in packing density. We can therefore confine ourselves to those layers shown in the second column of Table 1.

All the layers with T subcells are oblique. If the plane ab of a two-dimensional cell layer coincides with the plane a_0b_0 of the subcell, then the symbols of the layers will be $T[^1/_2, 0]$ and $T[-^1/_2, 0]$. In layers with T subcells, where each molecule has six neighbors, the translation vectors are $\pm a_0$, $\pm b_0$, and $\pm (a_0 + b_0)$.* The condition that the shift of any of these molecules shall not be more than unity still only permits the two layers $T[^1/_2, 1]$ and $T[-^1/_2, 1]$.

Table 1 gives all the possible layers thus predicted, together with the parameters of their two-dimensional cells and the angles φ_a, φ_b, and φ_c * between the molecular axes and the axes a, b, and the normal to the plane ab, respectively.

Kitaigorodskii further considered possible rhombic, monoclinic, and triclinic structures occurring in superimposed layers. In particular, structures of triclinic symmetry can be obtained by superimposing layers of any type – R, M, and T – with arbitrary shifts. It is necessary to appreciate, here, that layers can never be exactly superposed on each other, i.e., they cannot be associated with a reflection plane of symmetry, since, in this case, the "convexities" of the upper layer would be in contact with the "convexities" of the lower layer and dense packing would be impossible (see Fig. 9 a). This circumstance applies generally in organic crystal chemistry [2]. Since neighboring layers are always superposed with some shift, the c axis of the actual elementary cell, passing through identical points of the molecules of neighboring layers, cannot coincide with the direction c_0 of the molecular axis (Fig. 9b). These axes only coincide in the case of a two layer rhombic structure, in which the third layer is located under the first (Fig. 9 c).

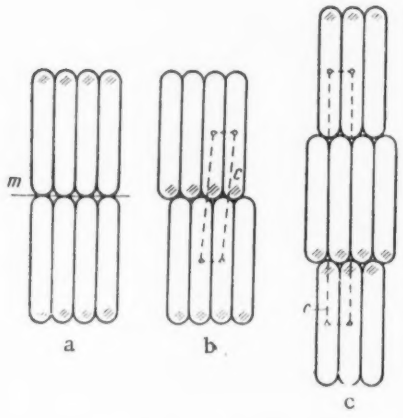

Fig. 9. Superposition of layers: a) The adjacent layers of molecules can never be associated with a reflection plane of symmetry, since dense packing could not then occur; b) in single layer structures, the axis c of the elementary cell does not coincide with the molecular axis c_0; c) in rhombic (two layer) structures, the c axis coincides with the direction of the molecular axis c_0.

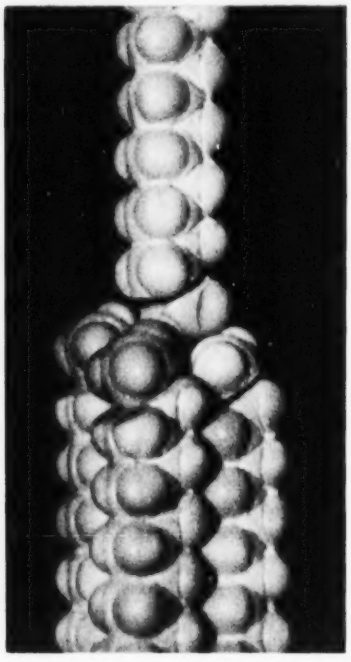

Fig. 10. The packing of molecules in triclinic n-paraffins.

An arbitrary shift is more favorable, from the point of view of dense packing, than a shift preserving monoclinic symmetry, or still more-so rhombic symmetry. Nevertheless, a triclinic shift will occur sometimes, since the achievement of a minimum free energy is associated not only with a tendency to the densest packing, but also with a tendency to preserve the highest possible molecular symmetry in the crystal.

* Considering, as usual, a γ type angle.

The complete characteristics of the structures derived by Kitaigorodskii are given in the references cited. These structures include those investigated by Müller, Shearer and Vand, and Smith. Such structures are not only appropriate to n-paraffins, but also to other long chain compounds where the aliphatic zigzag is the main factor in the packing. The theory accounts for the structural diversity shown by chain molecules, and explains why this diversity is mainly characteristic of the even members of the n-paraffin homologous series, whereas only two structural variants with rhombic cells can be expected for the odd members.

The Structure of Triclinic n-Paraffins. The above theory has been confirmed by a determination of the crystal structure of the paraffin n-$C_{18}H_{38}$ [28]. The course of investigation in this case was very different from that used in classical structural analysis. First of all, experimental values were obtained for the angles between the molecular axes and the axes of the elementary cells selected by Müller and Lonsdale: $\varphi_a = 74°$, $\varphi_b = 91°$, $\varphi_c \approx \varphi_c^* = 18°$. These agreed excellently with the corresponding theoretical values for layers T[$\pm$ 1/2, 0] (Table 1). They completely determined the type of subcell and the coordinates of the carbon atoms. The corresponding data is presented with allowance for corrections, whose application will be considered below. The triclinic subcell (T), containing two CH_2 groups, has the parameters –

$$\begin{array}{ll} a_0 = 4{,}3\text{A} & \alpha_0 = 90°, \\ b_0 = 4{,}8\text{A} & \beta_0 = 107{,}5°, \\ c_0 = 2{,}54\text{A}, & \gamma_0 = 107° \end{array}$$

The coordinates of the carbon atoms (the origin is at the center of a C–C bond) are –

$$\begin{array}{ll} x_1 = 0{,}008, & x_2 = 1 - x_1 \\ y_1 = 0{,}095 & y_2 = 1 - y_1 \\ z_1 = 1/4, & z_2 = 3/4 \end{array}$$

It was also shown that n-$C_{18}H_{38}$ crystals were built up from [T $-$ 1/2, 0] layers and not from T [+ 1/2, 0] layers. The structure of these crystals, produced by the only possible means of dense superposition of the layers, is shown by means of a model in Fig. 10. It will be recalled that the other n-paraffins, corresponding to the straight line B in Fig. 3, are isostructural with n-$C_{18}H_{38}$.

The Density of R and T Packings. The data in the above cited references enables us to compare the packing densities of molecules with R and T subcells. The precision with which the parameters are known is sufficient for this purpose, but it should be noted that the comparison cannot be exact, since it is between different substances although all of one type.

The parameter c_0 is 2.54 A in both cases, so that the packing density of the molecules in the subcell is determined by the area occupied by one molecule in a section perpendicular to the chain. The required cross-sectional area for the R subcell is

$$S_R = a_0 b_0 / 2 = 18{,}5_6\ \text{A}^2.$$

In order to find the corresponding value for the T subcell, it is necessary to project the face ab on to a plane perpendicular to the chain, and to calculate the area of the projection –

$$S_T = b_0 a_{\perp 0} \cos(\gamma_0 - 90°) = b_0 \sqrt{a_0^2 - \left(\frac{c_0}{2}\right)^2} \cos(\gamma_0 - 90°).$$

Substituting in this the values $a_0 = 4{,}28$ A, $b_0 = 4{,}82$ A, $\gamma_0 = 107°18'$, we obtain $S_T = 18.7_3$ A^2.

The small difference in density (less than 1%) accounts for the existence in nature of both types of subcell, R and T, since the energetic suitability of any structure is primarily determined by the packing density of the molecules.

It is appropriate to consider here a question which is of fundamental importance for the understanding of polymorphism in n-paraffins. How can we explain the stability of structures with the triclinic modification for

even n-paraffins with a number of carbon atoms n < 26, and the change to structures with the R subcell for n > 26 ? An answer can be obtained by starting with the assumption that the free energy of the actual T subcell is somewhat greater than that of the R subcell. It therefore follows that the energetic suitability of triclinic structures is ensured, since, as shown above, the triclinic packing of layers is, in general, more dense. But this advantage in the packing density of the end groups becomes relatively less the longer the molecule, and, with a high enough value of n, it finally becomes insufficient for a structure with the T subcell to be energetically preferable to a structure with the R subcell. We will return to this question in the second part of this review, when dealing with the experimental data on solid solutions of n-paraffins.

In any case, it is clear that the difference in free energies of crystals with R and T type packings is not very large. This follows from comparison of their densities, and also from the fact that a few percent of neighboring homologs as impurities can convert a triclinic into a rhombic structure. On this basis, Kitaigorodskii and Mnyukh [38] made a successful attempt to find a T packing in samples of polyethylene. Teare and Holmes [39], independently, found a triclinic modification in polyethylene, which they described as unstable, and confirmed the above considerations with regard to the R and T packings.

Recently, Kabalkina [40] made an x-ray investigation of the paraffins n-$C_{30}H_{62}$, n- $C_{32}H_{66}$, and n-$C_{34}H_{70}$ at pressures up to 15,000 atmospheres. She made an interesting discovery, namely the appearance of some triclinic phase in the structure, which persisted for a few days after reducing the pressure. The applied pressure was not hydrostatic, and this complicates the interpretation of the phenomenon.

Making the Molecular Form More Precise

In analyzing the packing of paraffin chain molecules, Kitaigorodskii and Mnyukh [41] came to the conclusion that it was desirable to apply a correction, shown in Fig. 11, to the form of the aliphatic molecule as found by the standard methods of organic crystal chemistry. This correction can be considered as the result of a redistribution of electron density in those places where there is strong overlap of the intermolecular spheres of atoms not joined by valency bonds. The increase in precision of the molecular form leads to complete agreement between the parameters of the "ideal" structure, obtained by geometrical construction, and the experimental measurements; this is shown in Fig. 12.

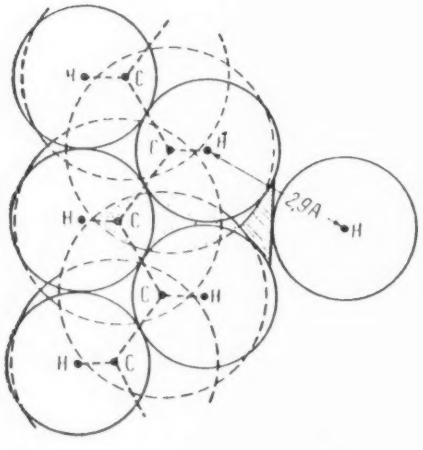

Fig. 11. Increase in precision of the molecular form of paraffin. There is an isolated region where there is overlap of the intermolecular spheres of neighboring carbon atoms not joined by valency bonds. The correction applied is shown in the form of a hatched area.

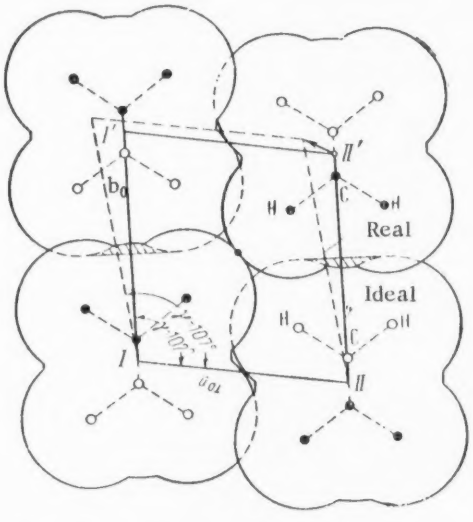

Fig. 12. Comparison of the "ideal" and experimental paraffin subcells.

The following subcell dimensions are used in this diagram (Fig. 12) – a_0 (theor.) = a_0(exp) = 4.28 A, $a_{\perp 0}$ = 4.08 A, b_0 (theor.) = 4.45 A, b_0(exp) = 4.82 A,

γ_0(theor.) = 102°, γ_0(exp) = 107° ($a_{\perp 0}$ is the projection of a_0 perpendicular to the chain axis). The cause of the difference becomes clear after introducing the correction to the molecular form. The existence of steric hindrance and the need to preserve H − H contact, at the point marked in the center of the cell, produces cell deformation in the direction shown by the arrow. The overlap region is hatched.

There is data available to show that a similar correction to the form can be applied in all other cases when there are neighboring atoms, not joined by valency bonds, in the molecule, at a spacing appreciably less than the sum of the intermolecular radii.

II. The Structure of Solid Solutions

The structural simplicity of n-paraffin crystals makes it possible to solve problems concerned with the structure of their solid solutions, which are of great interest both for an understanding of the properties of aliphatic chains in the condensed phase, and with respect to the theory of solid solutions of organic molecules.

Binary solid solutions of n-paraffins have been examined repeatedly by different authors. Their results have usually been expressed as composition diagrams of one form or another. A valuable idea was to compare the lengths of component molecules, so as to predict whether there would be continuous solubility. For the solution of this particular problem, at first glance the indicated approach appears to be by proportion. Indeed, since the form of an n-paraffin molecule in a crystal is a plane aliphatic zigzag of carbon atoms, it might be expected that all differences would depend on the molecular length factor. However, this leaves out of account the difference in symmetry of the even and odd molecules and of the crystals built up from them. Thus, Kravchenko [42, 43] attempted to make a generalization, concerned with the formation of either continuous solid solutions or eutectics, based only on the relative lengths of the component molecules. It soon appeared that such an approach was inadequate. He found that there was a break in the solubility in some systems with small differences in length between the component molecules, while the expected break did not occur in other cases. Also, his approach gave no explanation of the very large difference in types of composition diagrams for binary n-paraffin systems. It will be shown below that we can go very much further with the structural explanation of the solubility of n-paraffins.

A large number of composition diagrams for binary n-paraffin systems can be found in the literature. Unfortunately, many of the older ones are of poor technical quality, and are too incomplete and imprecise to be included in this review. In particular, the liquidus and solidus lines often run together, and many phase transitions remain unnoticed. However, composition diagrams have been determined with sufficient care for the following systems −

$C_8 + C_9$ [45]	$C_{16} + C_{18}$ [48]	$C_{21} + C_{31}$ [48]
$C_{12} + C_{13}$ [46]	$C_{17} + C_{18}$ [48]	$C_{30} + C_{32}$ [50]
$C_{13} + C_{14}$ [46]	$C_{18} + C_{20}$ [49]	$C_{30} + C_{34}$ [51]
$C_{14} + C_{15}$ [46]	$C_{19} + C_{20}$ [48]	$C_{30} + C_{36}$ [51]
$C_{15} + C_{16}$ [47]	$C_{21} + C_{23}$ [48]	$C_{35} + C_{36}$ [48]
$C_{16} + C_{17}$ [47]	$C_{20} + C_{30}$ [50]	

These are all shown in Fig. 13, where we have added the following symbols: T) modification with T subcell; R) modification with R subcell; H) modification with H subcell; M_R − monoclinic structure with R subcell; L) liquid phase. The dotted lines, shown on the diagrams, do not conflict with the condition for formation of continuous solid solutions.

Conditions for Formation of Solid Solutions

The general conditions for the formation of solid solutions by two organic substances have been considered by Kitaigorodskii [34, 52]. In organic chemistry, we are mainly concerned with solid solutions formed by substitution. The possibility of formation of solid solutions depends here only on the similarity in form and dimensions of the mixed molecules, and, in contradistinction to inorganic materials, this condition is necessary and

* Some of these diagrams are included in the review article [44].

sufficient. Continuous mutual solubility (i.e., over the whole concentration range) is possible only if one further essential condition is observed – the symmetries of the associated molecules must be the same in the pure component crystals.

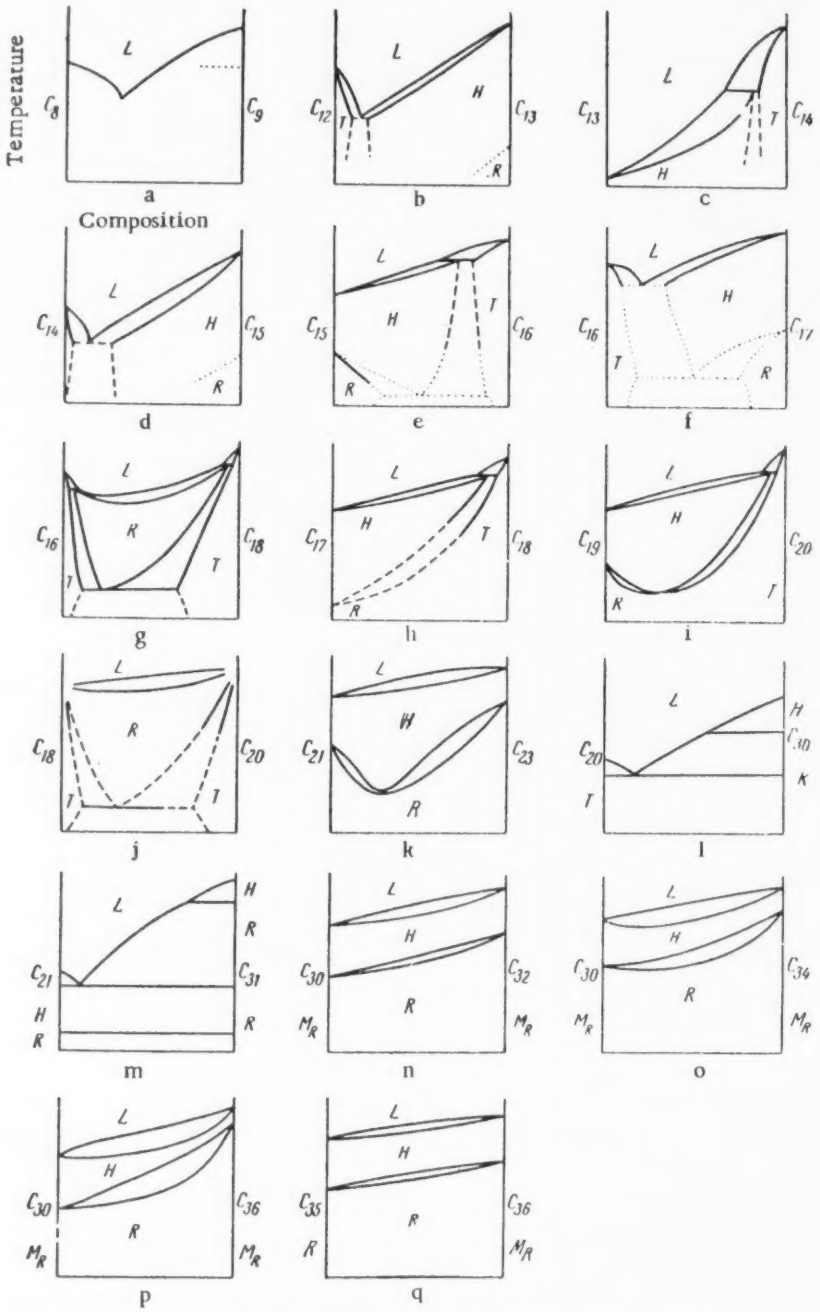

Fig. 13. Composition diagrams for n-paraffin binary systems.

Starting from these general principles, it is not difficult to formulate conditions for the formation of n-paraffin solid solutions. The requirement of similarity in form and dimensions of the mixed molecules simply implies, here, a small difference in length. A continuous series of solid solutions can only be formed from components having the same subcells – H and H, R and R, or T and T. Continuous mutual solubility is impossible

between components with different subcells – H and T, R and T, or H and R. This implies, in particular, that there is always a break in the solubility with systems of the type "even + odd," whereas, in systems of the type "odd + odd," this will depend only on the relative lengths of the molecules, since all odd n-paraffins are isomorphous with each other. These conclusions are confirmed by diagrams a, b, c, d, e, f, h, and i of Fig. 13. All these show a break in the solubility of the type H + T. At the same time, in the system n-C_{21} + n-C_{23}, continuous solid solutions are formed in all proportions of the types H + H and R + R, although the molecules n-C_{21} and n-C_{23} differ more in length than do, for instance, n-C_{19} and n-C_{20}.

It is understood that, for continuous solubility to occur, there should be uniform and real cells, but this cannot be detected in view of the properties of the materials under consideration and the restricted possibilities of the thermographic method, which is normally used to establish the composition diagram. Careful consideration of the diagrams in Fig. 13 shows that they indicate best of all the "solidus – liquidus" transitions, less precisely and fully the transitions in the solid state from one type of subcell to another, while they do not indicate the phase transitions in which the lateral packing of the chains (i.e., the subcells) is preserved but there is a change in the packing of the end groups. For instance, according to Mazee there is continuous solubility in the system n-C_{35} + n-C_{36}, but, strictly speaking, this is incorrect. In principle, by means of improved experimental technique, it should undoubtedly be possible to detect a break in the solubility (as with any "even + odd" n-paraffin system), since n-C_{35} has a rhombic true elementary cell, while n-C_{36} has a monoclinic one. However, the subcells of both components, and of any of their mixtures, are of the R type, so that the diagram is correct in an approximate sense. The systems n-C_{30} + n-C_{32}, n-C_{30} + n-C_{34}, and n-C_{30} + n-C_{36} (Fig. 13, n, o, and p) also show continuous solubility over the whole range, although the work of Piper and his co-workers [26] (Fig. 18) indicates that there should be a break in the solubility very close to the components axis, with the change from the "oblique" modification to the rectangle without a change in the subcell (R). Unfortunately, these materials were not pure enough, and, although this may not have been the reason, the transitions mentioned could not be detected. It should be noted, however, that there is no doubt about continuous solubility of the H + H type in these systems (including n-C_{35} + n-C_{36}).

Thus, when considering the literature data on binary n-paraffin systems, it should be borne in mind that the diagrams do not reflect all the phase transitions in the solid state, but only those accompanied by a change in the type of lateral packing of molecular chains. This is because changes in packing of the end groups, which do not affect the basic structural units, i.e., the subcells, produce such small thermal effects that they are outside the sensitivity limits of thermographic methods. Experimental difficulty is also increased by the slowness of phase transformation processes in the solid state.

When the condition of similarity in size of the mixed molecules is not fulfilled, it is natural to expect that solid solution formation is impossible. The symmetry factor, which is important when the above condition is fulfilled, is now a secondary factor. This is abundantly confirmed by the systems n-C_{20} + n-C_{30} and n-C_{21} + + n-C_{31} (Fig. 13, l and m). Eutectics are formed in both cases, and the diagrams are very similar, although the symmetries of the components are different.

The Rule of Mutual Interaction

Up to now we have concentrated attention on the possibility or impossibility of unrestricted solubility. However, we can proceed further to state an interesting general rule for the case of restricted solubility, based on the principle of dense packing of molecules in an organic crystal [49]. It is assumed that part of the molecules of n-paraffin A are mixed with the molecules of another n-paraffin B. Figure 14 shows diagrammatically what can happen when a shorter or longer molecule is introduced. We can conceive of the packing as unchanged if B < A. The solubility limit is approached when the number of "gaps" becomes large and the packing density drops appreciably. If B > A, then the introduction into the main component crystal of even a small number of molecules inevitably produces distortion. Thus, the following rule can be formulated. Under otherwise similar conditions, n-paraffins with shorter chains will dissolve in n-paraffins with longer chains, while preserving the structure (modification) of the solvent, to a greater extent than in the reverse case. Analysis of the composition diagrams of Fig. 13 shows that these contain a number of convincing examples of this rule and no exceptions to it. Some of these examples are illustrated in Fig. 15. This shows constant temperature sections through the diagrams of Fig. 13, which confirm the mutual interaction rule: a) is the system C_{21} + C_{23} confirming the rule for phase transitions of the type H $\rightleftharpoons$ R; b) is the systems C_{16} + C_{18} and C_{18} + C_{20}, giving three independent

confirmations (B > A, D > C, and B > C) for the phase transition T ⇌ R; c) is an unrealizable case which shows that B > C is actually an independent confirmation; d) is the system $C_{26} + C_{28}$ (x-ray data [26]) with phase transitions of the type "oblique layer ⇌ rectangular layer," but with the R subcell unchanged.

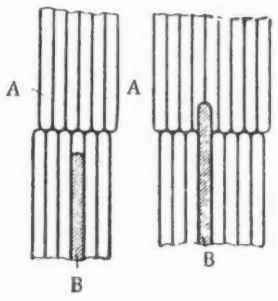

Fig. 14. Packing diagrams for the ends of long molecules, illustrating the lower energetic suitability of "projections" as compared with "gaps."

It should be noted that the only systems suitable for this purpose are those with components of the same crystal symmetry (otherwise, not all the other conditions are fulfilled) and with a solubility break at the temperature of the section. It is important that the data shown includes different types of phase transitions. It is reasonable to assume that a similar rule applies to other systems as well as to aliphatic ones, although it may be masked by other factors [53, 54].

Conventional and Concrete Symbols for Phases

The use of the normal literature symbols α and β (or S_α and S_β), which are based on physicochemical analysis (α represents the high temperature form, β the low temperature form), can often lead to confusion. Where possible, it is much more convenient to use concrete symbols which express the structural characteristics of the phase.

Phase diagram investigators often fall into this error; they assume a uniform phase type for different members of a homologous series, and denote it by the same conventional symbol. This error is illustrated by Mazee's data [48] in Table 2; the conventional symbols are as he used them.

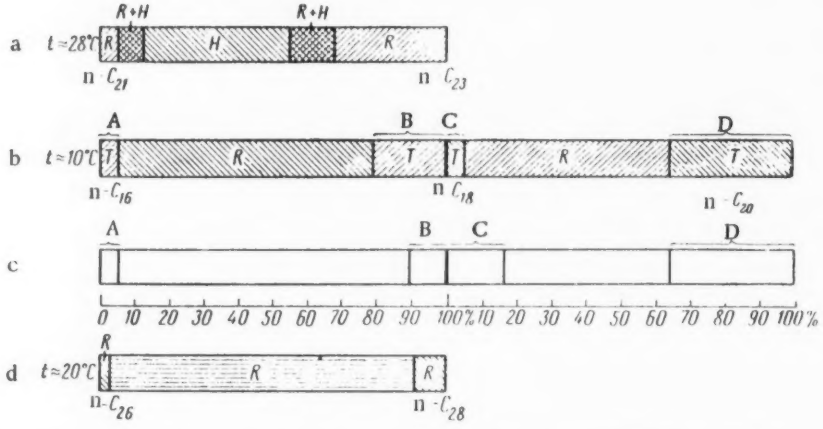

Fig. 15. Constant temperature sections through the n-paraffin binary system composition diagrams of Fig. 13, confirming the mutual solubility rule.

We may take as an example the system $n\text{-}C_{17} + n\text{-}C_{18}$ (Fig. 13, h), where errors resulted from neglect of the phase structural characteristics. Mazee observed that pure $n\text{-}C_{18}$ did not undergo equilibrium phase transitions in the solid state, from which he concluded that a single S_β modification existed along the $n\text{-}C_{18}$ axis. The mixture to the left should show enantiotropic phase transitions, since pure $n\text{-}C_{17}$ does. Arguing on these lines, Mazee denoted the solid phase above the transition point as S_α and below it as S_β. However, this is incorrect, since S_β for $n\text{-}C_{18}$ has a triclinic crystalline lattice, while S_β for $n\text{-}C_{17}$ has a rhombic lattice. This led to an erroneous representation of the phase transition curves in the solid state. In Mazee's composition diagram, the triclinic structure of $n\text{-}C_{18}$ altered continuously through a series of solid solutions to the rhombic structure of $n\text{-}C_{17}$, which is impossible. There should be a break in the solubility. The same author made a similar error in his description of the system $n\text{-}C_{19} + n\text{-}C_{20}$, where there is a gradual change in symmetry. Figure 16 shows two probable variants for the system $n\text{-}C_{17} + n\text{-}C_{18}$, which do not conflict with the condition for formation of solid solutions.

The most correct procedure would be to replace the conventional phase symbols by the concrete symbols for the true cells, but this is still impossible owing to the absence of the relevant data. However, the indication of subcell type on existing composition diagrams substantially clarifies the picture for the mutual solubility of n-paraffins. The inadequacy of many diagrams is very clear, even in the above considered restricted sense of what is achievable by the thermographic method. There is still much to be done by the x-ray powder method by phase analysis, using a temperature controlled camera.

TABLE 2

Binary system	Phase symbol S_{α}, actual cell	Phase symbol S_{β}, actual cell
$n\text{-}C_{16} + n\text{-}C_{18}$	R	T
$n\text{-}C_{17} + n\text{-}C_{18}$	H	R and T
$n\text{-}C_{19} + n\text{-}C_{20}$	H	R and T
$n\text{-}C_{21} + n\text{-}C_{31}$	H	R
$n\text{-}C_{35} + n\text{-}C_{36}$	H	R

Types of Composition Diagrams with Adjacent Homologs

Let us consider those of the diagrams in Fig. 13 where the components are immediate neighbors in the homologous series. They are shown in Table 3. All the odd components in these systems are isomorphous with each other, and so are the even ones. Under these conditions, it would be expected that all the diagrams considered would be similar, but, instead of this, we find an alternation in type. Taking note of what has been stated above on the mutual solubility of H and T modifications, the difference between the systems in the two columns of Table 3 may be written:

$$C_{2n-1}(H) + C_{2n}(T),$$
$$C_{2n+1}(H) + C_{2n}(T),$$

i.e., in the first case the even component with the triclinic modification has the longer chain length, while in the second case it has the shorter chain length. This is a striking example of the effect of the general factor of relative chain length, which was formulated above as a rule for the mutual solubility of two n-paraffins.

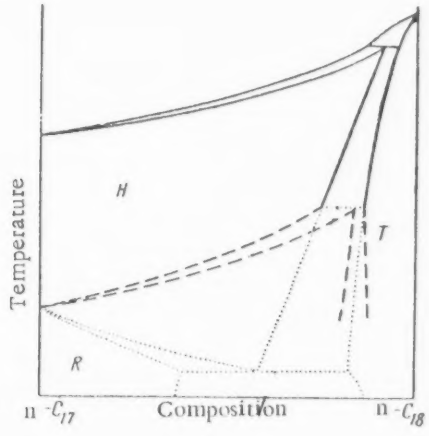

Fig. 16. Two possible variants for the composition diagram of the system $C_{17} + C_{18}$, which do not conflict with the condition for continuous solubility.

TABLE 3

Roozeboom Type IV	Roozeboom Type V
	$n\text{-}C_8 + n\text{-}C_9$
$n\text{-}C_9 + n\text{-}C_{10}$	
	$n\text{-}C_{10} + n\text{-}C_{11}$
$n\text{-}C_{11} + n\text{-}C_{12}$	
	$n\text{-}C_{12} + n\text{-}C_{13}$
$n\text{-}C_{13} + n\text{-}C_{14}$	
	$n\text{-}C_{14} + n\text{-}C_{15}$
$n\text{-}C_{15} + n\text{-}C_{16}$	
	$n\text{-}C_{16} + n\text{-}C_{17}$
$n\text{-}C_{17} + n\text{-}C_{18}$	
$n\text{-}C_{19} + n\text{-}C_{20}$	
$n\text{-}C_{2n^*-1} + n\text{-}C_{2n}$	$n\text{-}C_{2n} + n\text{-}C_{2n+1}$

* n is always a whole number.

The Solubility Break in Systems with T Components

The absence of a continuous series of solid solutions was observed in a study of the binary system n-C_{18} + + n-C_{20} [49], in spite of the isomorphism of the component crystals, which have triclinic subcells of similar size and with the same symmetry. Over a definite concentration range, with a sufficient content of solute in solvent, they form solid solutions of a different rhombic (R) modification. The same has been observed in the system n-C_{16} + n-C_{18}. We may ask why there is not a continuous series of solid solutions on the basis of a T subcell, although it would appear that all the conditions for this are fulfilled. The phenomenon can be explained if we suppose (see part I of this review) that the triclinic structures of n-paraffins acquire stability as the result of the high packing density of the molecular layers, but that the T subcell itself is less stable than the R subcell. It is clear that the higher symmetry of the R subcell is important in this connection, since the tendency of a structure to have maximum symmetry is now well established. On the other hand, it follows from theory [2] that the formation of a triclinic true cell, as the result of an arbitrary shift in the superposition of molecular layers, always leads to the maximum packing density of these layers. We can now understand why there is not continuous solubility in the systems n-C_{16} + n-C_{18} and n-C_{18} + n-C_{20}, although the component structures are isomorphous and the molecules differ little in length. Mixing with a different length component inevitably disturbs the end group packing density, so that the triclinic structure becomes less stable than the rhombic, and the result is a structure with a stable R subcell.

The Problem of Molecular Packing in Solid Solutions of n-Paraffins

The problem of molecular packing in solid solutions of n-paraffins and their derivatives has for a long time attracted the attention of investigators. Hengstenberg [55], investigating n-paraffin mixtures from C_{60} to C_{80} did not find any lines on the x-ray patterns corresponding to a large interplanar spacing (which we shall call the interlayer spacing), and therefore proposed a scheme for the crystalline structure of solid solutions in which the end groups were arranged randomly, but there was complete order in the lateral packing (Fig. 17, a). However, later investigators in this field always found the expected interlayer periods with various samples, and it is possible that, with improvement in experimental technique, (00*l*) reflections would be found with Hengstenberg's samples. Ott and Slagle [56], working with fatty acids from C_{10} to C_{18}, observed something approaching Vegard's law – a smooth linear change in d_{001} with change in mixture composition. Hess and Kiessig [57] investigated soap mixtures. They interpreted the clear reflections in the x-ray patterns and the continuous change in these with change in composition, as shown in Fig. 17, b. The end polar groups are packed in true planes, separated by uniform spacings, but the opposite ends of the chains are bent and packed quite densely, because aliphatic chains are highly flexible. The authors suggest that this picture is also valid for other chain compounds containing hetero-groups – fatty acids, fatty acid esters, ketones, etc. – but is hardly applicable to the n-paraffins themselves. However, Piper and his co-workers [26], working with mixtures of n-paraffins differing in length by one or two CH_2 groups, observed one system of clear 00*l* reflections. Ewald [58], Hess, and other investigators explained this as the result of the small difference in chain length between the mixed components. In this case, a plane can be traced through the ends of the molecules, although less strictly, since this conception exists simultaneously with clear low order reflections.

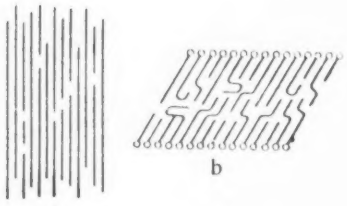

Fig. 17. a) Structural model of a solid solution of a system of chain molecules, preserving the dense zigzag form for the carbon atom chains, but with random packing of the ends; b) structural model of a solid solution of a system of chain molecules, containing hetero-atoms in the molecular chains located in parallel equally spaced planes.

The problem was further investigated by Kitaigorodskii and Mnyukh [59]. The idea behind their investigation was as follows. Different mechanisms for the formation of solid solutions may be anticipated, depending on whether the solvent paraffin has a longer or shorter chain length than the solute. The relation between interlayer spacing and composition was investigated experimentally. The choice of binary systems was dictated by the conditions that the structures of the components should be isomorphous, that a continuous series of solid solutions should be formed over a wide concentration range, and that there should be a maximum difference between the numbers of CH_2 groups in the two components. In contrast to the work of Piper and his co-workers (Fig. 18), the latter condition made it possible to establish in more

detail the shape of the curves in the "interlayer spacing – composition" diagrams. This condition was satisfied by the systems n-C_{30} + n-C_{34} and n-C_{30} + n-C_{36}. X-ray exposures were carried out with a low angle camera. Figure 19 shows the results. The experimental points near the y axis are less reliable. It is clear that there are two separate regions, showing the difference in character of the solid solution formation process, depending on whether the dominant structure is that of the longer or shorter component.

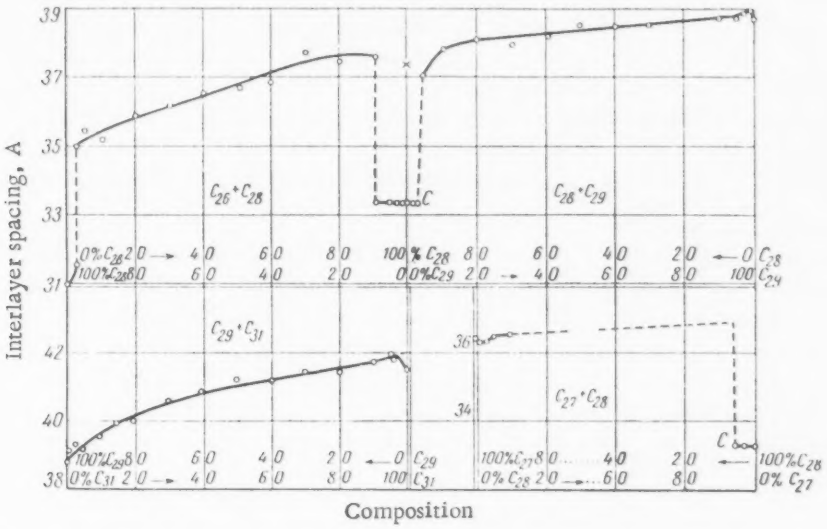

Fig. 18. "Interlayer spacing – composition" diagrams for some binary n-paraffin systems.

Thus, there is not a linear relation between interlayer spacing and composition. The curve lies above the line joining the points for the pure components. It should be noted that this interlayer spacing curve also represents the change in volume curve of the elementary cell, since it has been shown that the lateral packing density of the chains does not depend on the composition. The mean mass of a molecule in solid solution varies linearly with composition, whereas the densities of the components are almost the same, so the curves shown must be considered as representing the relative densities of the solid solution crystals.

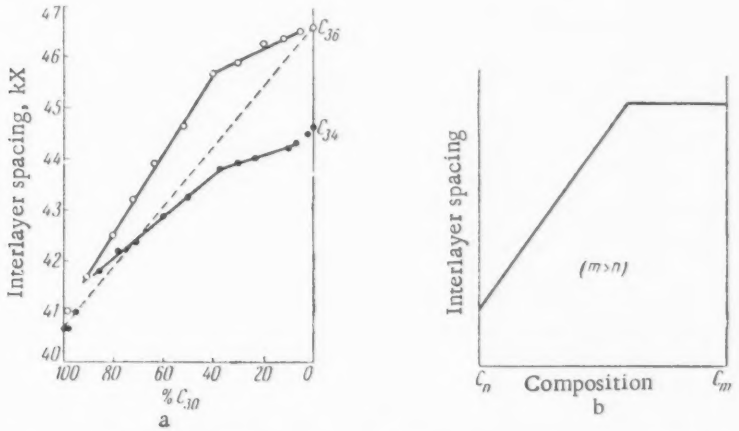

Fig. 19. a) "Interlayer spacing – % composition" diagrams for the systems C_{30} + C_{34} and C_{30} + C_{36} [60]; b) the ideal case explained in the text.

It was shown earlier that, with the dissolution of a shorter chain length paraffin, the conceivable structure was unaltered up to the percentage composition where the packing density dropped appreciably. From this point of view, in relation to Fig. 14, the variation of interlayer spacing with composition should correspond more to the horizontal part of the curve shown in Fig. 19, b. This horizontal part of the curve corresponds to solid solutions in which the gaps, caused by replacement of long molecules by shorter ones, are not filled. Experiment shows that there is some departure from this ideal mechanism.

The results of this investigation show that the structure suffers a greater change if the distortion, resulting from the superposition of layers, is caused by the appearance of projections instead of cavities (this is evident from the slopes of the curve in Fig. 19, a, before and after the discontinuity). This is in agreement with all the above discussed conceptions and would be expected, because the intermolecular (van der Waals) attraction curve is steep on the repulsion side and slopes more gradually on the attraction side. Thus, the tolerance of gaps without structural distortion is associated with a smaller increase in energy than is the complementary compression in the projection region.

Finally, it must be emphasized that the available experimental data is in conflict with any attempt to explain the structure of n-paraffin solid solutions in terms of an idealized crystal lattice (such as an alternation of layers in the crystal) without irregularities in the end group region. An idealized ordered alternation of layers (each consisting of one sort of molecule), or any other conceivable "ideal" method of molecular packing in the mixed crystal, when associated with the existence of low angle x-ray patterns showing a single system of clear 00*l* lines, requires that there should be a linear relation between interlayer spacing and composition; but this is refuted experimentally. Also, the manner of strict alternation should change with the slightest change in composition, which is very improbable. On the other hand, however, there are some unpublished results by Smith which indicate that there are conditions under which it is possible to grow n-paraffin mixed crystals with an ideal order of alternating layers. Thus, it is clear that the problem of molecular packing in n-paraffin solid solutions still contains many interesting features, and is a worthwhile field for further investigation.

In conclusion, we must make reference to a review [60], which gives a very detailed analysis of the literature, and to two experimental papers [61, 62], devoted to questions which have been discussed here.

LITERATURE CITED

1. V. A. Kargin, A. I. Kitaigorodskii, and G. L. Slonimskii, Kolloid. Zhur. 19, 131 (1957).*
2. A. I. Kitaigorodskii, Organic Crystal Chemistry [in Russian] (Izd. AN SSSR, Moscow, 1955).
3. K. S. Pitzer, Faraday Soc. Disc. 10, 73 (1951).
4. W. J. Taylor, Chem. Phys. 16, 257 (1948).
5. H. M. M. Shearer and V. Vand, Acta Cryst. 9, 379 (1956).
6. J. R. Brathovde and E. C. Lingafeler, Acta Cryst. 11, 729 (1958).
7. B. K. Vainshtein and Z. G. Pinsker, Doklady Akad. Nauk SSSR 72, 53 (1950).
8. A. Müller and W. B. Saville, J. Chem. Soc. 127, 599 (1925).
9. A. Müller, Proc. Roy. Soc. A 120, 437 (1928).
10. A. E. Smith, J. Chem. Phys. 21, 2229 (1953).
11. C. W. Bunn, Trans. Faraday Soc. 35, 482 (1939).
12. C. S. Fuller and C. L. Erickson, J. Am. Chem. Soc. 59, 344 (1937).
13. C. S. Fuller and C. J. Frosch, J. Phys. Chem. 43, 323 (1939).
14. C. S. Fuller and C. J. Frosch, J. Am. Chem. Soc. 61, 2575 (1939).
15. C. S. Fuller, et al., J. Am. Chem. Soc. 64, 154 (1942).
16. Yu. V. Mnyukh, Zhur. Fiz. Khim. 33, 2076 (1959).
17. E. von Sydow, Arkiv. Kemi 9, 231 (1956).
18. V. Vand, Acta Cryst. 4, 104 (1951).
19. A. Müller, Proc. Roy. Soc. A 127, 805 (1930).
20. A. Müller, and K. Lonsdale, Acta Cryst. 1, 129 (1948).
21. A. A. Schaerer, et al., J. Am. Chem. Soc. 77, 2017 (1955).
22. W. M. Mazee, Rec. trav. chim. 67, 197 (1948).

* Original Russian pagination. See C. B. translation.

23. A. Müller, Proc. Roy. Soc. A 124, 317 (1929).
24. R. Kohlhaas and H. Soremba, Z. Krist. 100, 47 (1938).
25. S. H. Piper, et al. J. Chem. Soc. 127, 2194 (1925).
26. S. H. Piper, et al. Biochem. J. 25, 2072 (1931).
27. J. D. Hoffman, J. Chem. Phys. 20, 541 (1952).
28. A. I. Kitaigorodskii and Yu. V. Mnyukh, Izvest. Akad. Nauk SSSR, Otdel. Khim. Nauk., 12, 2088 (1959).*
29. A. Müller, Proc. Roy. Soc. A 138, 514 (1932).
30. A. Eucken, Z. Electrochem. 45, 126 (1939).
31. J. Timmermans, Les constantes physiques des composes organiques cristallises (Paris, 1953).
32. A. I. Kitaigorodskii, Doklady Akad. Nauk SSSR 124, 861 (1959).*
33. A. A. Schaerer, G. G. Bayle and W. H. Mazee, Rec. trav. chim. 75, 513 (1956).
34. A. I. Kitaigorodskii, Kristallografiya 2, 456 (1957).
35. A. I. Kitaigorodskii, Kristallografiya 2, 646 (1957).
36. A. I. Kitaigorodskii, Acta Cryst. 10, 802 (1957).
37. T. Schoon, Z. Phys. Chem. B 39, 385 (1938).
38. A. I. Kitaigorodskii and Yu. V. Mnyukh, Doklady Akad. Nauk SSSR 121, 115 (1958).*
39. P. W. Teare and D. R. Holmes, J. Pol. Sci. 24, 496 (1957).
40. S. S. Kabalkina, Doklady Akad. Nauk SSSR 125, 114 (1959).*
41. A. I. Kitaigorodskii and Yu. V. Mnyukh, Doklady Akad. Nauk SSSR 121, 291 (1958).*
42. V. M. Kravchenko, Acta Physicochim. URSS 21, 335 (1946).
43. V. M. Kravchenko, Collected Papers on Physical Chemistry [in Russian] (Izd. AN SSSR, Moscow-Leningrad, 1947), p. 329.
44. N. A. Nechitailo and G. B. Ravich, Uspekhi Khim. 26, 640 (1957).
45. J. Smittenberg, et al. J. Am. Chem. Soc. 60, 18 (1938).
46. R. Sabzgeber, Compt. rend. 240, 1642 (1955).
47. S. A. Yuganova, Candidate's Dissertation, Central Scientific Research Inst. of Aviation Fuels and Oils [in Russian] (1950).
48. W. M. Mazee, Anal. Chim. Acta 17, 97 (1957).
49. A. I. Kitaigorodskii, Yu. V. Mnyukh, and N. A. Nechitailo, Kristallografiya 3, 298 (1958).
50. N. A Nechitailo, Doklady Akad. Nauk SSSR 116, 613 (1957).*
51. A. V. Topchiev and N. A. Nechitailo, Doklady Akad. Nauk SSSR 117, 629 (1957).*
52. A. I. Kitaigorodskii, Doklady Akad. Nauk SSSR 113, 604 (1957).*
53. R. M. Myasnikova and A. I. Kitaigorodskii, Kristallografiya 3, 160 (1958).
54. A. I. Kitaigorodskii and Liang Tung-ch'ai, Kristallografiya 5, 238 (1960).
55. J. Hengstenberg, Ann. Physik. 84, 272 (1927).
56. E. Ott and F. B. Slagle, J. Phys. Chem. 37, 257 (1933); J. Am. Chem. Soc. 55, 4404 (1938).
57. K. Hess and H. Kiessig, Chem. Ber. 81, 327 (1948).
58. P. P. Ewald, Handbuch der Physik, herausgeg. von H. Greiger and K. Scheel. (Springer-Verlag, 1933) Vol. 23, Chap. 2.
59. A. I. Kitaigorodskii and Yu. V. Mnyukh, Vysokomolek. Soed. 1, 128 (1959).
60. V. Daniel, Adv. Phys. 2, 450 (1953).
61. P. W. Teare, Acta Cryst. 12, 294 (1959).
62. S. Barbezat-Debreuil, Compt. rend. 246, 2907 (1958).

* Original Russian pagination. See C. B. translation.

BRIEF COMMUNICATIONS

OXANIUM COMPOUNDS OF OXYGEN

Ya. K. Syrkin

M. V. Lomonosov Moscow Institute of Fine Chemical Technology
Translated from Zhurnal Strukturnoi Khimii, Vol. 1, No. 3, pp. 389-390,
September-October, 1960
Original article submitted June 22, 1960

In oxonium compounds, it is well known that, in addition to the two bonds by unpaired $2p_x$ and $2p_y$ electrons, oxygen forms a third active bond by means of the unshared pair of $2p_z$ electrons. Thus, all three 2p orbitals are occupied in oxonium compounds. The configuration in the presence of the three neighbors has C_{3v} symmetry (a pyramid with oxygen at the vertex). Except for the stable H_3O^+ ion (for which there is a special reason), the oxonium compounds are mostly of low stability. Thus, the trialkyl oxonium compounds of Meerwein and compounds of the type $(CH_3)_2O \cdot HCl$ are very unstable.

However, in addition to these, compounds of another type are possible, namely oxanium compounds, in which there are two donor bonds by the two unshared pairs $2s^2$ $2p^2$ in addition to the two normal unpaired 2p electron bonds. As a result, oxygen can give four hybrid σ bonds directed to the vertices of a tetrahedron. This condition exists to some extent in the lattices of BeO, ZnO, PtO, PdO, etc.

The oxanium state can arise when 1) the neighboring atoms have vacant orbitals, 2) the neighboring atoms show electron affinity, and 3) electron shift from the oxygen is accompanied by a delocalization of negative charge which stabilizes the system.

As an alternative to these four σ bonds, it is also possible for the oxygen to form three σ and one π bond: $\sigma^3\pi$ (three σ bonds in a plane with D_{3h} symmetry, and a fourth π bond delocalized between the oxygen and three neighboring atoms). This is the case with $[O(HgCl)_3]^+Cl^-$ [1]. The structure of this compound can be represented diagrammatically as follows: there are two positive charges on the oxygen and one negative charge shared between the three surrounding atoms, so that each O–Hg bond is $^1/_3$ double. The HgOHg angle is 120°. (The negative charge can also be partly distributed over the inner chlorine atoms).

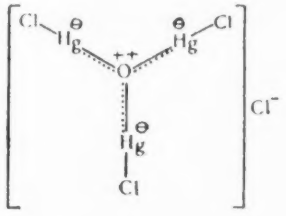

It is considered that the compounds $[(C_6H_5)_3O]^+X^-$ (where X is an anion), synthesized by Nesmeyanov and Tolstaya [2], are of this type. Unlike the very unstable trialkyl oxonium compounds of Meerwein, these compounds are quite stable and only decompose above 150°. It is evident that this is not a triphenyl oxonium but a triphenyl oxanium compound, in which the unshared electron pairs of the oxygen ($2s^2$ and $2p^2$) are shifted to the aromatic rings, so that the oxygen gives three hybrid σ bonds and one π bond, and a single negative charge is delocalized between the nine ortho and para positions of the benzene rings. The structure is shown diagrammatically below.

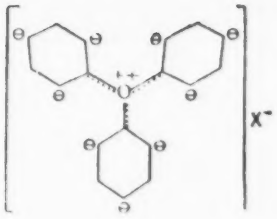

If this description is correct, then 1) the triphenyl oxanium compounds should show ortho-para orientation, and 2) the oxygen and the neighboring atoms of the benzene rings should lie in a plane. Owing to considerable delocalization of the negative charge in the π bond, these compounds should be considerably more stable than their trialkyl analogs, where such delocalization and such a state for the oxygen are impossible.

If oxygen is bonded to only two neighboring atoms with empty orbitals, then it is possible for the oxanium state to occur with a linear configuration of the atoms Me $\leftarrows$ O $\rightrightarrows$ Me (for instance Ru $\leftarrows$ O $\rightrightarrows$ Ru), where the oxygen forms two σ and two π bonds.

Oxanium oxygen can evidently also exist in a series of other compounds.

For the sake of precision, it should be noted that the oxanium state does not denote tetravalent oxygen in the ordinary sense, i.e., in the form of a neutral atom in which one of the unshared pair of $2p_z$ electrons is promoted to a 3s orbital, since such promotion with change in the principle quantum number would involve too great an expenditure of energy. For this reason, the structure $(CH_3)_2OHCl$, with oxygen forming four ordinary covalent bonds, is incorrect.

LITERATURE CITED

1. S. Scavnicar and D. Grdenic, Acta Cryst. 8, 275 (1955).
2. A. N. Nesmeyanov and T. P. Tolstaya, Doklady Akad. Nauk SSSR 117, 626 (1957). *

LITHIUM URANATE (V) $LiUO_3$

L. M. Kovba and A. N. Golubenko

M. V. Lomonosov Moscow State University

Translated from Zhurnal Strukturnoi Khimii, Vol. 1, No. 3, pp. 390-392, September-October, 1960
Original article submitted July 16, 1960

An x-ray investigation has been made of the products of thermal dissociation of α-Li_2UO_4. A scheme has been proposed for the dissociation, and structures have been considered for all the phases formed, including $LiU^{V}O_3$.

Lithium uranate (V) was first obtained by Rüdorff and Leutner [1] by the interaction of lithium monouranate Li_2UO_4 with uranium dioxide at 650-750°. The authors considered that lithium uranate (V) crystallized with rhombic or monoclinic syngony, but did not give any data except for some Debye photographs, without

* Original Russian pagination. See C. B. translation.

stating what radiation was used. Sodium and potassium uranates (V) give crystals of the perovskite type [2]. According to Rüdorff and Leutner [1], uranium dioxide is formed by the dissociation of Li_2UO_4. They did not detect any intermediate products.

We established that two dissociation products were formed by the dissociation of Li_2UO_4 at 933°. The x-ray photograph (FeK radiation) of one (Table 1) of these phases was analyzed on the assumption of a hexagonal cell with a = 5.406 ± 0.001 kX and c = 7.506 ± 0.004 kX. The systematic absence of lines with $h + k + l \neq 3n$ showed that the cell was rhombohedral. The parameters of the latter were: a = 4.039 kX and $\alpha = 85° 03'$. The cell must be considered as a distorted primary cube. The volume of the rhombohedral cell was 63.5 A^3, which is close to the semisum of the volumes of the Li_2O and U_2O_5 cells (67.5 A^3) and to the semisum of the volumes of the Li_2O and $UO_2 + UO_3$ cells (61.8 A^3).* This showed that one $LiUO_3$ formula unit could be assigned to the cell.

TABLE 1

Debye X-Ray Powder Pattern of Lithium Uranate (V)*

I	$10^4/d_H^2$	hkl	$10^4/d_R^2$	I	$10^4/d_H^2$	hkl	$10^4/d_R^2$	I	$10^4/d_H^2$	hkl	$10^4/d_R^2$	I	$10^4/d_H^2$	hkl	$10^4/d_R^2$
10	633	101	634	8	6104	131	6106	6	3369	211	3370	6	7763	116	7758
8	1166	012	1166	6	6249	205	6267	6	3901	122	3902	4	8000	042	8006
8	1376	110	1369	3	6380	006	6389	4	4104	300	4104	8	8784	134	8768
6	2005	021	2001	6	6642	312	6638	4	4883	015	4898	8	8850	321	8842
6	2530	202	2522	8	7074	223	7070	4	5463	220	5472	6	9160	107	9153
8	2976	113	2966	4	7483	401	7474	6	5696	303	5702	10	9371	232	9374
3	3311	104	3296	6	7641	125	7636	8	6066	214	6034	8	9574	410	9576

* In constructing the intensity scale, we used the ratio $I_\alpha : I_\beta = 5 : 1$ instead of the usual 7-8 : 1.

It is stated in the literature [1] that $LiUO_3$ crystallizes with rhombic or monoclinic syngony, and the impression has arisen that lithium uranate (V) exists in two polymorphic modifications. In order to check this assumption, we synthesized the material by sintering lithium monouranate with uranium dioxide in a platinum boat at 650-750°. However, in this case, we obtained a hexagonal uranate (V) with a = 5.406 ± 0.002 kX and c = 7.502 ± 0.004 kX. Thus, the uranates (V) of lithium, sodium, and potassium have similar cells:

$LiUO_3$	$NaUO_3$ [2]	KUO_3 [2]
Rhombohedral cell	Monoclinic cell	Cubic cell
$a = 4{,}039\ kX$ $\alpha = 85°03'$	$a \sin\beta = b = c \sin\beta = 4{,}129\ kX$; $\beta = 88°36'$	$a = 4{,}290\ kX$.

These all belong to the perovskite type (sometimes with distortion of the cubic cell), as is illustrated by a comparison of their Debye x-ray powder patterns (see figure). When samples were taken from the surface of the material, then lines of a second phase appeared in the x-ray photographs of the dissociation products. The lines of this unknown phase could be analyzed on the assumption of a face-centered cell with a = 5.375 ± 0.005 kX (Table 2). This phase could not be one of the uranium oxides,** since UO_2 and $UO_{2.25}$ have large lattice constants (a = 5.458 ± 0.001 kX for UO_2 and 5.430 ± 0.005 kX for $UO_{2.25}$). Considering the ease with which phases of the type $(Me, U)O_{2\pm x}$ can be formed from many di- and trivalent metals (the lattice constants of such

* The volume of the U_2O_5 cell was calculated from the data of [3], which possibly refers to a metastable phase. The cell volume of the α modification was taken for UO_3.

** This was also shown by the equilibrium pressure of oxygen (5.55 mm Hg at 933°).

oxides are 5.30 - 5.40 A), particularly from magnesium, and since lithium has an ionic radius close to that of magnesium, it is reasonable to assume the formation of a phase $(Li, U)O_{2\pm x}$.

Debye x-ray powder patterns for the uranates of a) lithium, b) sodium, and c) potassium; the index data for $LiUO_3$ refer to the rhombohedral cell.

TABLE 2

Comparison of Debye X-Ray Powder Patterns of UO_2 and $(Li, U)O_{2\pm x}$

UO_2			$(Li, U)O_{2\pm x}$			UO_2			$(Li, U)O_{2\pm x}$		
hkl	*I*	$10^4/d^2$	*I*	$10^4/d^2_H$	$10^4/d^2_R$	*hkl*	*I*	$10^4/d^2$	*I*	$10^4/d^2_H$	$10^4/d^2_R$
111	8	1007	8	1034	1038	400	5	5370	2	5528	5538
200	4	1342	10 *	1376	1384	331	10	6376	6	6567	6576
220	10	2685	8	2779	2769	420	8	6712	4	6944	6922
311	10	3692	8	3806	3807	422	10	8054	6	8310	8306
222	4	4027	6 *	4104	4153	333 } 511 }	10	9061	4	9335	9345

* A strong $LiUO_3$ line also occurs here.

It can be seen from Table 2 that the line intensities of the $(Li, U)O_{2\pm x}$ phase correspond with those of UO_2, showing that these oxides are isostructural. From the absence of superlattice lines in the Debye x-ray powder patterns of $(Li, U)O_{2\pm x}$, it may be reasonably argued that there is a statistical distribution of U and Li atoms, with a single true system. This confirms our assumption as to the analogy between $(Li, U)O_{2\pm x}$ and the mixed oxides $(Me, U)O_{2\pm x}$. Formation of the phase $(Li, U)O_{2\pm x}$ is associated with a further loss of lithium oxide, which takes place first from the sample surface. Thus the thermal dissociation process is as follows (assuming that the final product is uranium dioxide [1] or $UO_{2.25}$, the latter being more likely at about 1000°): $Li_2UO_4 \rightarrow LiUO_3 \rightarrow (Li, U)_{2\pm x} \rightarrow UO_{2.25}$.

SUMMARY

1. The products formed by the thermal dissociation of lithium monouranate α-Li_2UO_4 are first $LiUO_3$ and then $(Li, U)O_{2\pm x}$.

2. Lithium uranate (V) has a rhombohedral distorted structure of the perovskite type, with lattice parameters (in the hexagonal aspect) a = 5.406 ± 0.001 kX and c = 7.506 ± 0.004 kX.

3. $(Li, U)O_{2\pm x}$ has a fluorite type structure, similar to that of uranium dioxide and the series of mixed oxides $(Me, U)O_{2\pm x}$.

LITERATURE CITED

1. W. Rüdorff and H. Leutner, Z. anorg. Chem. 292, 193 (1957).
2. L. M. Kovba, et al., Doklady Akad. Nauk SSSR 120, 1042 (1958).
3. R. E. Rundle, et al., J. Am. Chem. Soc. 70, 99 (1948).

* Original Russian pagination. See C. B. translation.